Data assimilation experiments at NARL

Amit P Kesarkar

Weather and Climate Research Group,

National Atmospheric Research Laboratory, Gadanki, Tirupati District, Andhra Pradesh 517112

Team: Dr. Jyoti N Bhate, Dr. V P M Rajasree, Dr. Pampi Malakar,

Dr. Arpita Munsi and Ms. Pavani Goriparthy

Presentation in workshop on data assimilation in weather and climate models

Data Assimilation- recap and outline of presentation

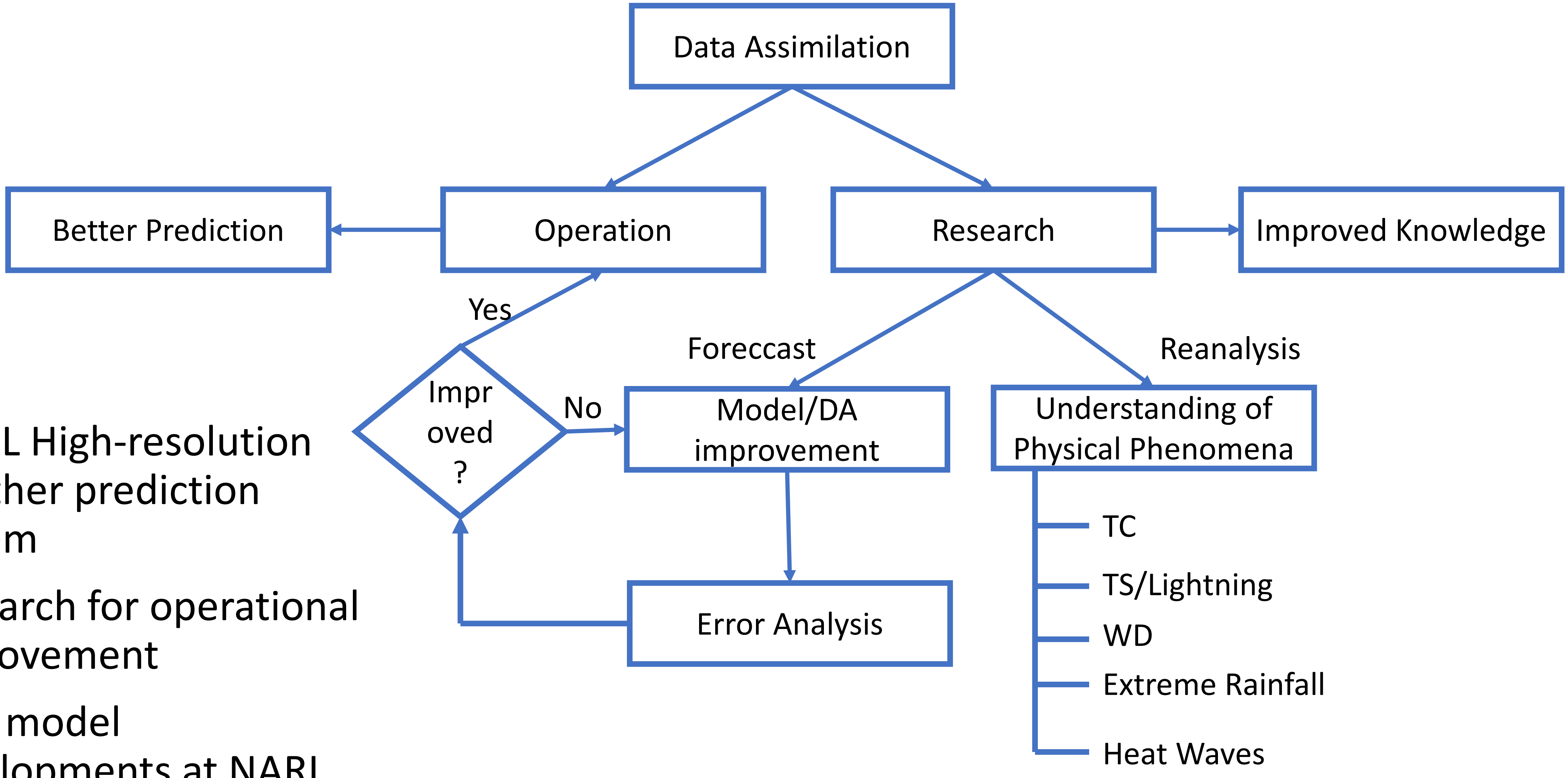

- NARL High-resolution weather prediction system
- Research for operational improvement
- New model developments at NARL

High Resolution Weather Prediction Over South Andhra Pradesh: Chittoor Project

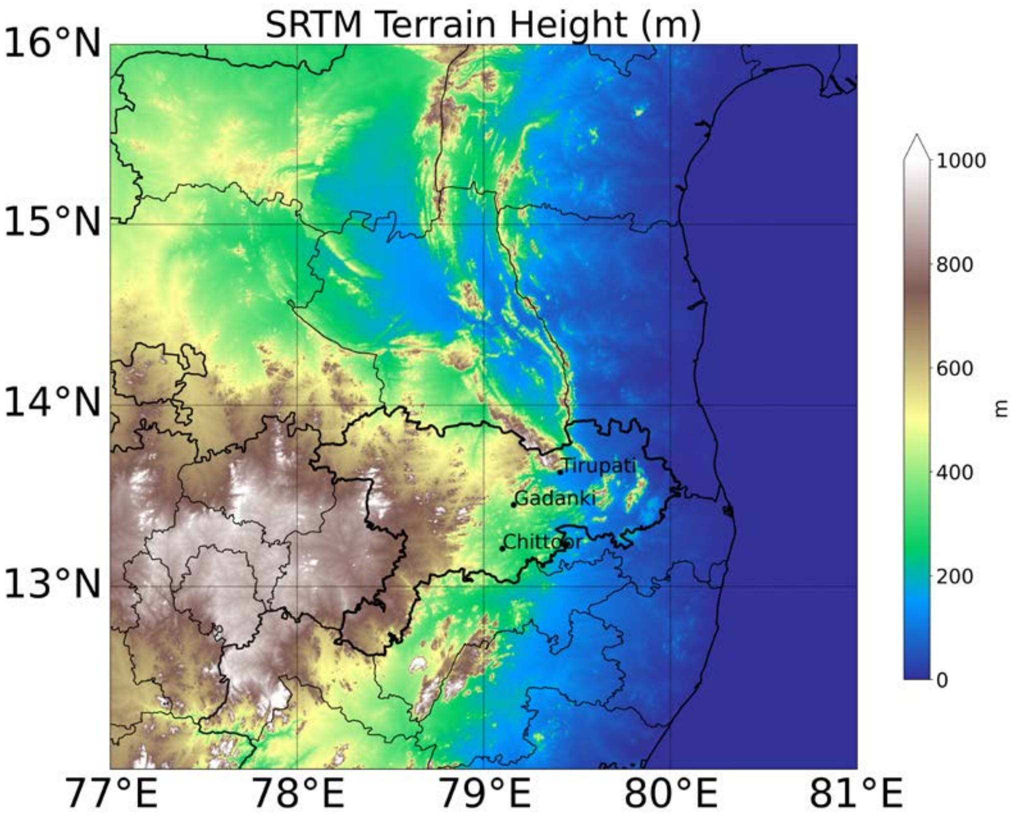

Objectives:

- To develop a high-resolution weather prediction system for Mandal-level predictions over the heterogeneous terrain of the Chittoor district and neighborhood.
- To validate with the weather observation systems available at NARL
- Continuously improve weather predictions by developing new parameterization techniques
- To develop AI/DL algorithms for bias corrections
- To develop computational clouds for multiplatform GIS-based dissemination of the weather predictions

Kesarkar A., Bhate J.N., Pavani G., Varma H., Panchal A. (2023) A verification of high-resolution weather forecast over Chittoor region. NARL report no. DOS-NARL-TD-UC-DEC-2023-01.

High Resolution Weather Prediction for South Andhra Pradesh

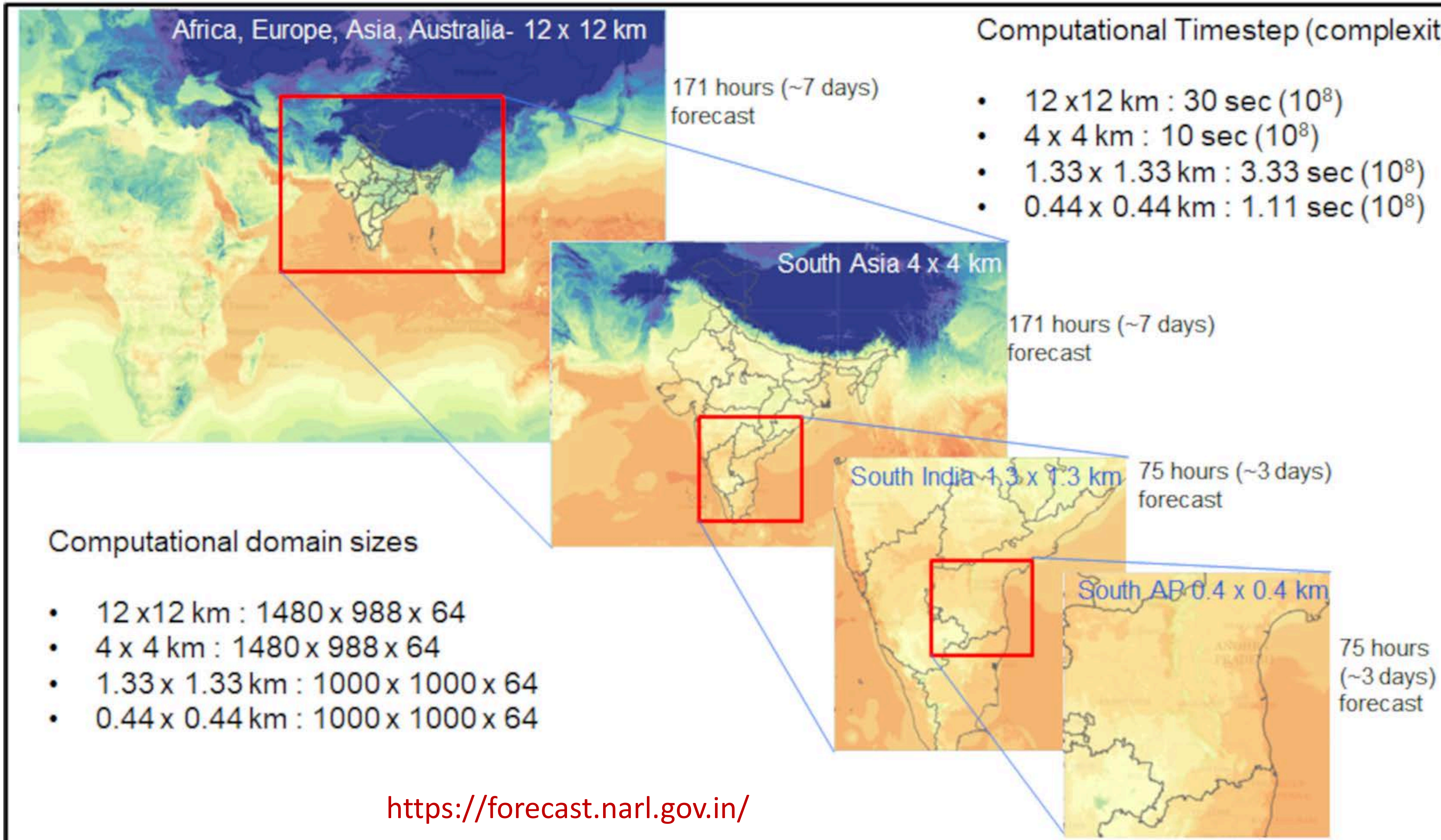

Computational Timestep (complexity)

- 12 x12 km : 30 sec (10^8)
- 4 x 4 km : 10 sec (10^8)
- 1.33 x 1.33 km : 3.33 sec (10^8)
- 0.44 x 0.44 km : 1.11 sec (10^8)

Computational domain sizes

- 12 x12 km : 1480 x 988 x 64
- 4 x 4 km : 1480 x 988 x 64
- 1.33 x 1.33 km : 1000 x 1000 x 64
- 0.44 x 0.44 km : 1000 x 1000 x 64

https://forecast.narl.gov.in/

High Resolution Weather Prediction for South Andhra Pradesh

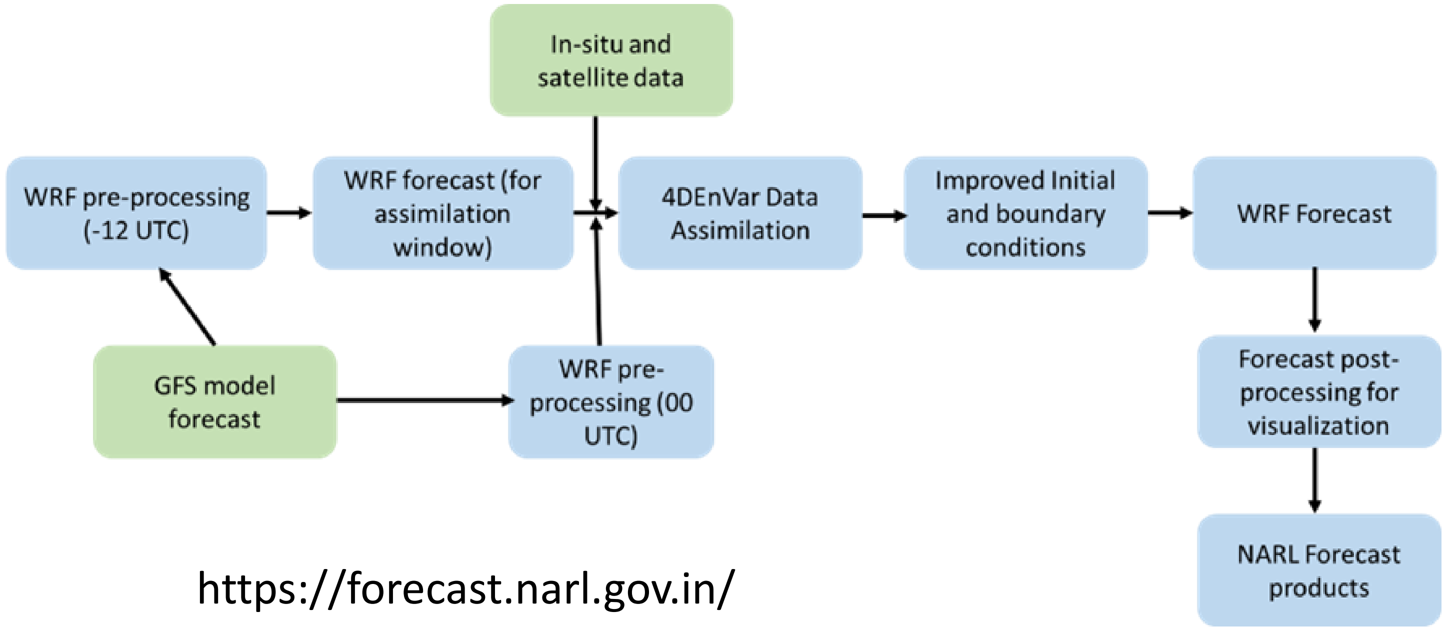

https://forecast.narl.gov.in/

Model configuration for Chittoor weather forecast

- The advanced four-dimensional ensemble variational (4DEnVAR)data assimilation technique
- The vertical levels are increased to 64.
- The highest resolution forecast over south Andhra Pradesh is 0.44km.
- Insitu/Satellite radiance data assimilation in cyclic mode

- Initial and Boundary conditions:
- Observations Assimilated
  - Prepbuffer data (Surface and Upper air observations)
  - AMSU,HIRS (NOAA series)
  - MHS,MTIASI (METOP)
  - GPSRO (METOP-A/GRAS)
  - ATMS (Suomi NPP and NOAA-20)
  - AMSR2 (GCOM-W1)
  - INSAT-3D
- Data Assimilation technique: 4DEnVar

Development of a high-resolution weather forecast system for the Chittoor district: verification

GPM-IMERG rainfall (mm)

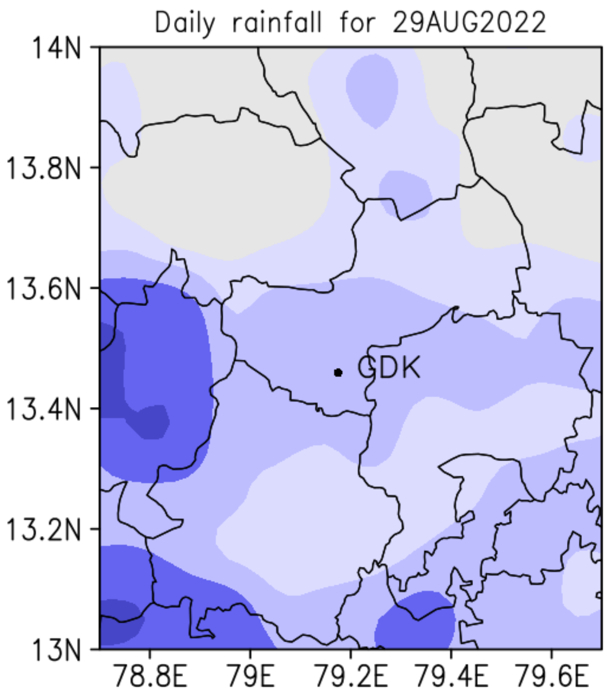

WRF model simulated rainfall (mm)

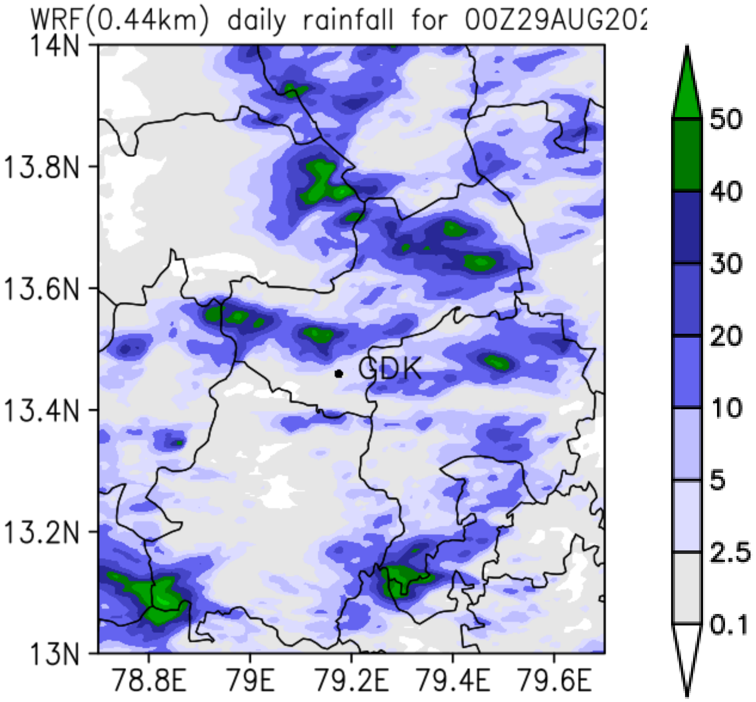

Time series over a grid point near Gadanki

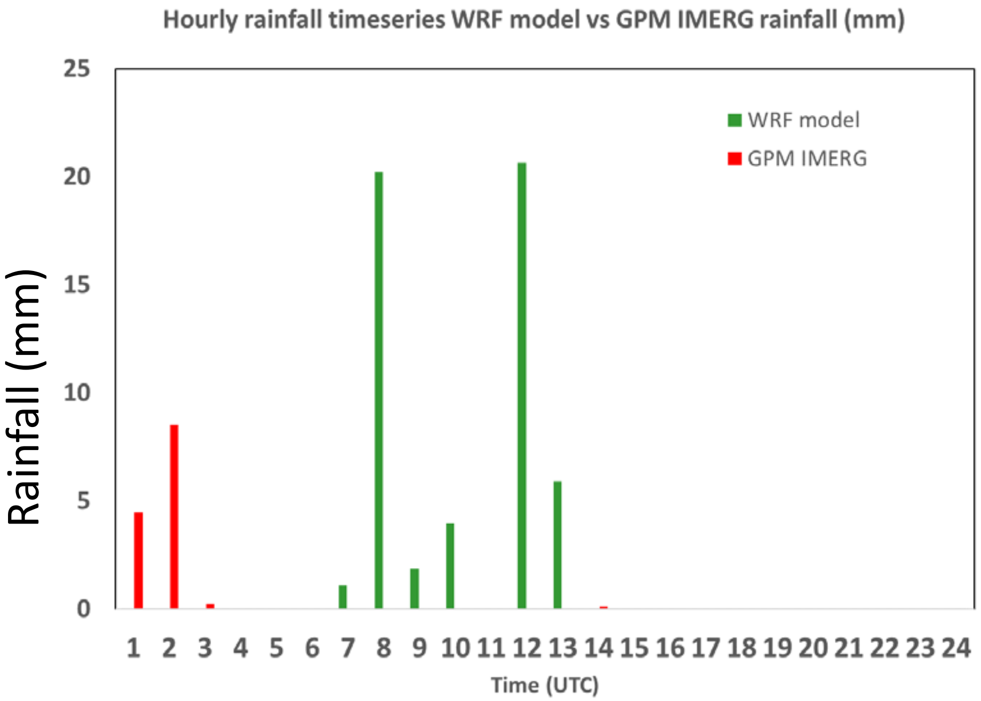

- New forecast system is able to capture the rainfall pattern at high resolution over Chittoor region.
- The forecast system is over estimating the rainfall with a time delay of 4-5 hours in model simulation.
- The time delay in rainfall is due to the time delay in simulating the surface fluxes.

~25 km IMD rainfall (mm)

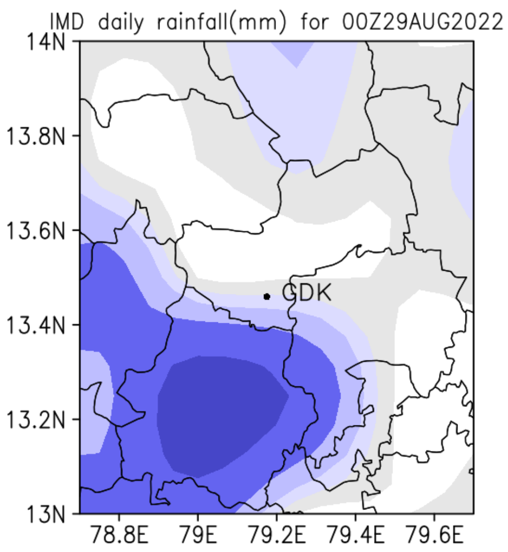

~11 km GPM-IMERG rainfall (mm)

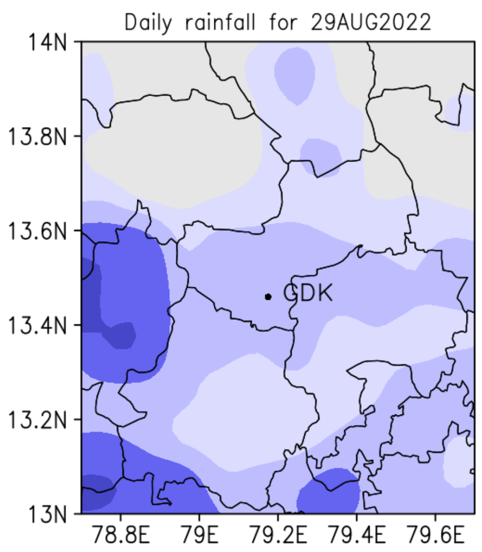

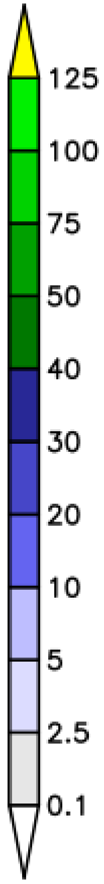

WRF 12km rainfall (mm)

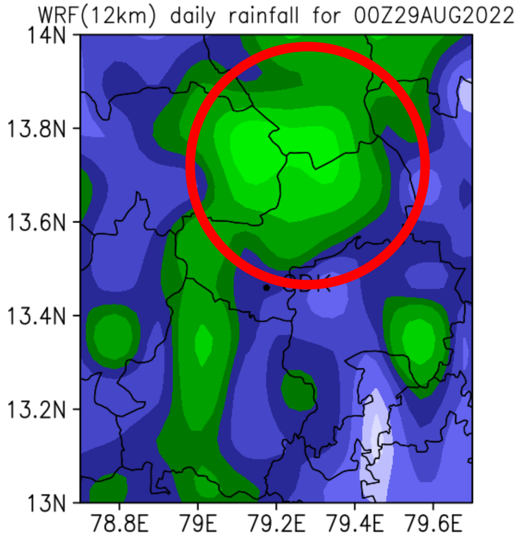

WRF 4km rainfall (mm)

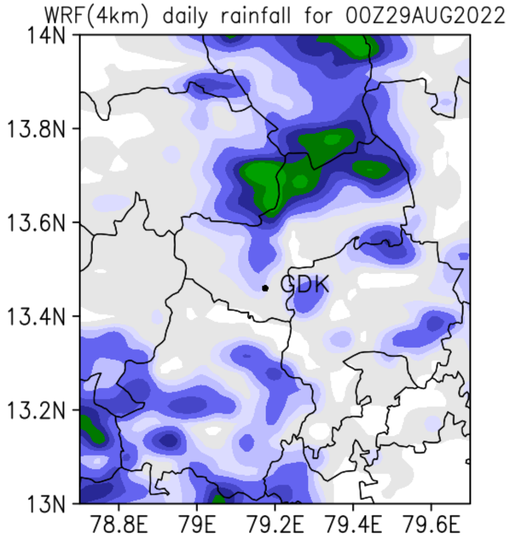

August 29, 2022 Daily rainfall comparison

WRF 1.33km rainfall (mm)

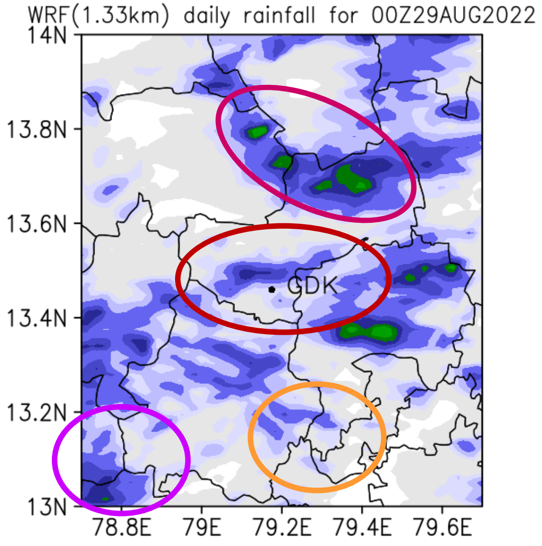

WRF 0.44km rainfall (mm)

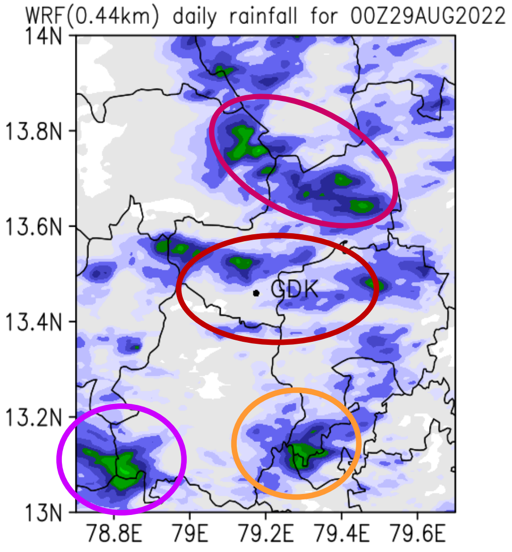

- The high-resolution spatial data(sub-kilometer scale) is not available.
- GPM-IMERG data underestimates over heterogeneous terrain.
- IMD data is based on the rain gauge network, and it is not densely populated.

Verification of High resolution rainfall forecast over Chittoor

Forecast skill scores over Chittoor region October to December 2022

12km

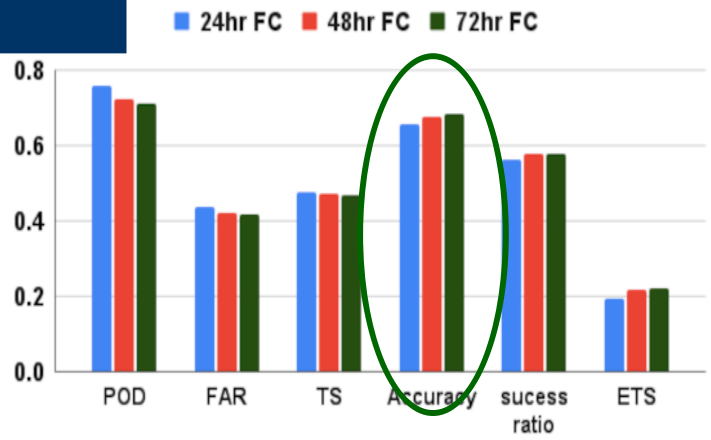

4km

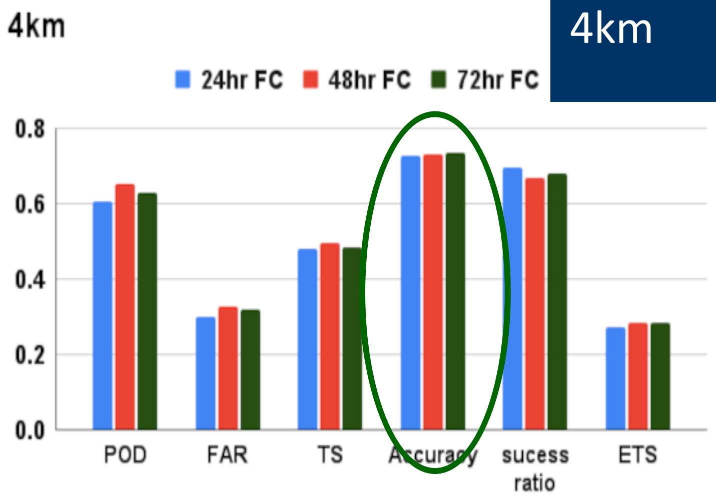

1.33km

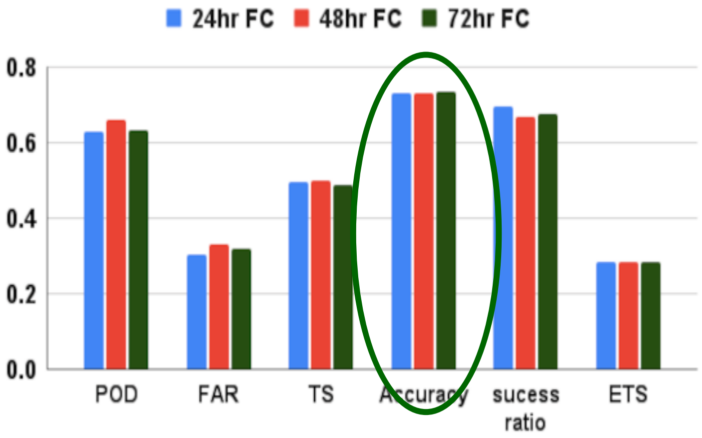

0.44km

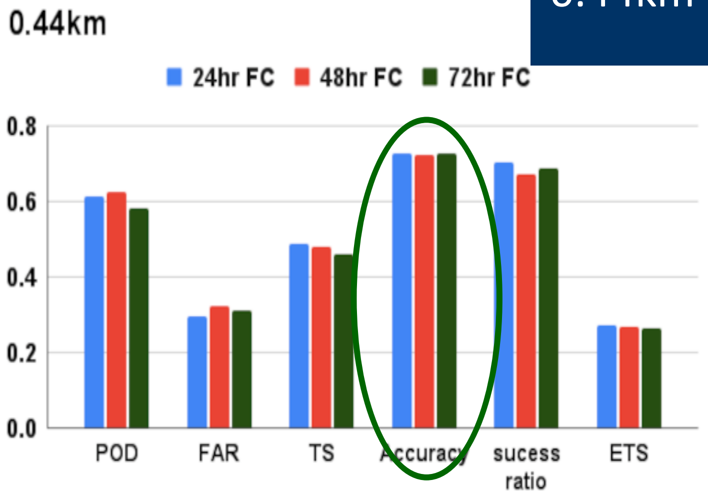

The overall accuracy is 75% for the season.

Rainfall verification for 0.44km rainfall forecast over Ananthapur and SriSathyasai districts

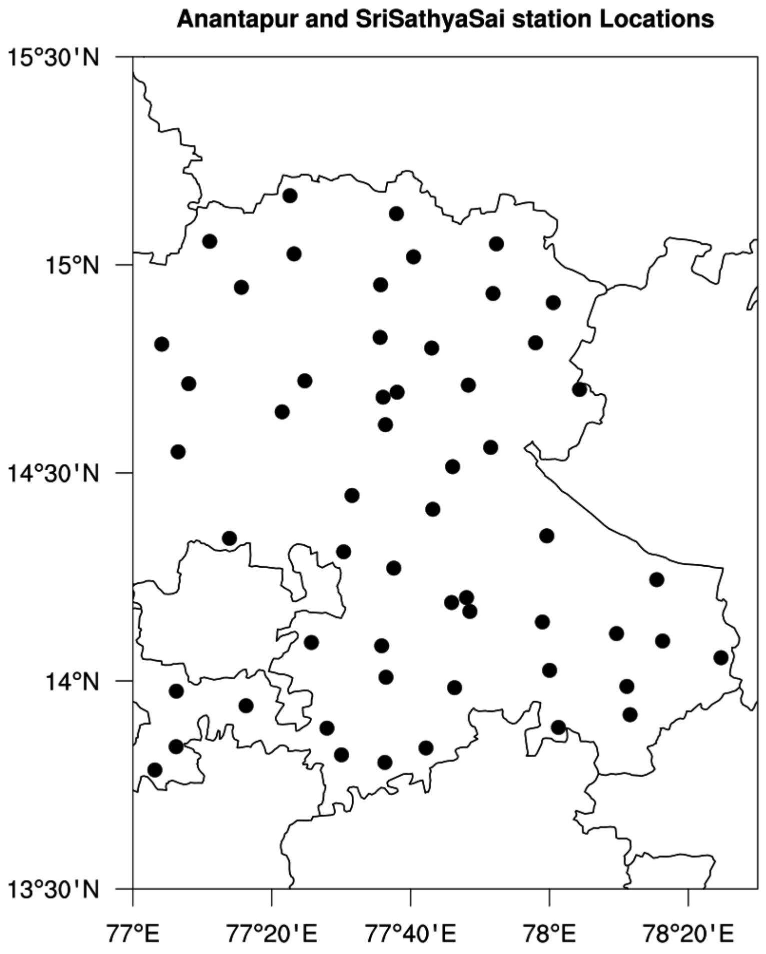

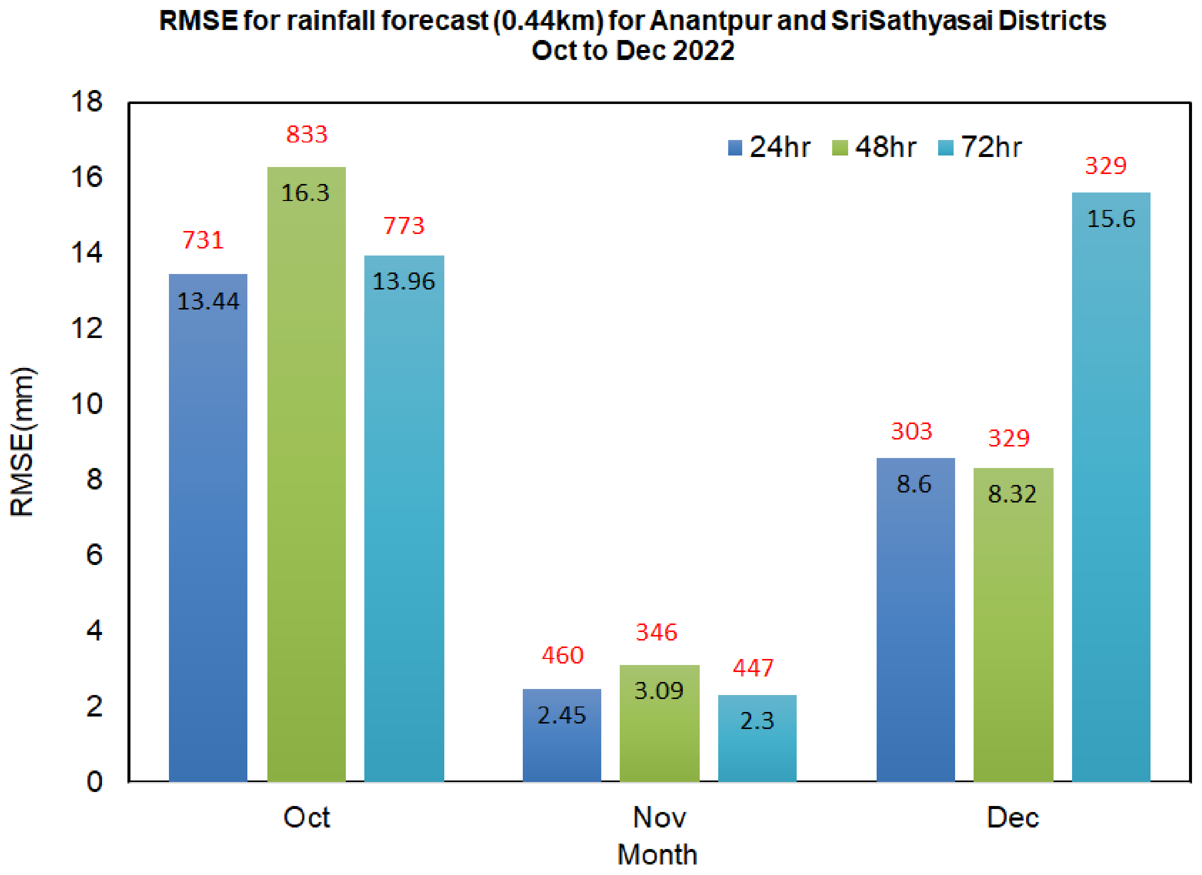

- Rainfall forecasts for 24, 48, and 72 hours lead time are verified over the Ananthapur and SriSathyasai districts (55 locations) using AWS data from ANGRAU.
- The maximum rainfall events (~42%) were in October followed by November(~27%) and December (~19%).

Rainfall verification for 0.44km rainfall forecast over Ananthapur and SriSathyasai districts

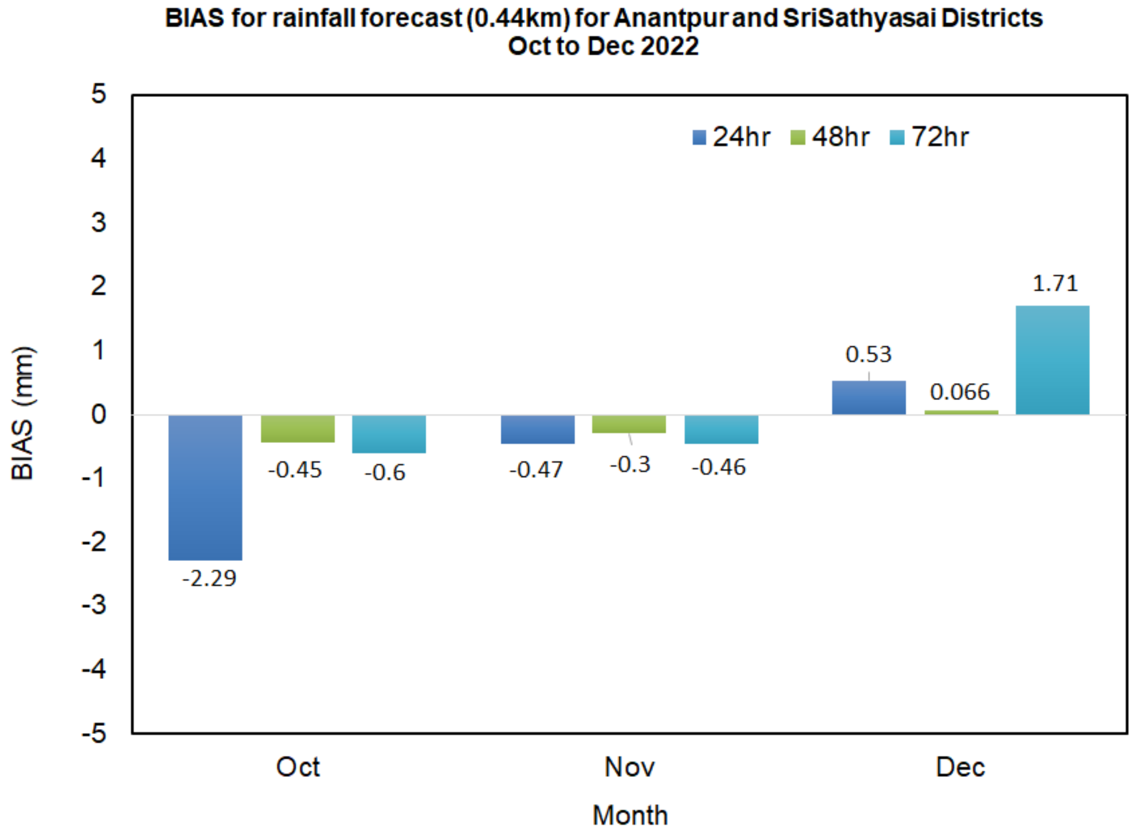

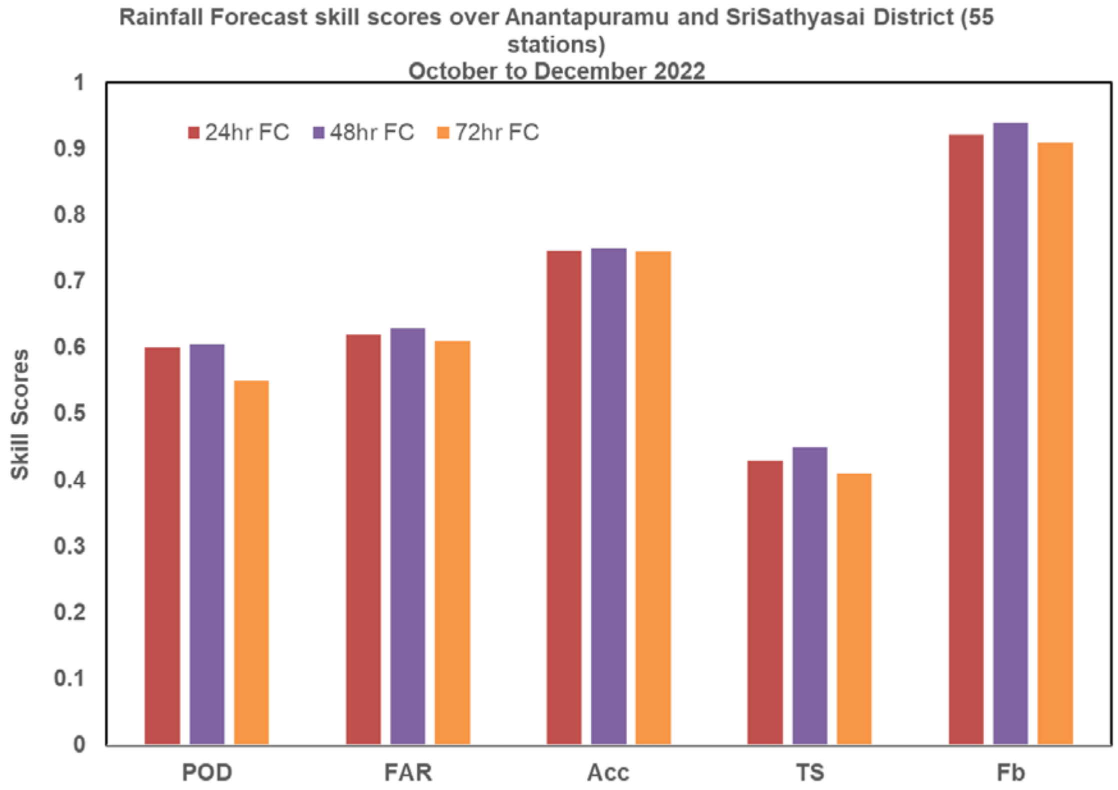

- The average bias in rainfall is within ± 2.3mm. The maximum RMSE is 16.3mm during heavy rainfall of about 80 mm
- The accuracy of rainfall forecast is 75% up to 3 days forecast.

Tropical cyclones over North Indian Ocean (2016-2020)

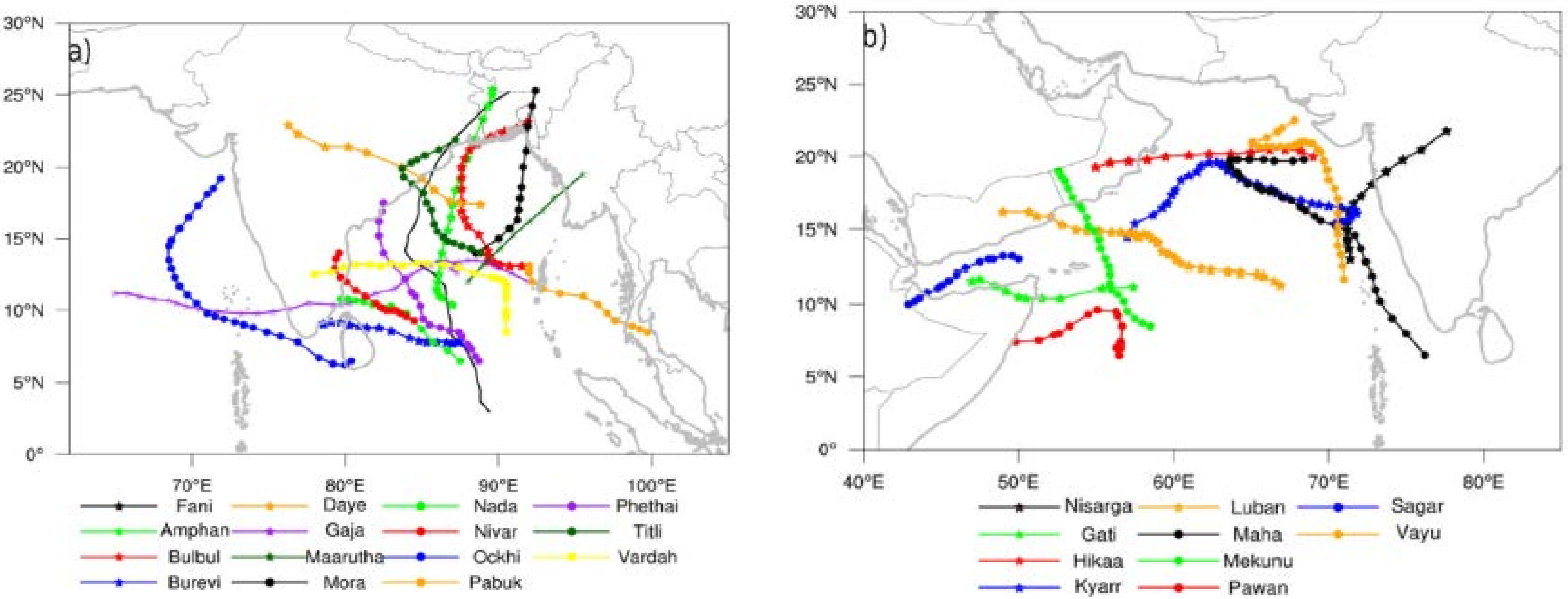

Pavani, G., Bhate, J., Kesarkar, A., Panchal, A., & Krishna, P. V. (2023). Verification of tropical cyclone motion and rainfall forecast over North Indian Ocean. Journal of Earth System Science, 132(3), 114.

Track Errors upto 120 hours of lead time

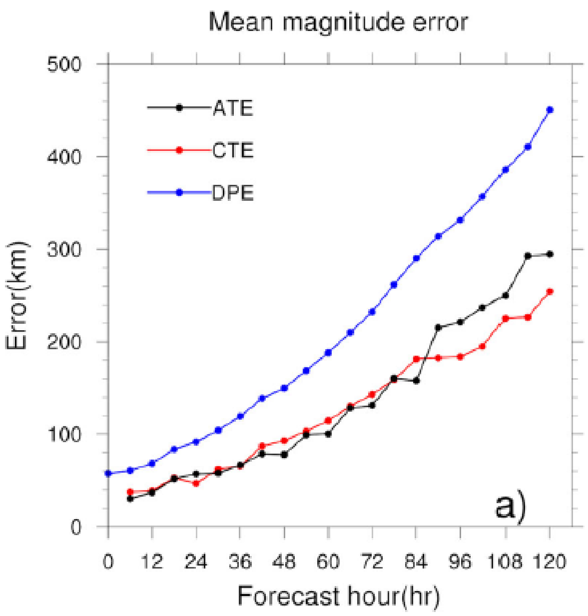

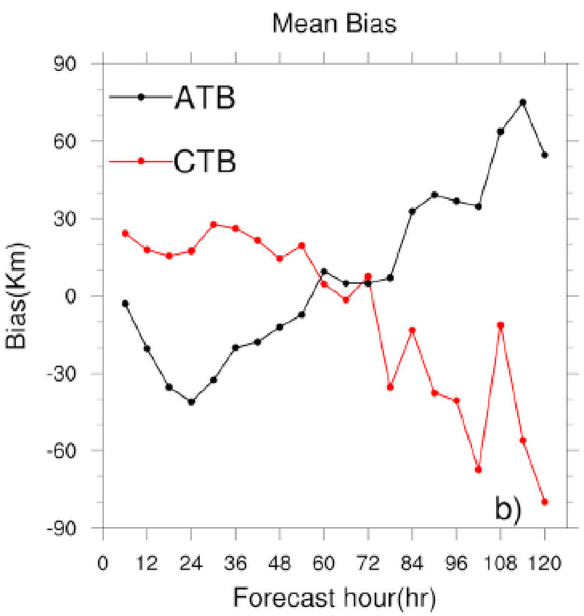

- All the errors increases with the forecast lead time.
- CTE has higher values for most of the lead times before 72 hours and lower values at later lead times compared to ATE.
- The positive bias in CTE indicates that the forecast track is eastward of the observed track till 72-hr lead, time and the negative bias in CTE shows that the forecast track is the west side of the observed track for further lead time.
- The negative bias in AT (across-track) indicates that forecast track is behind the observed track) till 72-hr and the positive bias shows that the forecast track is ahead of the observed track for the higher lead time.

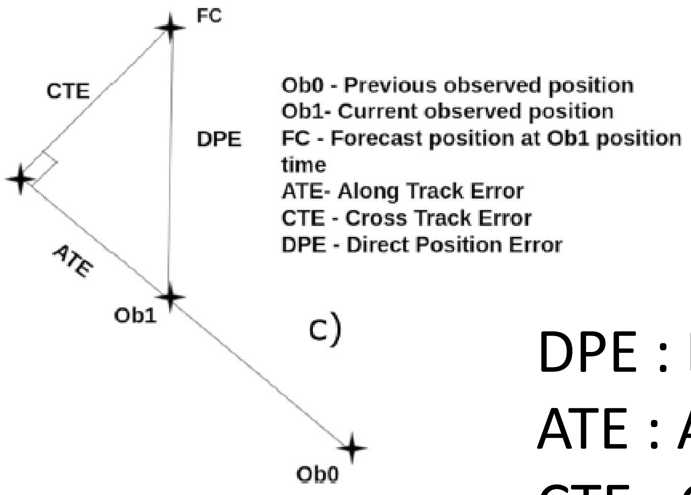

DPE : Direct Position Error (km)
ATE : Across Track Error (km)
CTE : Cross Track Error (km)

Research for Improvement of Operational predictions

- Tropical cyclones
- Thunderstorms
- Western Disturbances
- Impact of Meteorological assimilation on atmospheric chemistry

Multiscale Nature of Tropical Cyclone evolutions

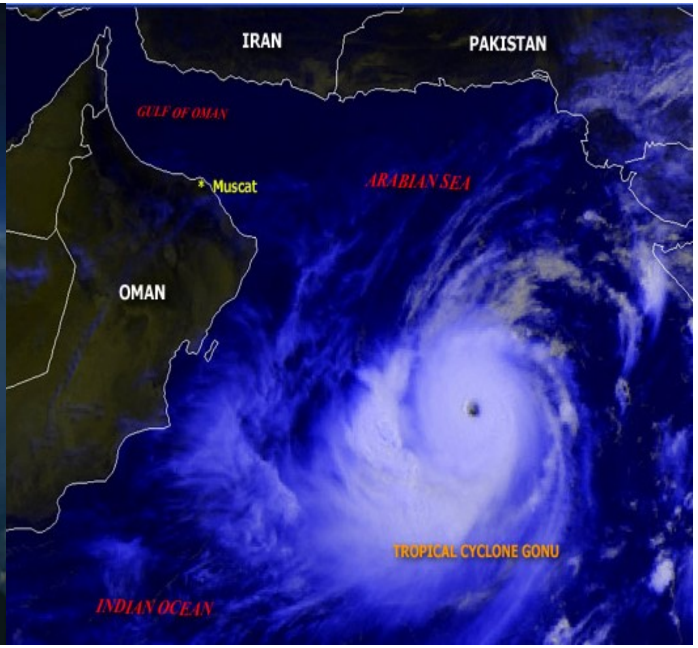

"The pathway by which cumulus convection organizes to form a large scale tropical cyclone vortex is an unsolved problem in dynamic and tropical meteorology"

Hendrics et al. 2004,
Montgomery et al. 2006

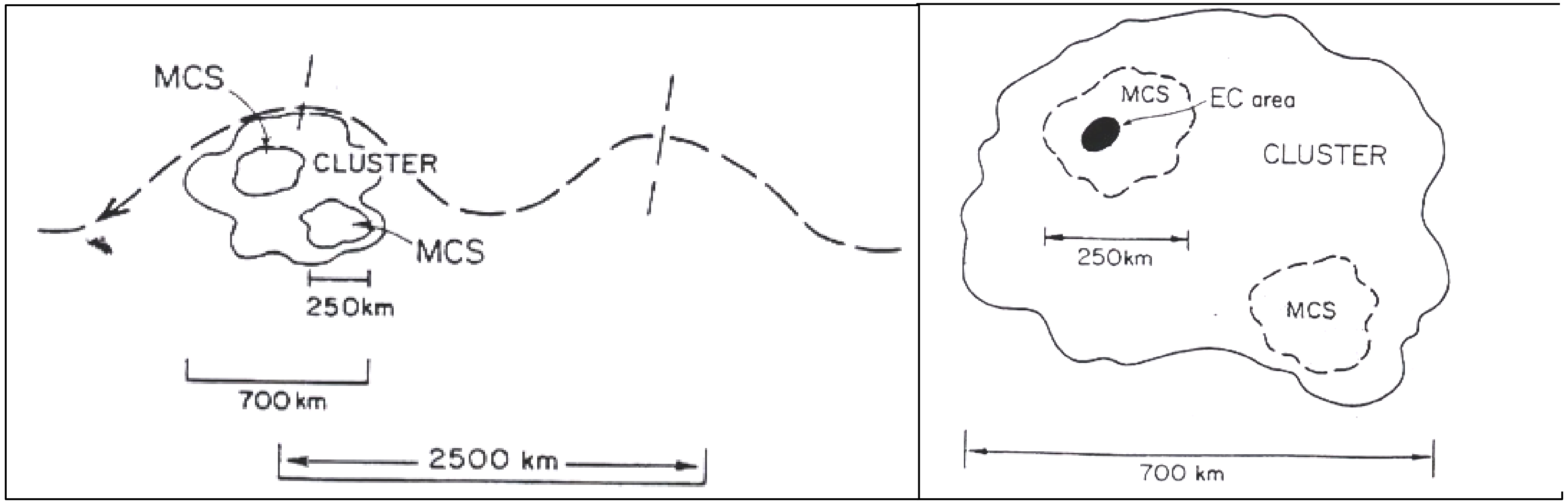

Gray, 1998

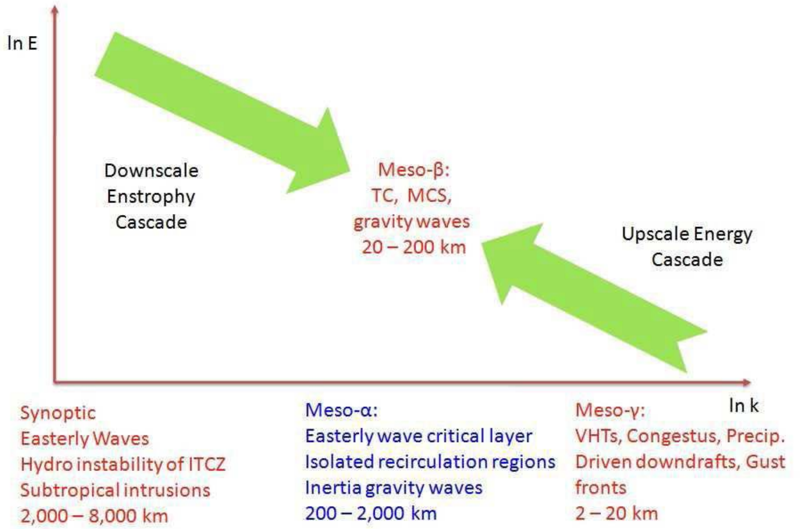

DMW 2009, Fig.:Ref Montgomery and Smith

Cyclone Agni High Resolution (1km) Simulation - Nudging

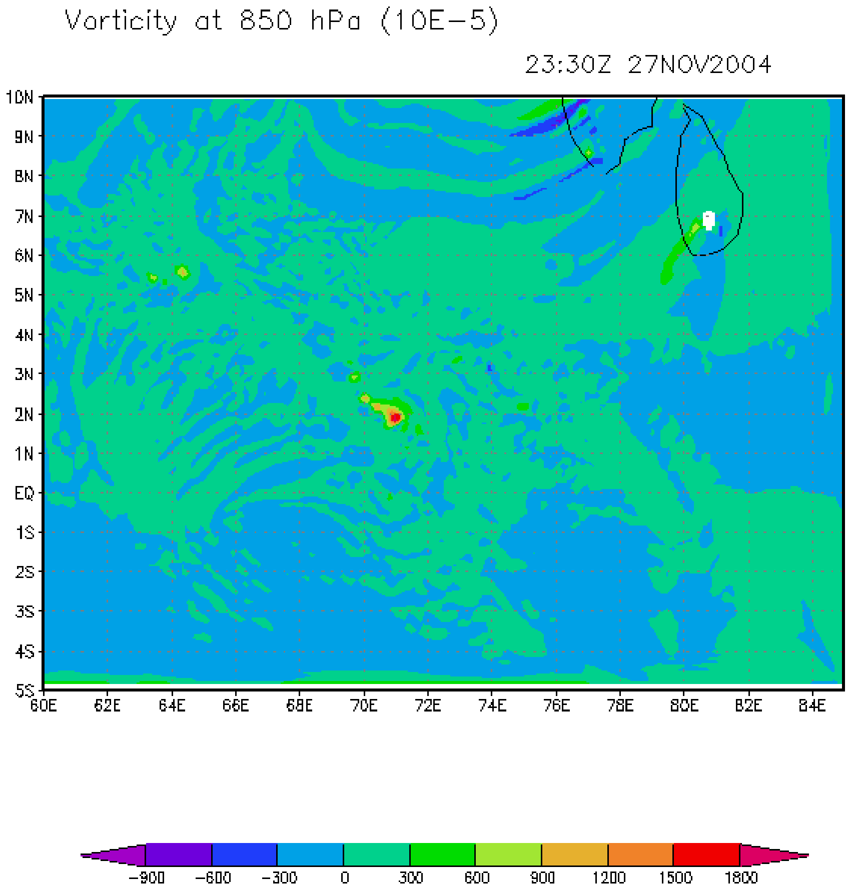

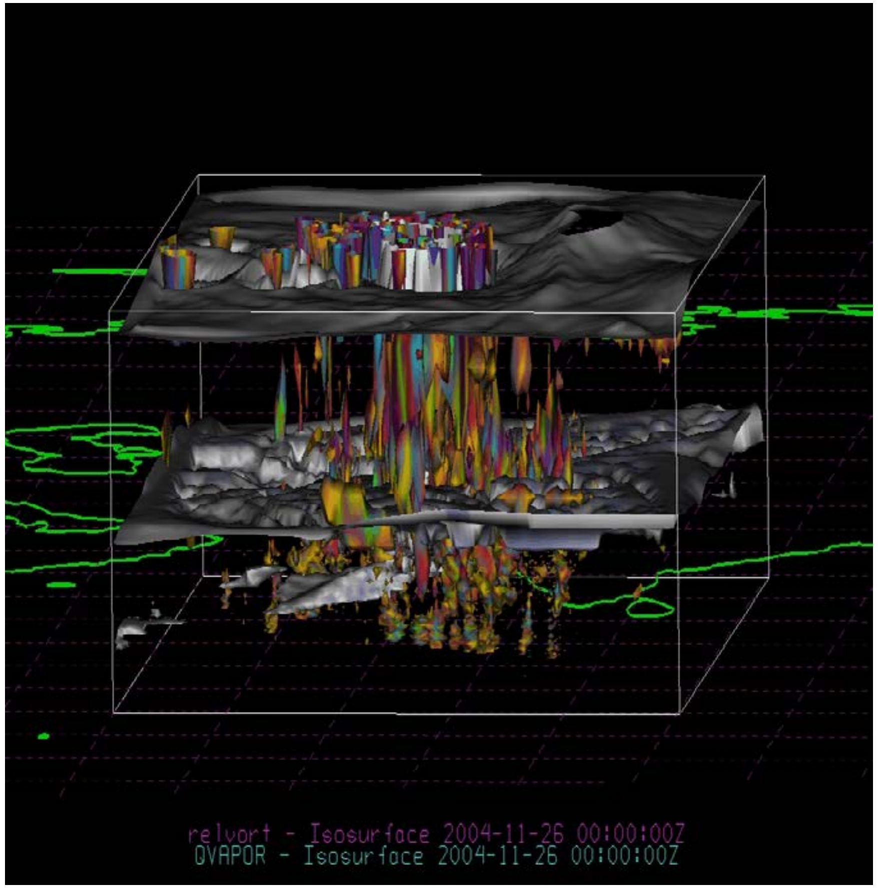

Kesarkar et al. 2006, Genesis of tropical cyclone Agni: Physical Mechanisms,
http://www2.mmm.ucar.edu/wrf/users/workshops/WS2006/abstracts/PSession03/P3_2_Kesarkar.pdf

Dynamical Downscaling-Tropical Cyclogenesis

Very Severe Cyclonic Storm Phailin (8-14 October 2013)

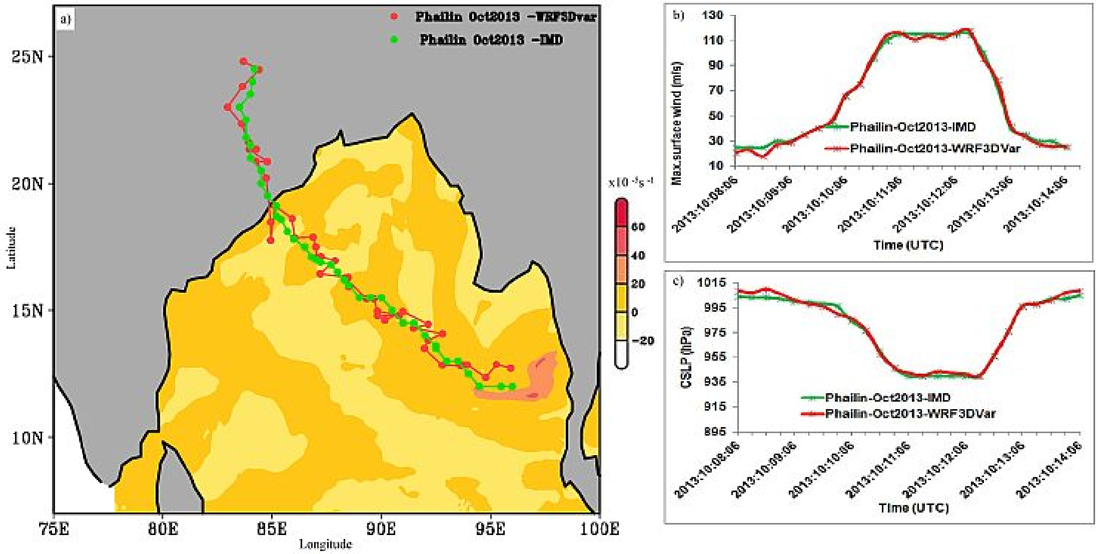

Very Severe Cyclonic Storm Lehar: 23-28 November 2013

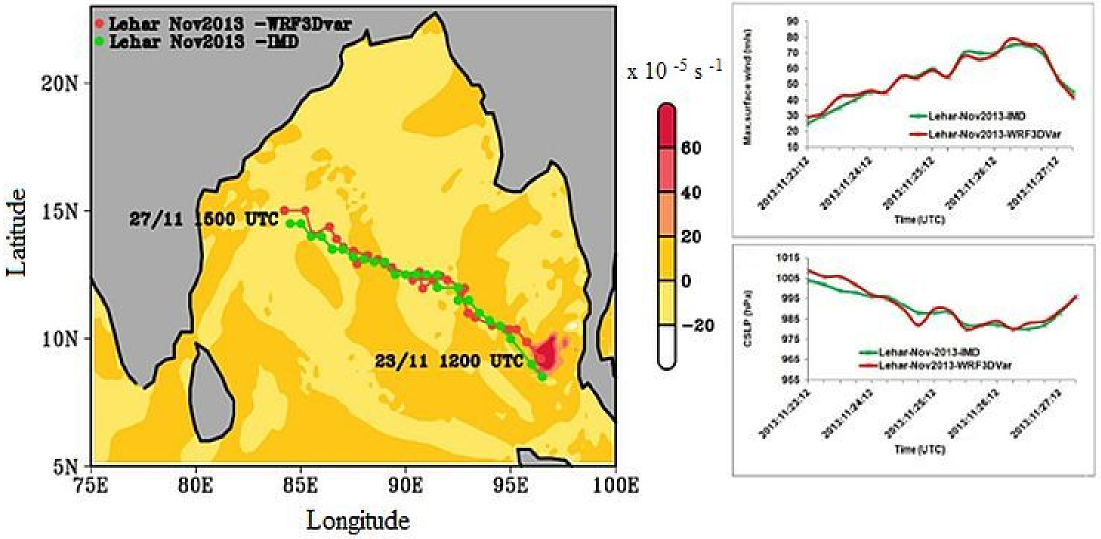

Very Severe Cyclonic Storm Madi: 6-13 December 2013

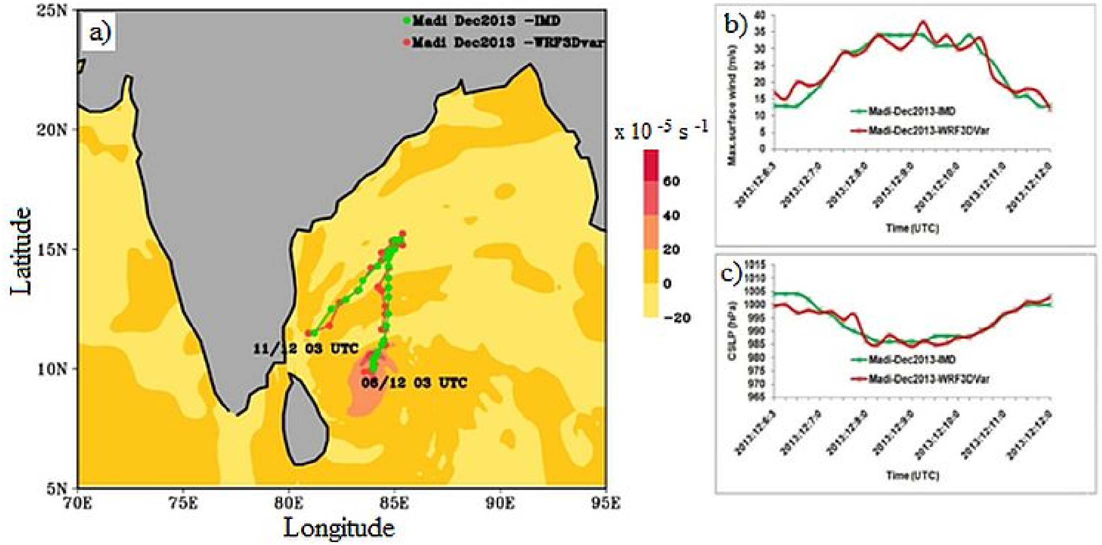

Very Severe Cyclonic Storm-Hudhud 7-14 October 2014

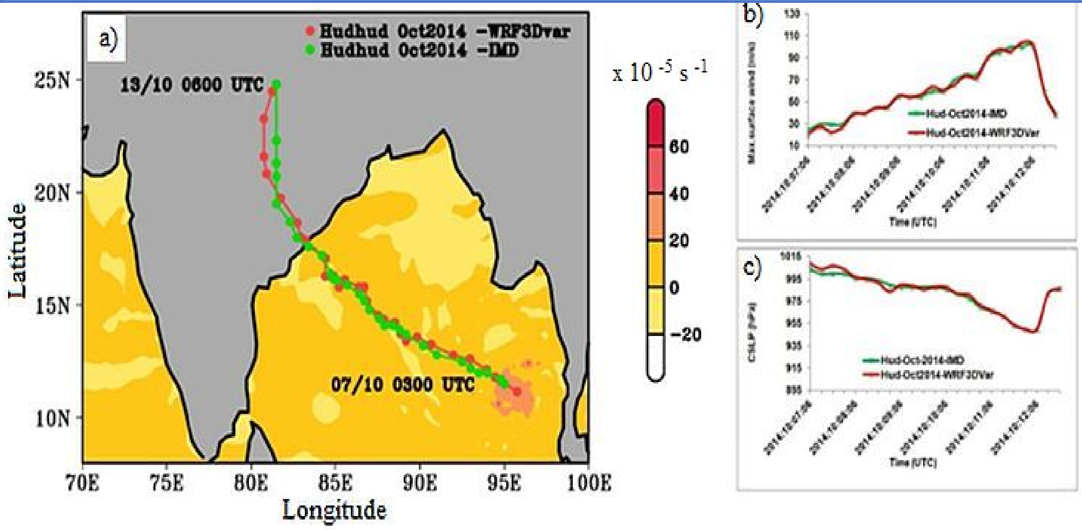

Rajasree et al. 2017a,b JGR Atmosphere

Presence of VHTs in the pre-genesis environment

Phailin

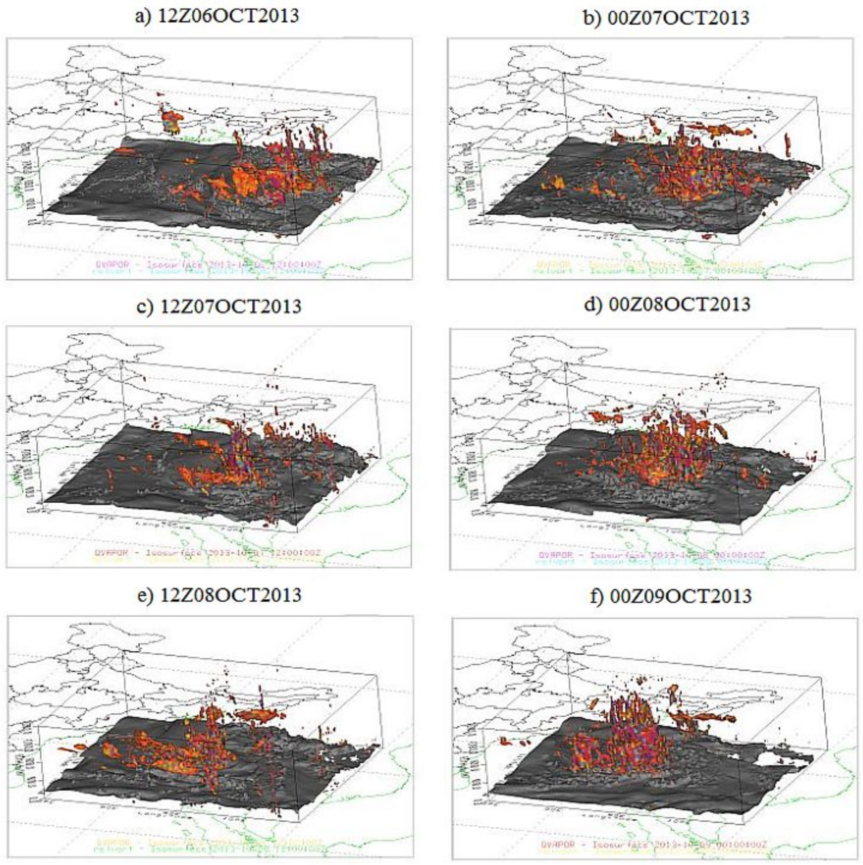

Lehar

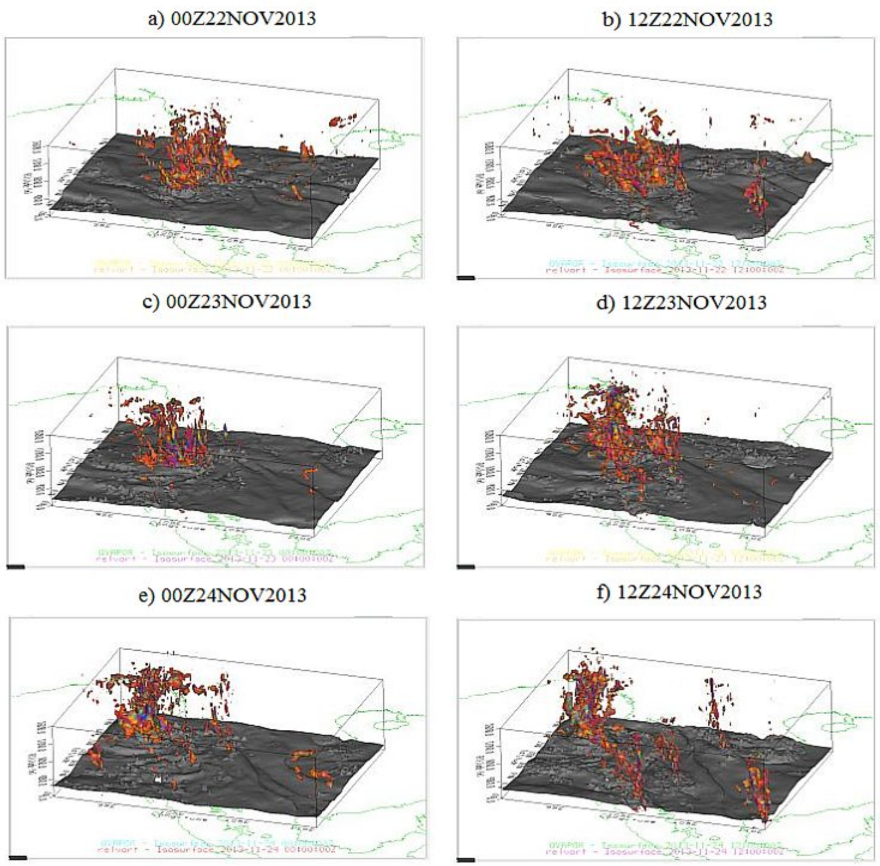

Relative vorticity iso-surface tilts from west to east with height

Rajasree, V. P. M., A. P. Kesarkar, J. N. Bhate, U. Umakanth, V. Singh, and T. Harish Varma (2016), Appraisal of recent theories to understand cyclogenesis pathways of tropical cyclone Madi (2013), J. Geophys. Res. Atmos., 121, 8949–8

Presence of VHTs in the pre-genesis environment

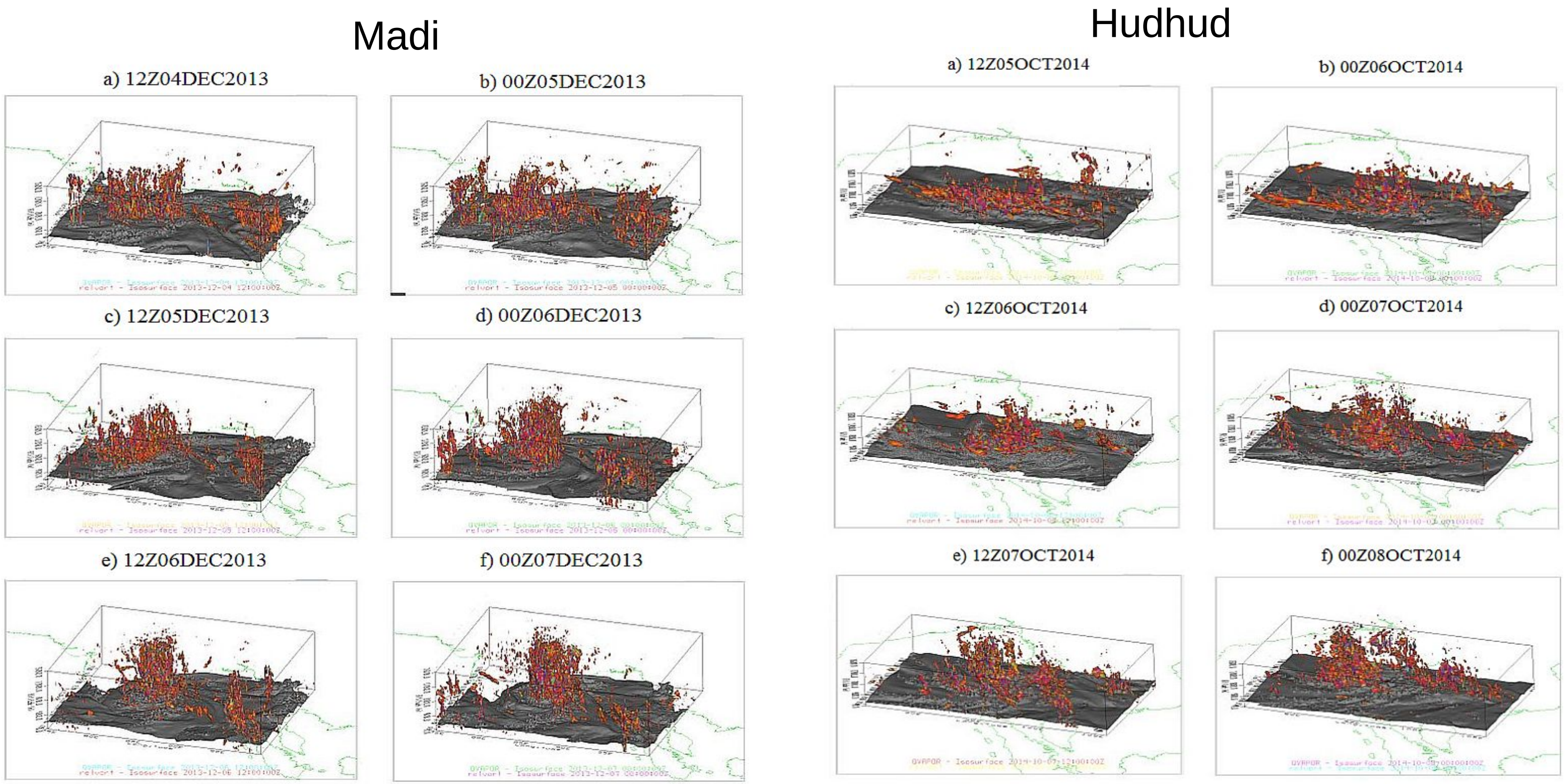

VHTs are found be more vigorous as the genesis nears

Rajasree, V. P. M., A. P. Kesarkar, J. N. Bhate, U. Umakanth, V. Singh, and T. Harish Varma (2016), Appraisal of recent theories to understand cyclogenesis pathways of tropical cyclone Madi (2013), J. Geophys. Res. Atmos., 121, 8949–8

Florence 3-12 September 2006; Very Severe Cyclonic Storm

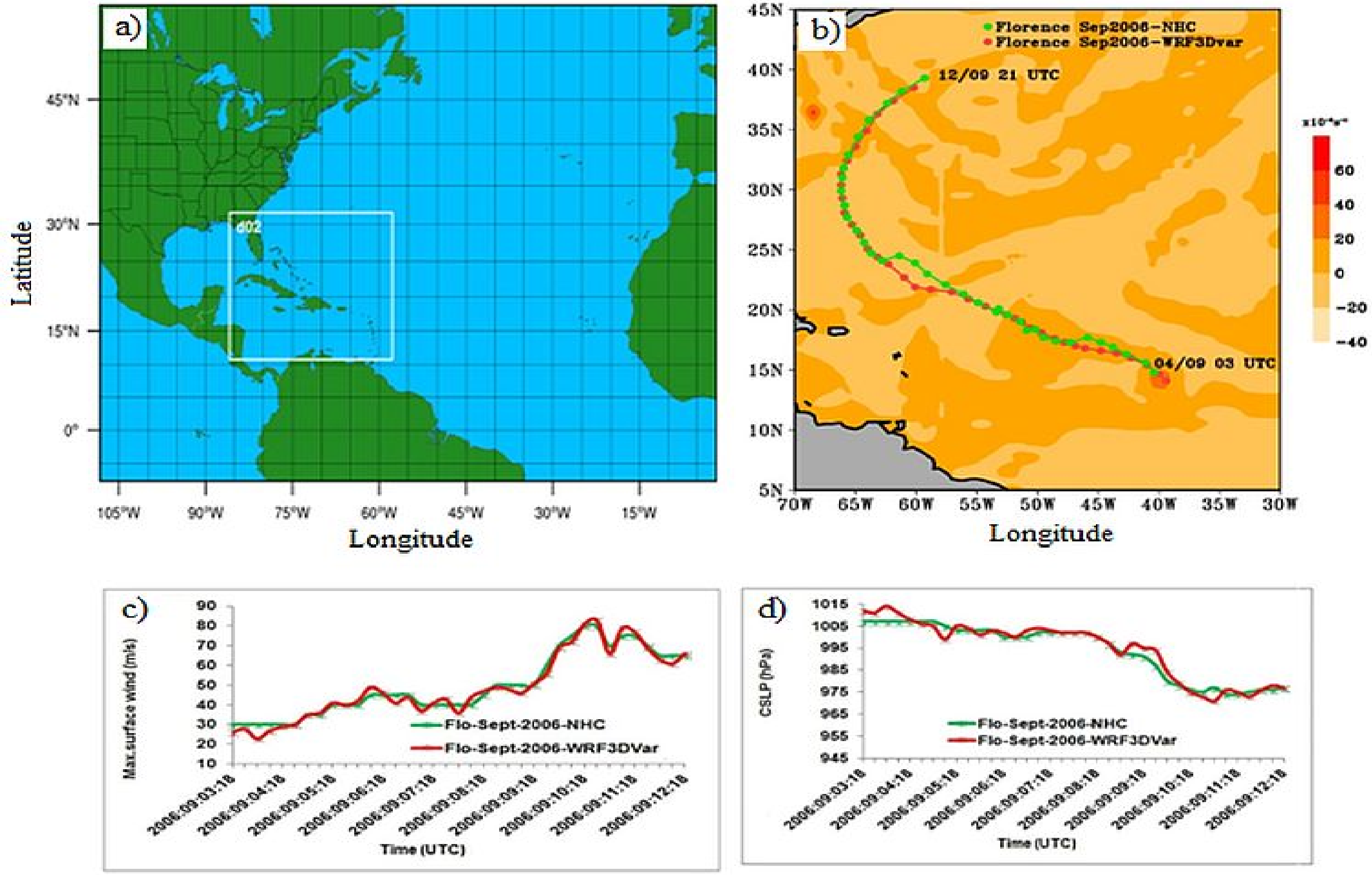

Dry air intrusion into the core of the vortex of Florence cyclone causing delay in intensification

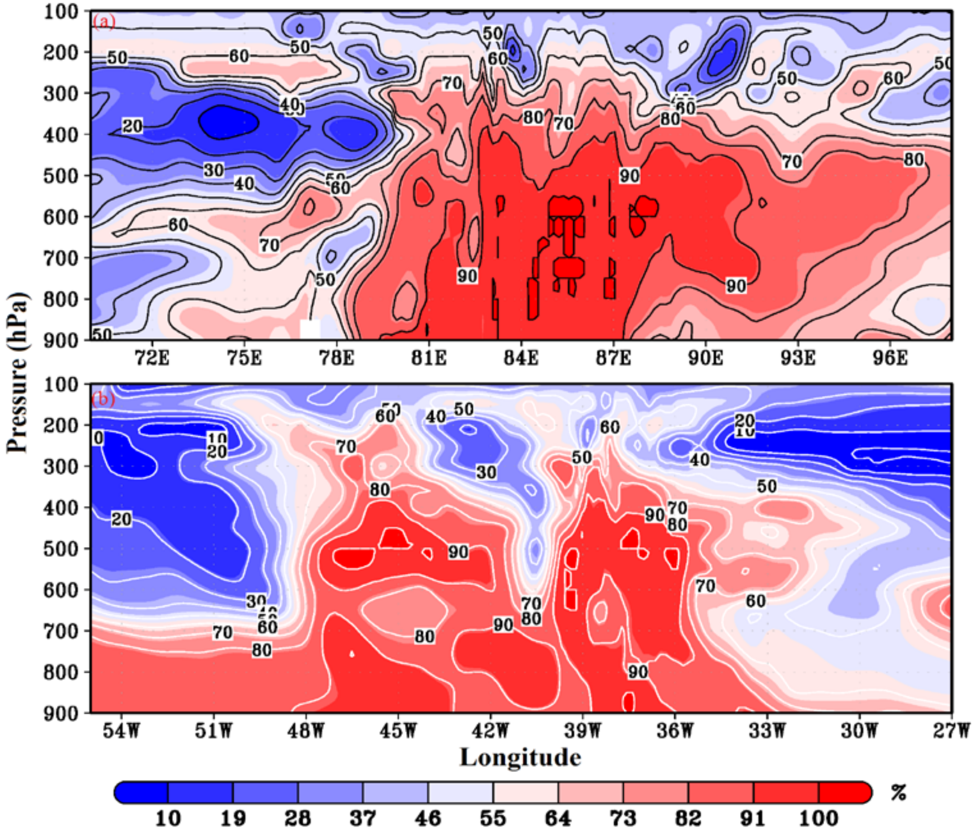

- Comparison of Bay of Bengal Cyclone with Atlantic Ocean Cyclone
- Madi and Florence originated from westward moving disturbances

Rajasree, V. P. M., A. P. Kesarkar, J. N. Bhate, V. Singh, U. Umakanth, and T. Harish Varma (2016), A comparative study on the genesis of North Indian Ocean tropical cyclone Madi (2013) and Atlantic Ocean tropical cyclone Florence (2006), *J. Geophys. Res. Atmos.*, 121, 13,826–13,858, doi:10.1002/2016JD025412.

Dynamical Downscaling-Tropical Cyclone Evolution

Rapid Intensification and Eyewall replacement cycle

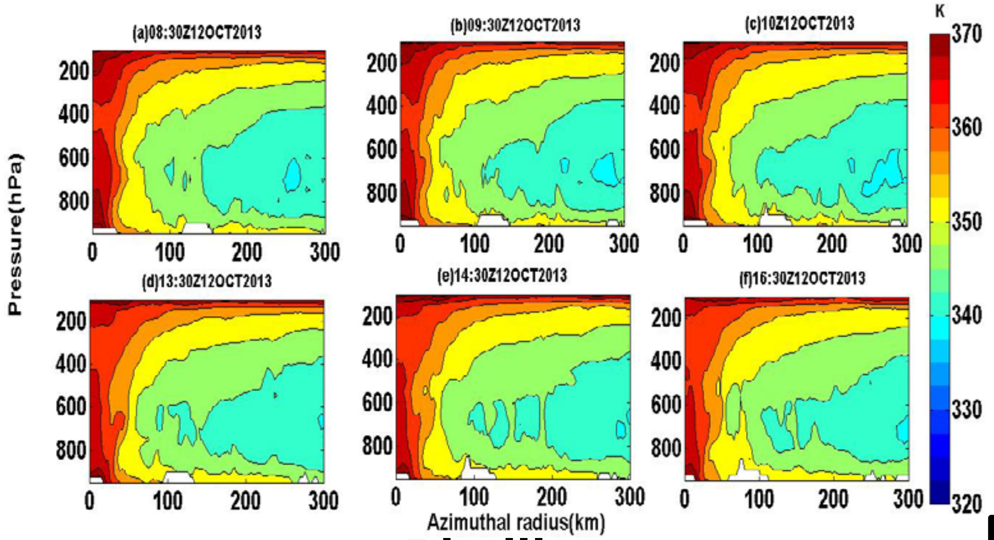

Phailin

- The analysis of vorticity indicated that solenoidal term played a crucial role in the development of secondary eyewall.
- The secondary maxima was observed in the wind speed. The angular momentum budget is being analysed to understand the mesoscale processes causing inner eyewall to rotate faster than the outer eyewall.

Impact of Dust on Rapid weakening of Tropical Cyclone Lehar

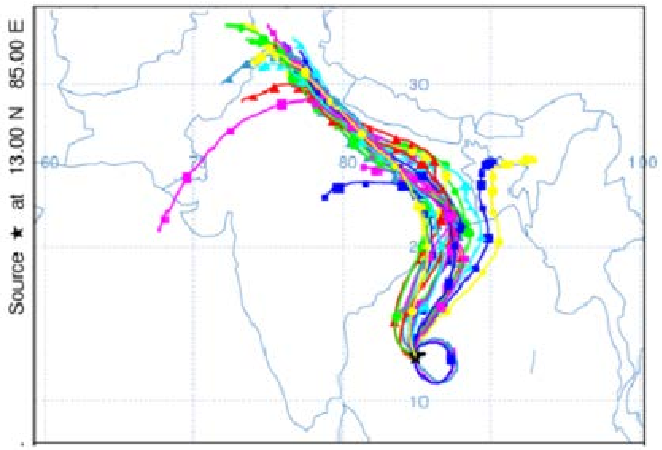

The dry air advection from the north of the storm is found to be a primary contributor for the weakening along with high deep layer shear in the weakening environment.

- The dry mass intrusion in boundary layer / lower tropospheric levels for intensified cyclones cause the rapid weakening and hence decay of the cyclone.
- Dry air intrusion in the spiral bands in lower tropospheric levels cause rapid weakening followed by dissipation of tropical cyclones.

OCKHI

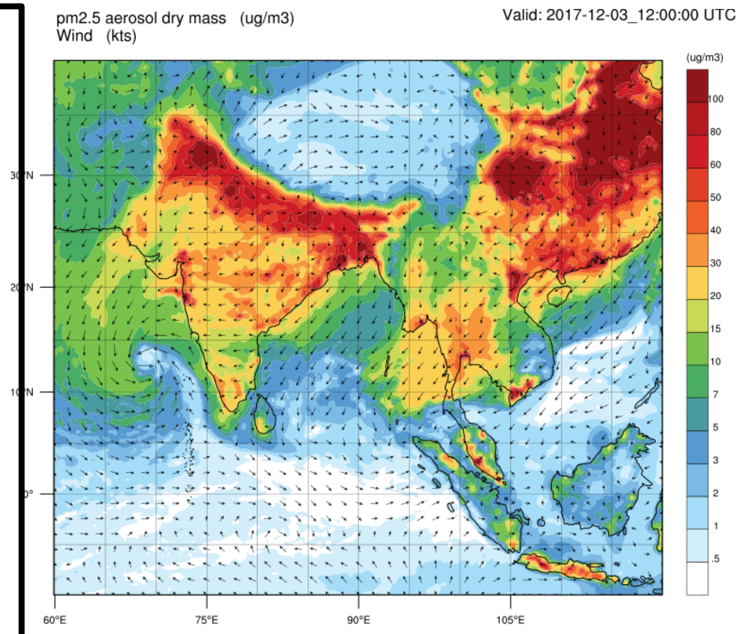

Appraisal of Reanalysis Datasets

Aim: Comparison of reanalysis dataset with respect to structure and intensity representation of tropical cyclone over North Indian Ocean

- ❖ Which global reanalysis/analysis dataset provides the better representation of TCs structure and intensity over NIO?
- ❖ Why do we need high-resolution downscaling?

Malakar, P., Kesarkar, A. P., Bhate, J. N., Singh, V., & Deshamukhya, A. (2020). Comparison of reanalysis data sets to comprehend the evolution of tropical cyclones over North Indian Ocean. *Earth and Space Science*, 7, e2019EA000978. https://doi.org/10.1029/2019EA000978

Appraisal of Reanalysis Datasets

- Global reanalysis datasets have coarse resolution which range between 0.5°x0.5° and 0.125°x0.125°. They can be used in regional weather prediction models as initial and boundary conditions. They are also used for understanding different physical mechanisms associated with tropical cyclone (TC) evolution and to understand the role of environmental factors associated with TC evolution.
- Although reanalysis datasets provide complete spatial and temporal data coverage over long time period and are used to study different climatological aspects of TCs, a good representation of TCs in reanalysis data is important in order to use these datasets to understand TCs interaction with climate system.
- We have compared four reanalysis datasets for evaluating the representation of track, intensity and structure of 28 TC occurred over northern Indian Oceans during 2006-2015.
- Aim of this study is to find out the best representation of TCs evolution in reanalysis datasets Over North Indian Ocean.

ECMWF ERA-Interim reanalysis. (0.125^{o}X0.125^{o})

JRA55 55-year reanalysis project (0.5^{o}X0.5^{o})

Modern-Era Retrospective analysis for research and applications, version 2 (MERRA-2) reanalysis (0.5^{o}X0.5^{o})

Global Forecast System (GFS) analysis produced by NCEP (0.5^{o}X0.5^{o}

IMD best track dataset

Malakar et al. 2020, Earth and Space Science

Track, Intensity and MSLP errors

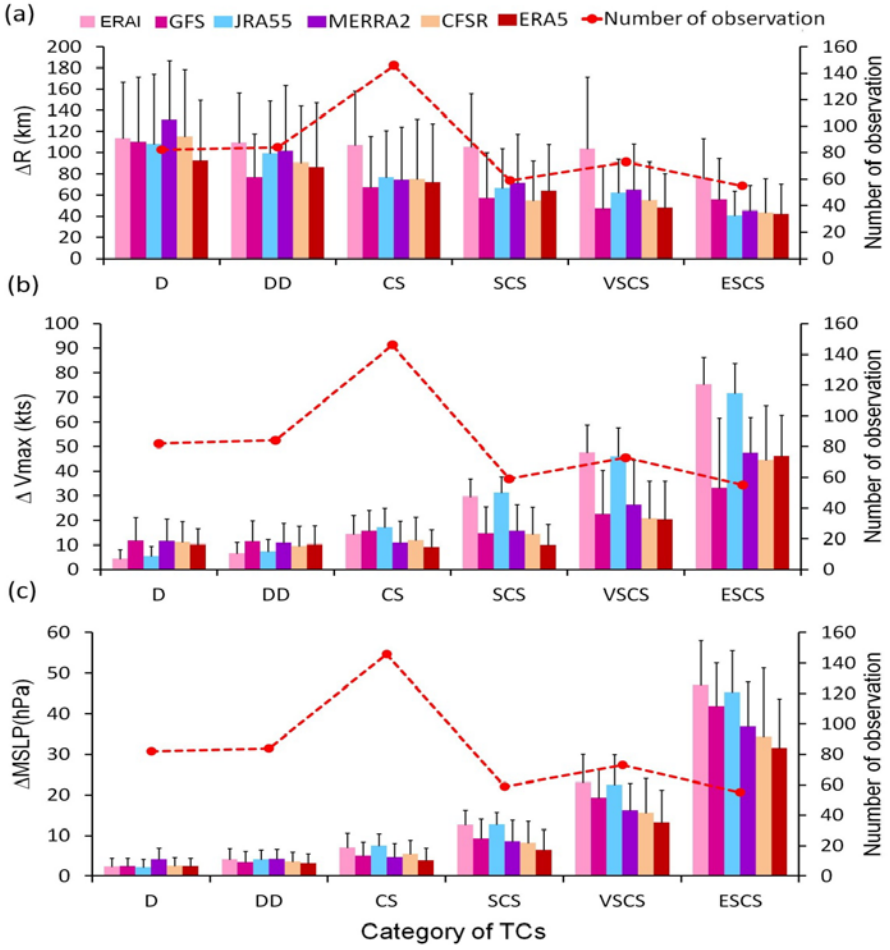

Contingency table for Intensity Prediction

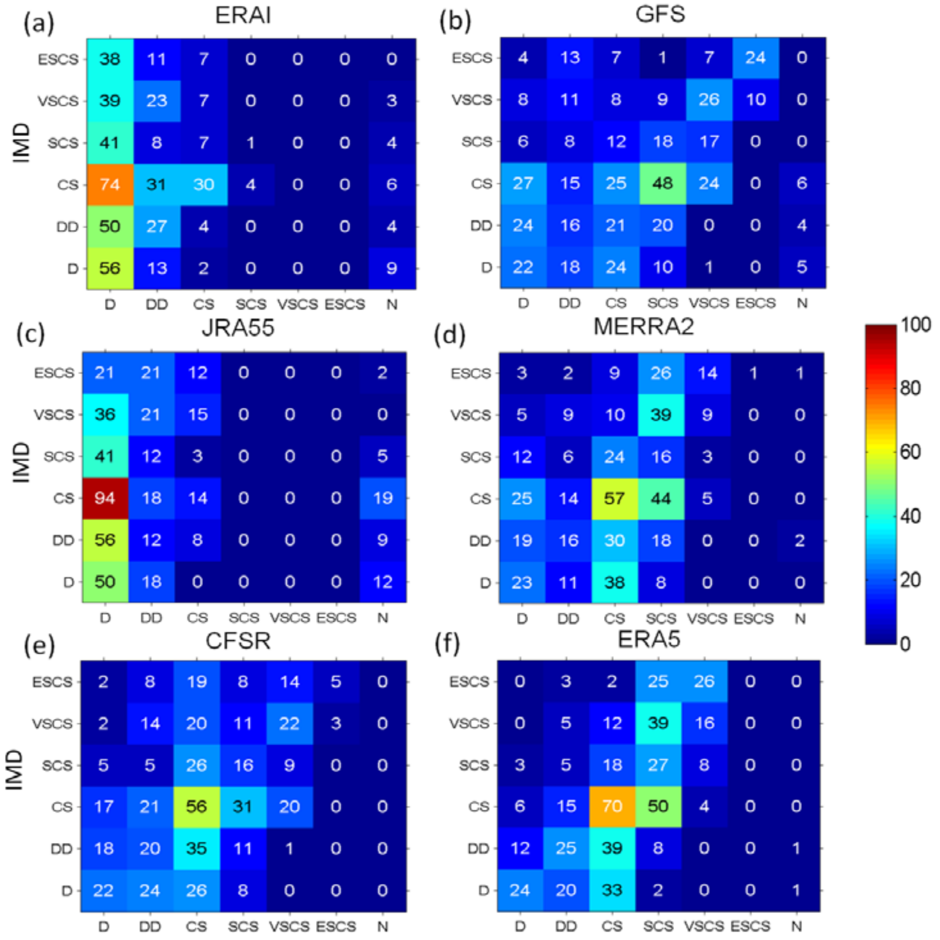

- Errors in track (intensity and MSLP) increase (decrease) with the intensification of TCs
- Overall Track error is minimum in GFS analysis followed by ERA5 and CFSR reanalysis respectively.
- Overall error in MSLP and Vmax are minimum in ERAI at weak stage (D and DD) in ERA5 during intensified stages (CS, SCS, VSCS) , in GFS during ESCS stage followed by CFSR dataset.

- ERAI and JRA55 mostly underestimate the intense stages of TCs to CS stage.
- Only MERRA2 , GFS analysis and CFSR are able to represent TC's ESCS intensity stage
- ERA5 is able to represent TC's Intensity till VSCS stage appropriately and more accurately in CS stages

Diabatic heating

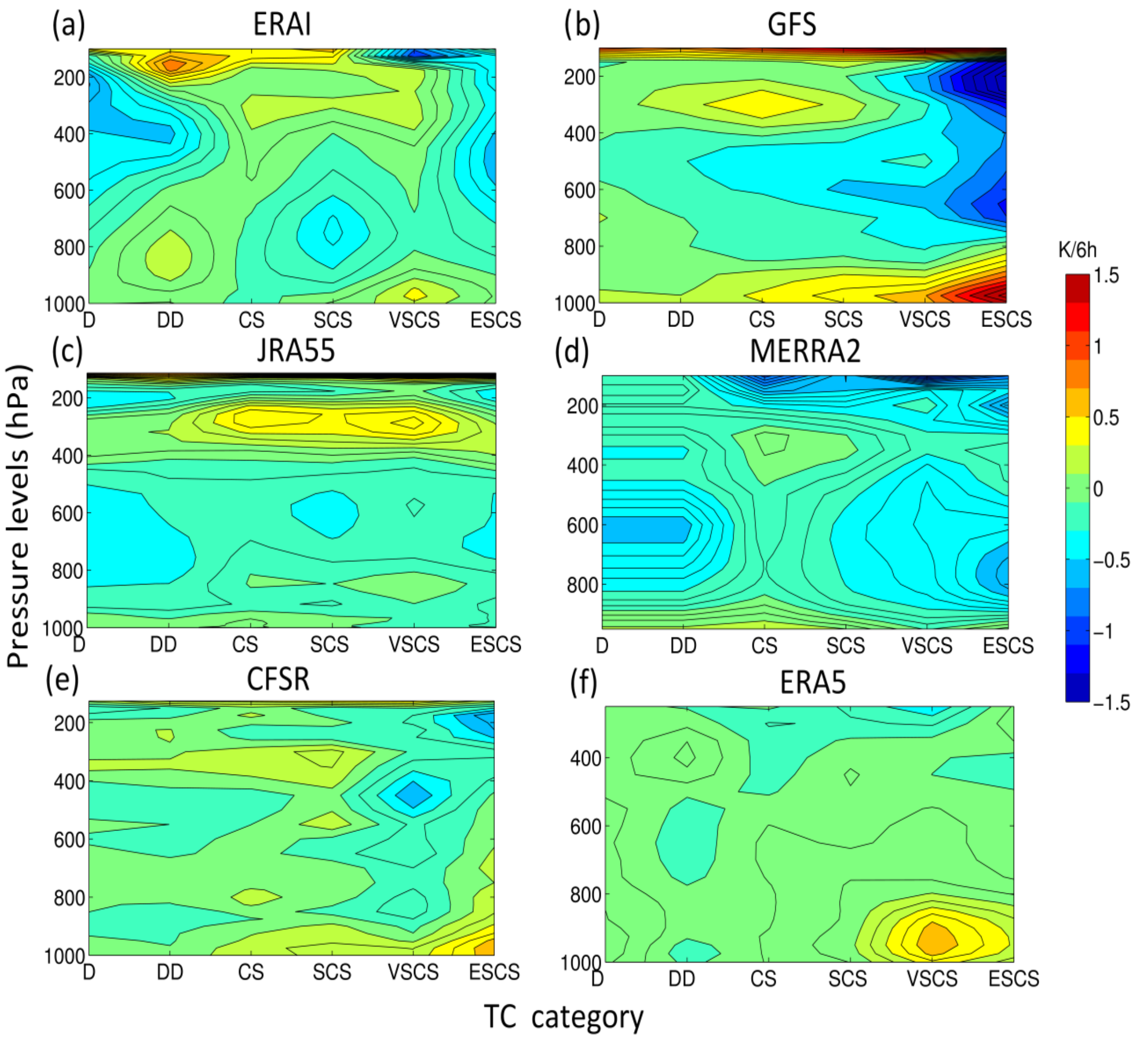

Horizontal wind

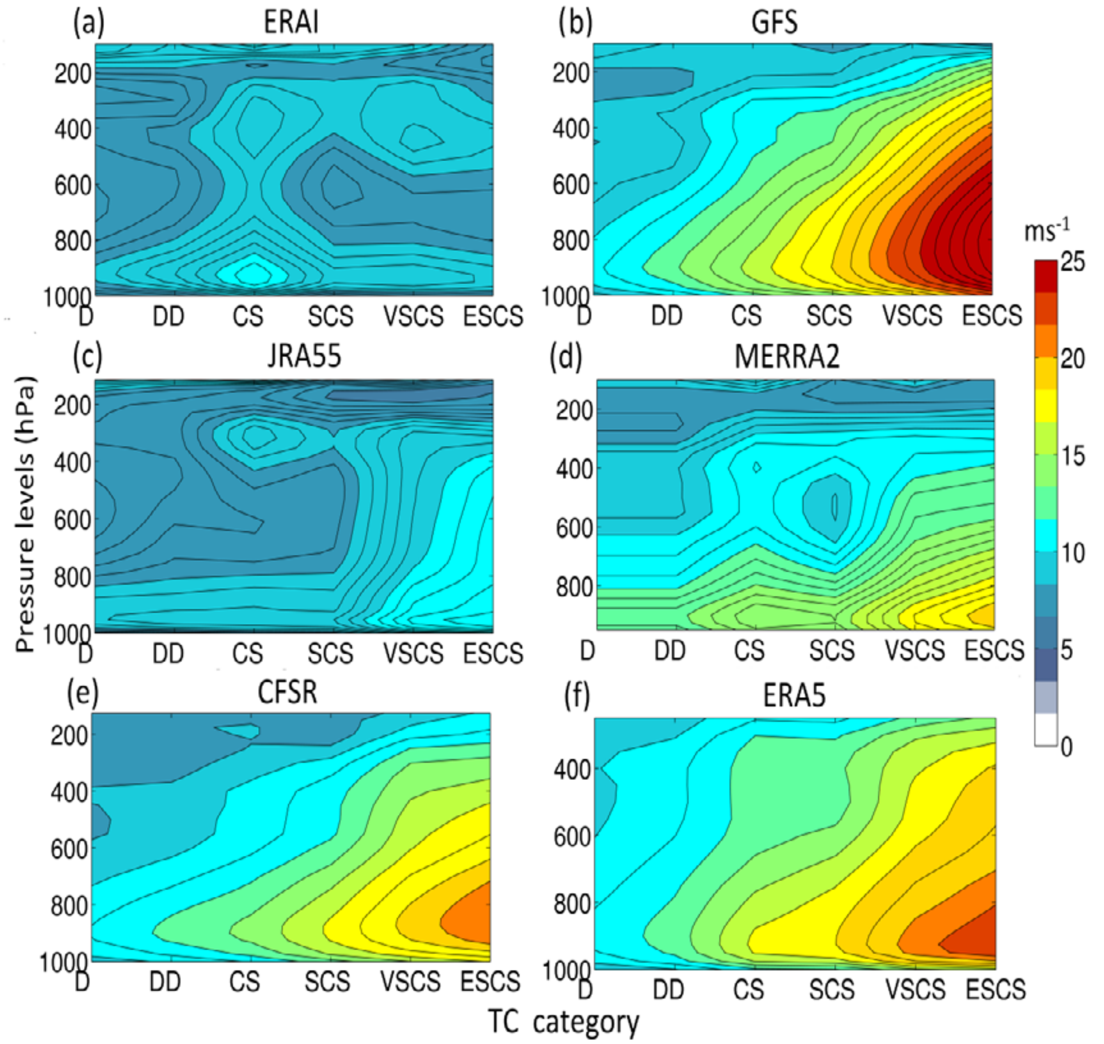

- **Diabatic heating is better represented in GFS analysis followed by CFSR and ERA5 reanalysis.**
- **GFS analysis captures the horizontal wind structure of TCs more realistically, followed by ERA5, CFSR, and MERRA2, respectively.**

Relative Vorticity

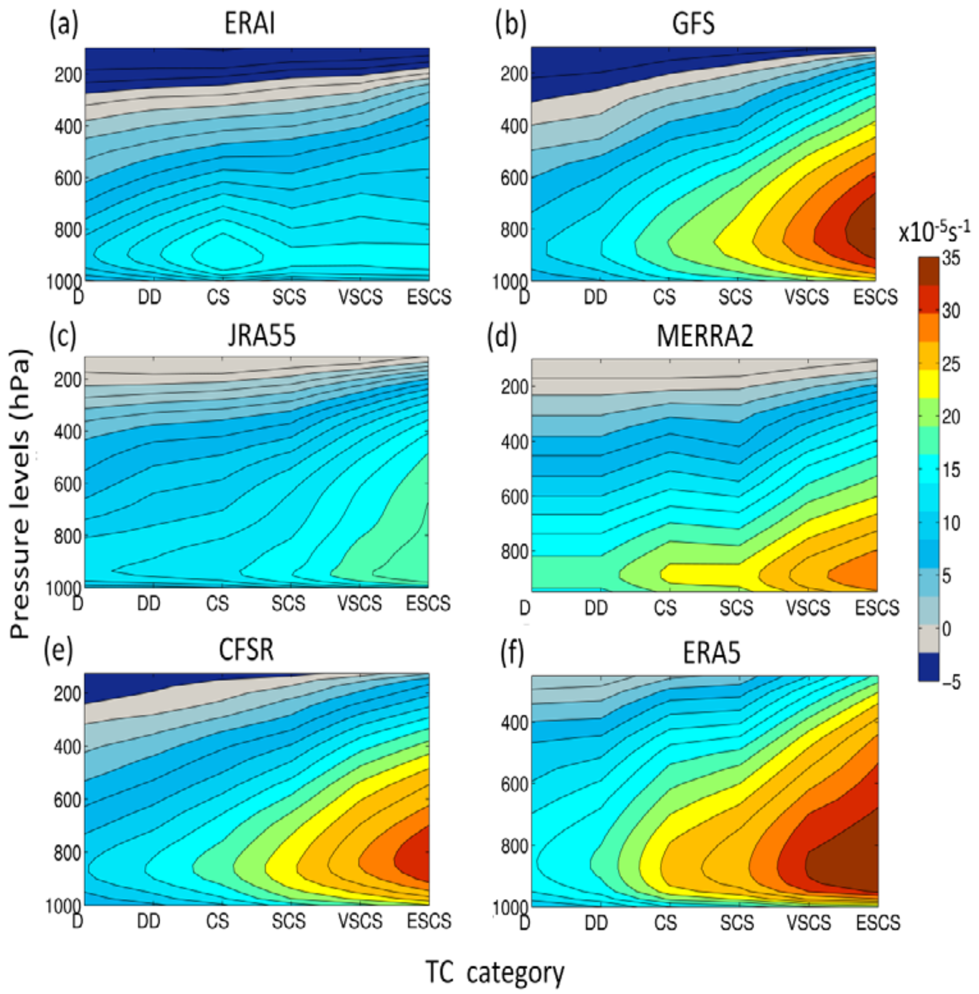

Convergence

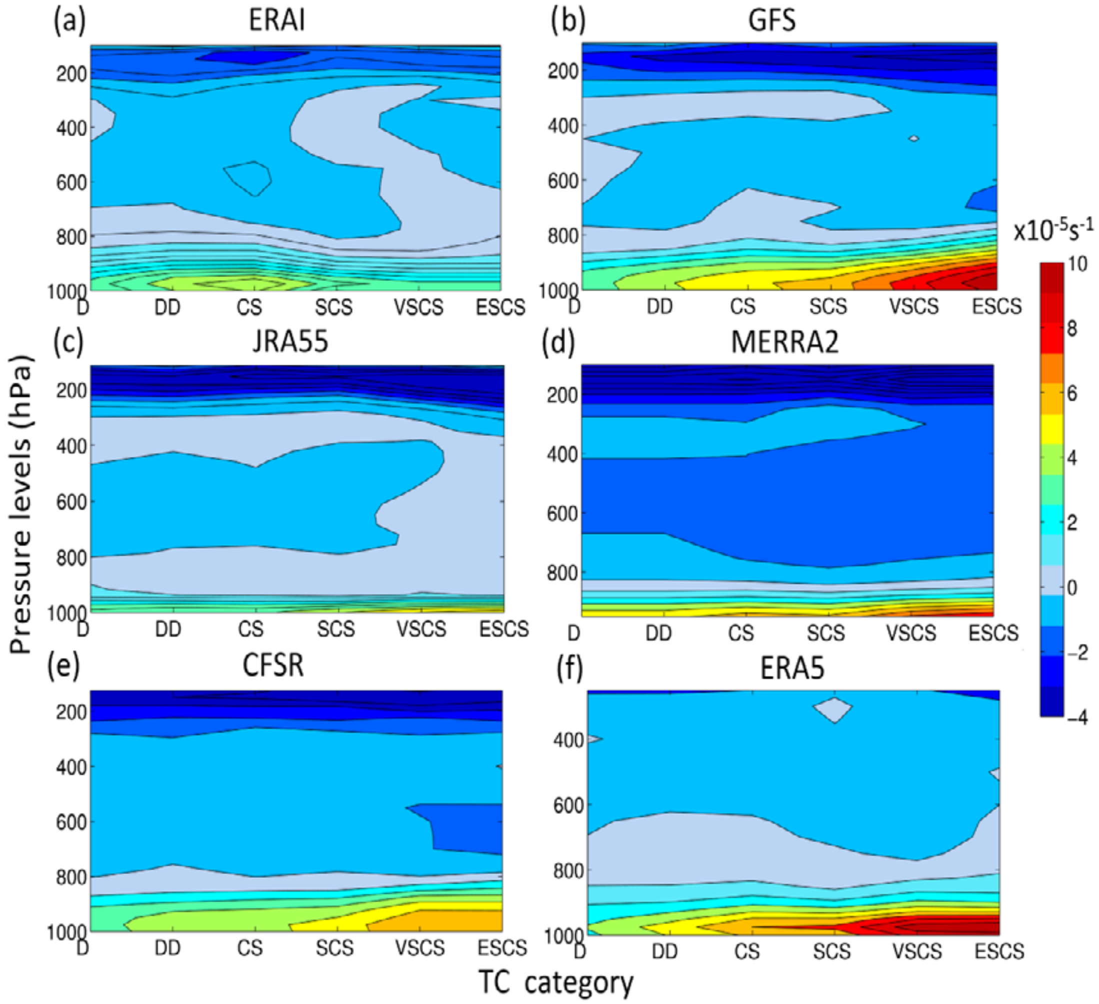

- GFS analysis captures the relative vorticity structure of TCs more realistically, followed by ERA5, CFSR, and MERRA2, respectively.
- GFS analysis captures lower-level convergence and upper-level divergence of TCs more realistically, followed by ERA5, CFSR, and MERRA2, respectively.

Summary of the paper

- Overall track error is minimal in GFS analysis, followed by ERA5 and CFSR reanalysis, respectively.
- GFS and CFSR better represent TC’s intensity since this dataset can only capture the highest intensity stage.
- Composite structure shows the significant improvement of ERA5 over ERAI in TCs structure and intensity (from contingency table) representation.
- Dynamical downscaling is crucial for obtaining a better representation of TCs to study the physical mechanisms involved in their evolution.
- GFS analysis is better than the other 5 reanalysis datasets to provide initial and boundary conditions in the mesoscale-model for TC simulation over NIO.

Data Assimilation techniques: Which Technique better?

Sensitivity of simulation of intensity and structure of tropical cyclones to data assimilation

- Which DA techniques improve initial conditions and provide better track and intensity simulation of TCs?
- Which simulation captures the rapid intensity change and the structure of TCs more accurately?

Malakar, P., Kesarkar, A. P., Bhate, J. N., Singh, V., & Deshamukhya, A. (2020). Comparison of reanalysis data sets to comprehend the evolution of tropical cyclones over the North Indian Ocean. *Earth and Space Science*, 7, e2019EA000978. https://doi.org/10.1029/2019EA000978

Data Assimilation techniques: Which Technique better?

Data assimilation combines the observations and short range forecasts to determine perfect initial condition

3DVAR

$$J(x) = \frac{1}{2}(x - x_b)^T B^{-1}(x - x_b) + \frac{1}{2}[H(x) - y]^T R^{-1}[H(x) - y]$$

4DVAR

$$J(x_0) = \frac{1}{2}(x_0 - x_0^b)^T B^{-1}(x_0 - x_0^b) + \frac{1}{2}\sum_{i=1}^{N}[H_i(M_i(x_0)) - y_i]^T R_i^{-1}[H_i(M_i(x_0)) - y_i]$$

3DEnVAR

$$J(x_1, \alpha) = \beta_s \frac{1}{2}(x - x_b)^T B^{-1}(x - x_b) + \beta_e \frac{1}{2}\sum_{i=1}^{N} \alpha_i^T C^{-1}\alpha_i + \frac{1}{2}[y - H(x_1 + x_e')]^T R^{-1}[y - H(x_1 + x_e')]$$

4DEnVAR

$$J(x_1, \alpha) = \beta_s \frac{1}{2}(x - x_b)^T B^{-1}(x - x_b) + \beta_e \frac{1}{2}\sum_{i=1}^{N} \alpha_i^T C^{-1}\alpha_i + \frac{1}{2}\sum_{k=1}^{K}[y_k - H_k(x_1 + x_{e,k}')]^T R_k^{-1}[y_k - H_k(x_1 + x_{e,k}')]$$

Where,

- X_b : background
- y : observation
- **H:** observation operator
- **R:** observation error covariance
- B : background error covariance
- **M:** the forecast model, and the whole assimilation window is split into i observation windows.
- X_0 : the control variable
- **C:** the correlation matrix
- N is the number of observational vectors distributed over time.

$$x_e' = \sum_{i=1}^{N} \alpha_i \cdot x_i'$$

x_i' ensemble perturbation for the i[th] ensemble

α_i ensemble perturbation weight

β_s and β_e Are the weights assigned for the static and ensemble

Appraisal of DA Techniques: **4DVAR, 3DEnVAR and 4DEnVAR**

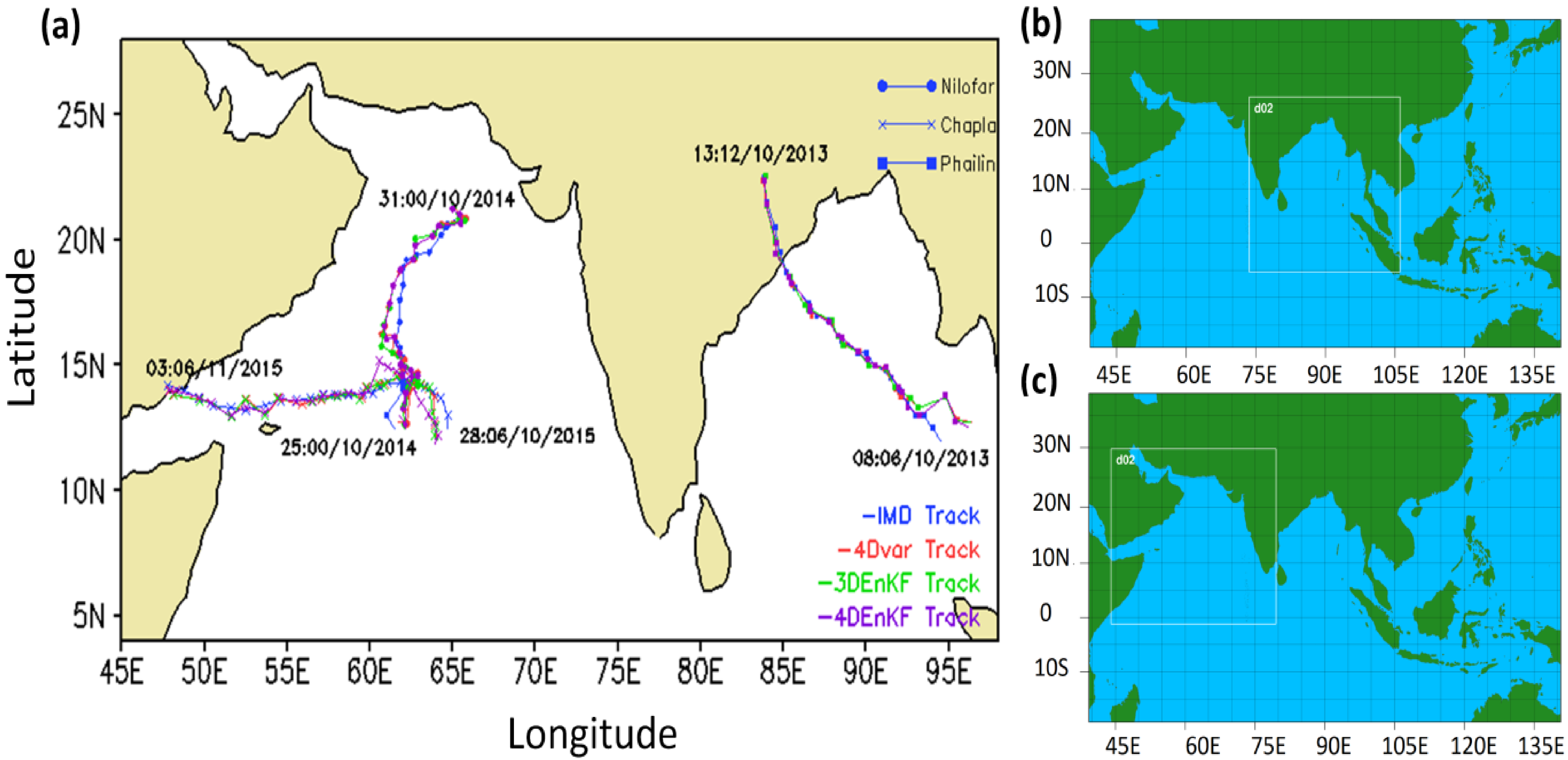

Model Simulated track matched well with IMD best track for all sets of experiments.

Malakar et al. 2020 ESS

Experimental setup

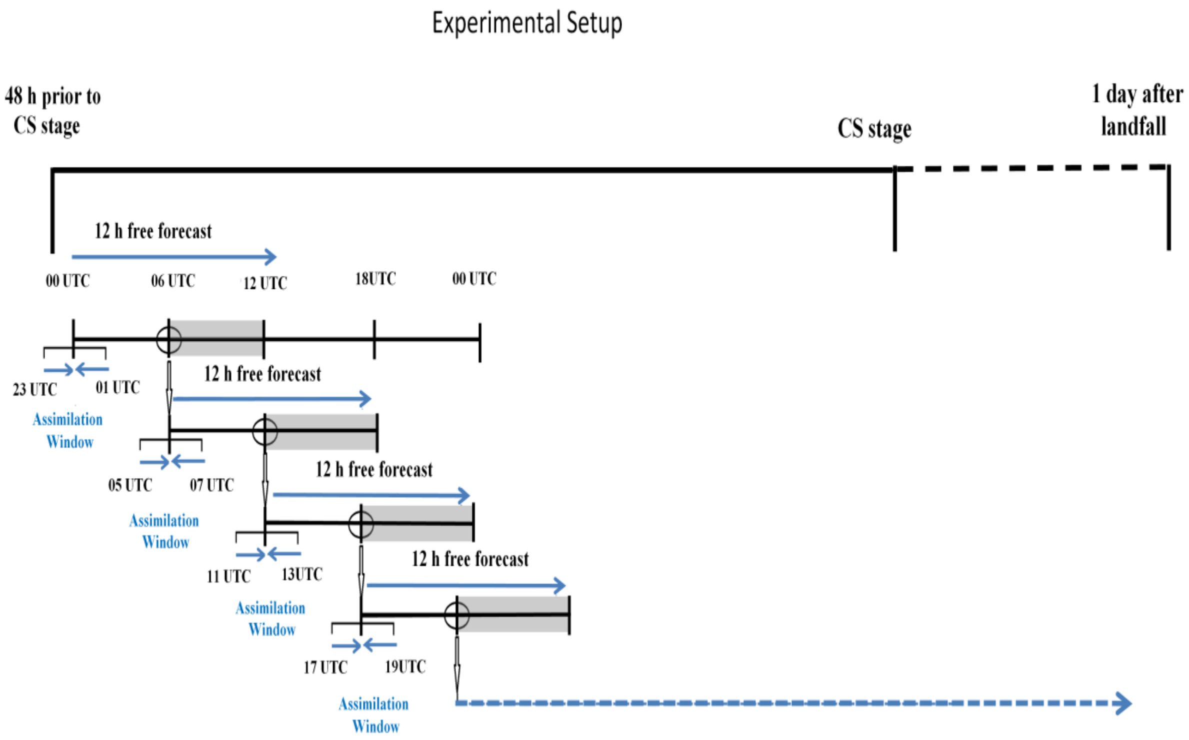

Computational and Information System laboratory

NCAR UCAR

Assimilated observations and satellite radiance (1°X1°)

Radiosonde , pilot balloon, aircraft, ship, buoy, and GPSRO

Satellite Sensors	Satellite Platform
AMSU A	NOAA 15,16,18, EOS Aqua and METOP-2
IASI	NOAA-15, 16, 17
AIRS	NOAA-17,18, and METOP -2
MHS	EOS Aqua

Data assimilation in continuous cyclic mode

IMD and model simulated Radar reflectivity of TC Phailin

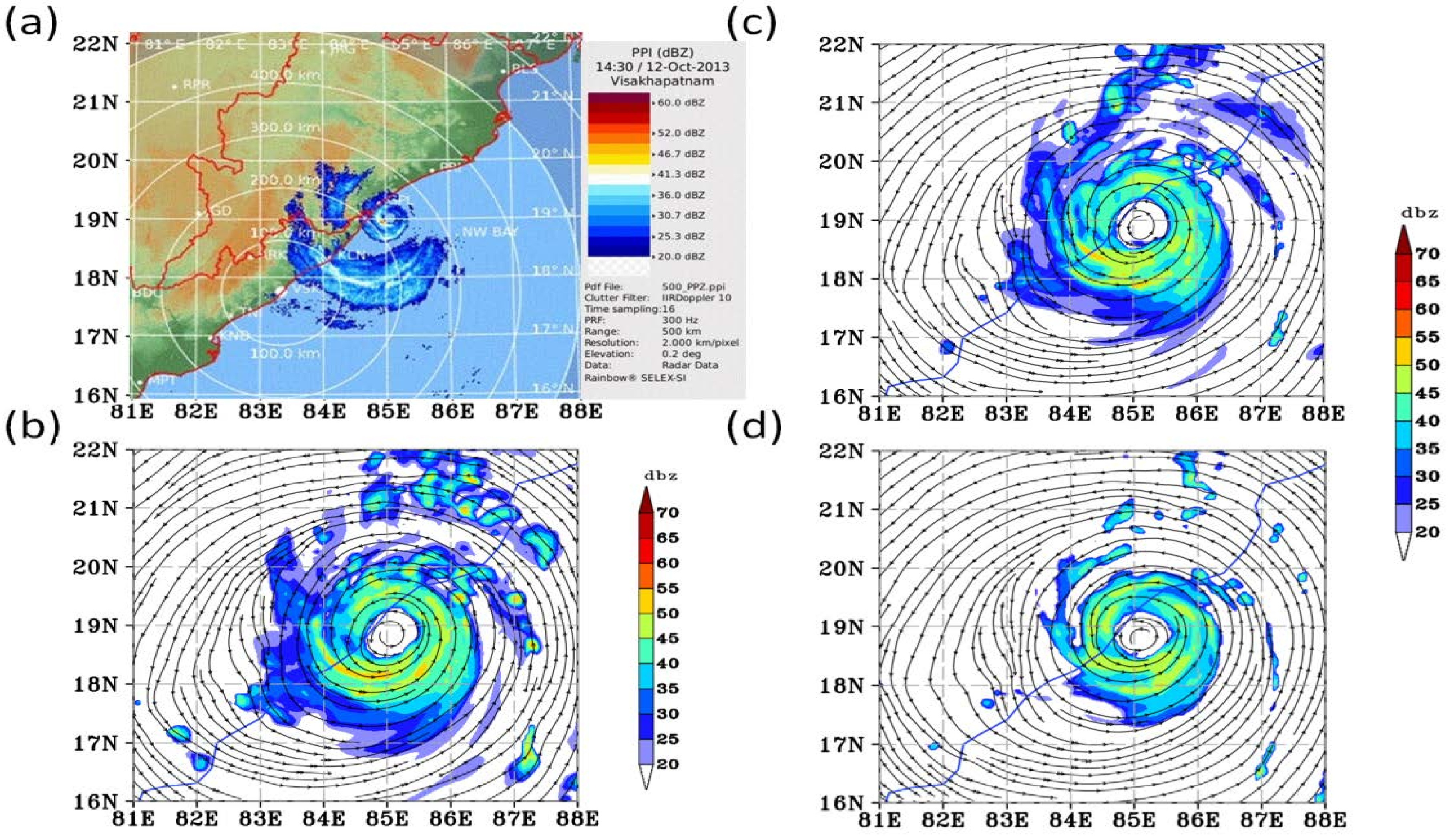

(a) IMD
(b) 3DEnVAR
(c) 4DVAR
(d) 4DEnVAR

Simulated reflectivity shows the position of the TC Phailin match well with observation and the spatial spread in dBZ is maximum in 4DVAR and minimum in the 4DEnVAR simulation

Error in track (ΔR), Intensity (ΔVmax) and mean sea level pressure (ΔMSLP) with respects to IMD best track dataset.

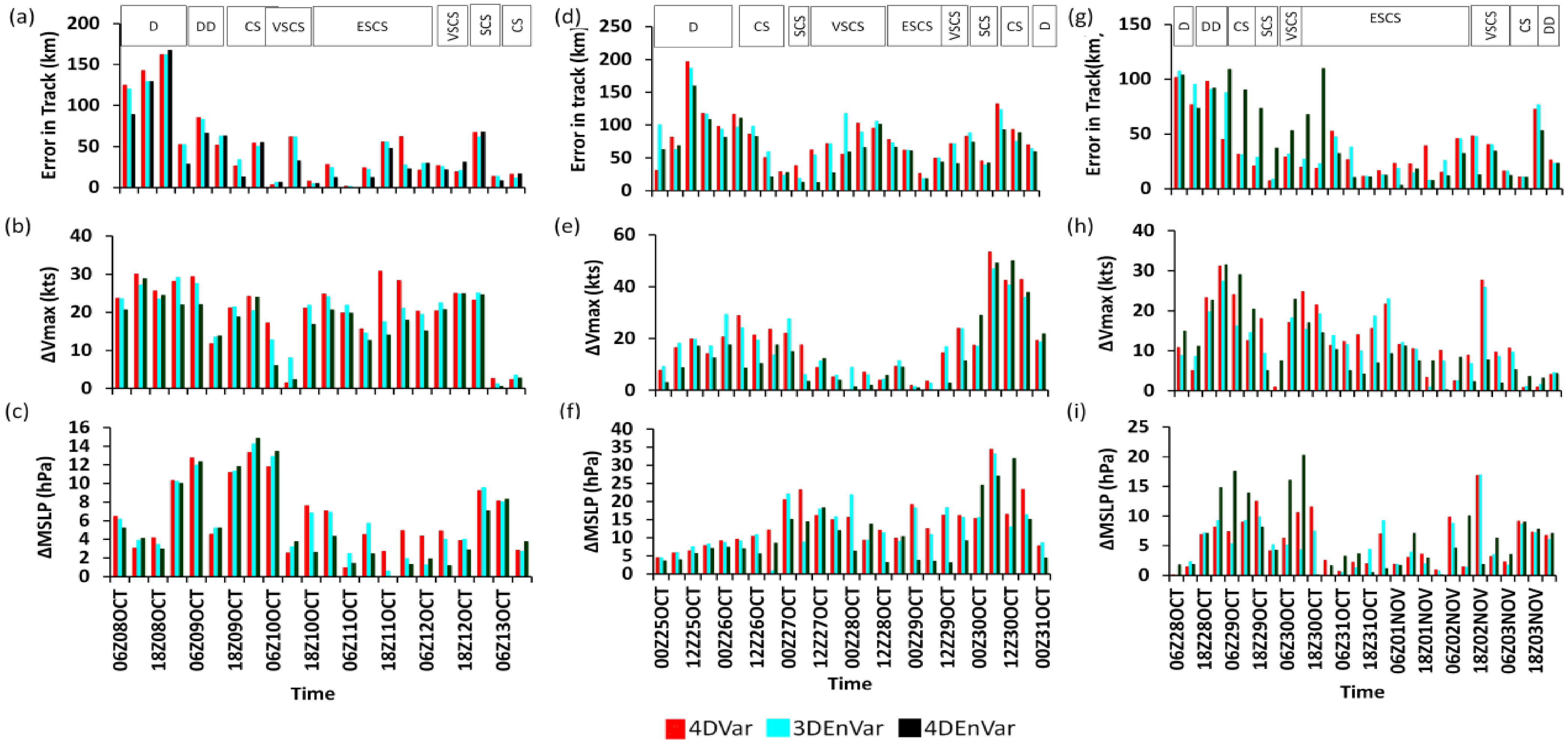

- Maximum track error in all experiment is around 200 km at the time of genesis and decrease there after.
- At the most intense stages ΔVmax is reducing compared to weaker stages .
- 4DEnVAR gives better representation of Track , Vmax and MSLP compared to 4DVAR and 3DEnVAR techniques.

Skill scores of rainfall simulations

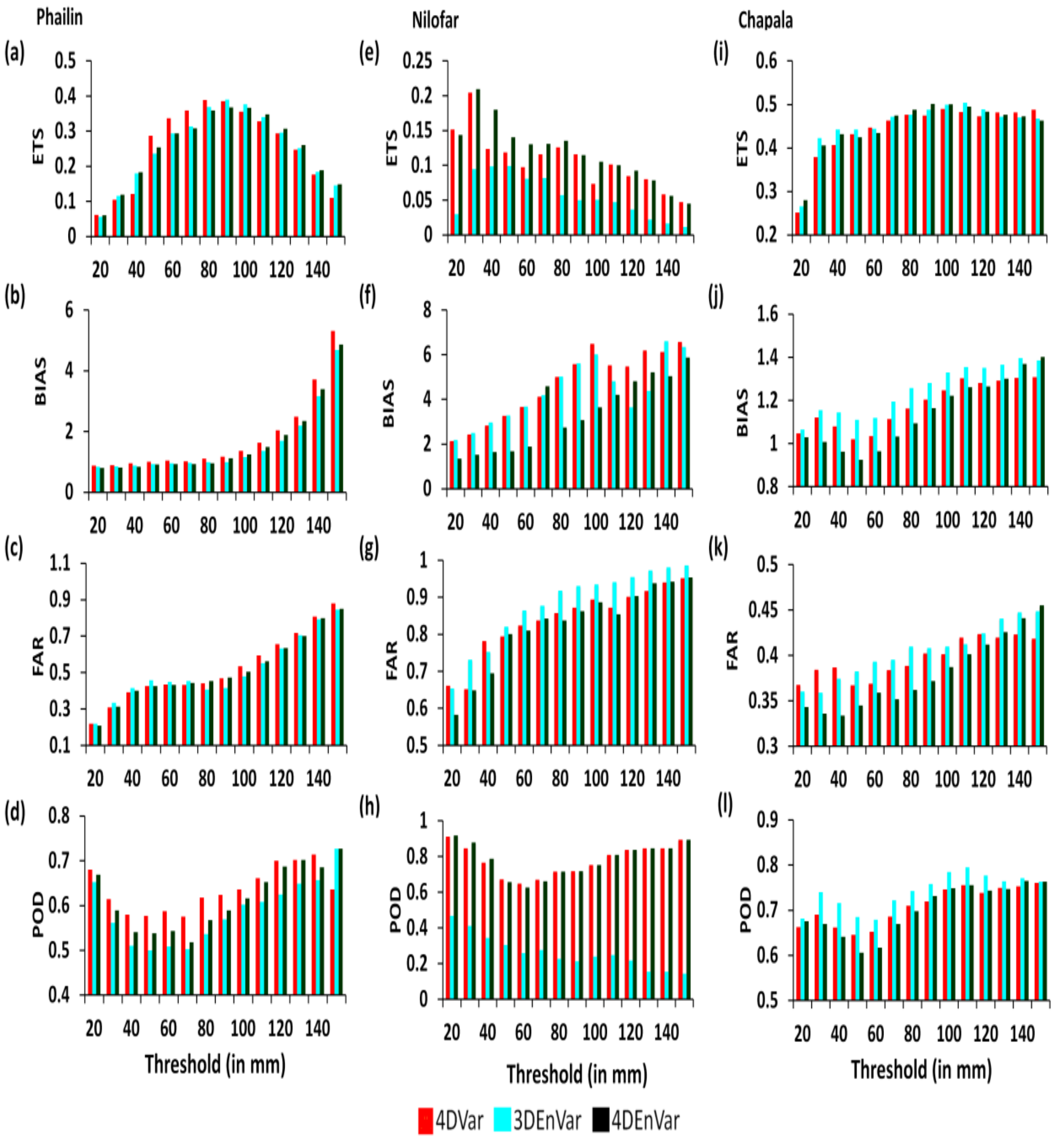

- 4DEnVAR method show less bias for rainfall exceeding 100 mm.
- 4DVAR and 4DEnVAR has better POD of rainfall.
- 4DVAR and 4DEnVAR has less FAR of rainfall.

Surface wind distribution

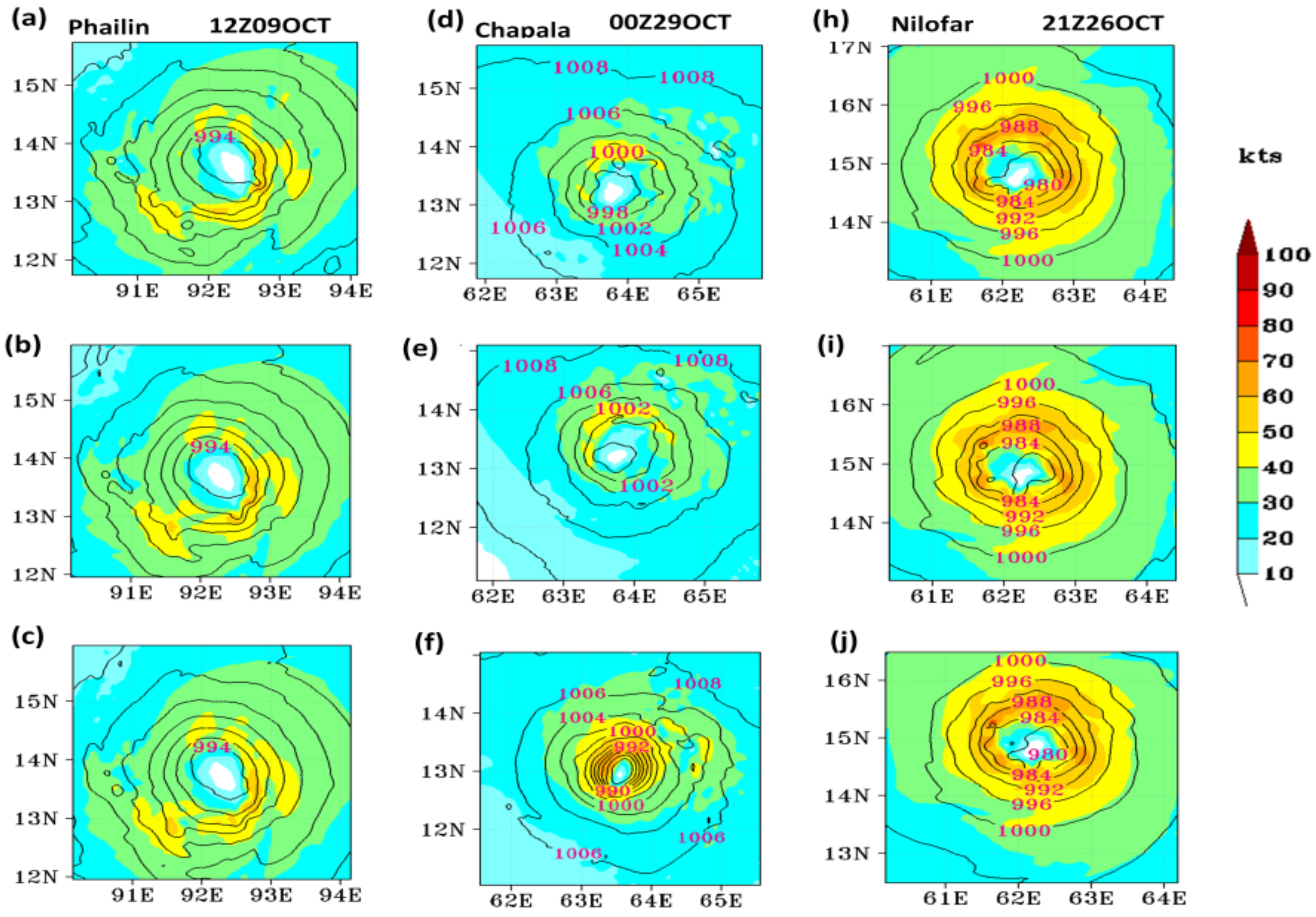

Spatial distribution of minimum sea level pressure (hPa) and maximum surface wind (knots) from all three simulations

Rapid Intensification

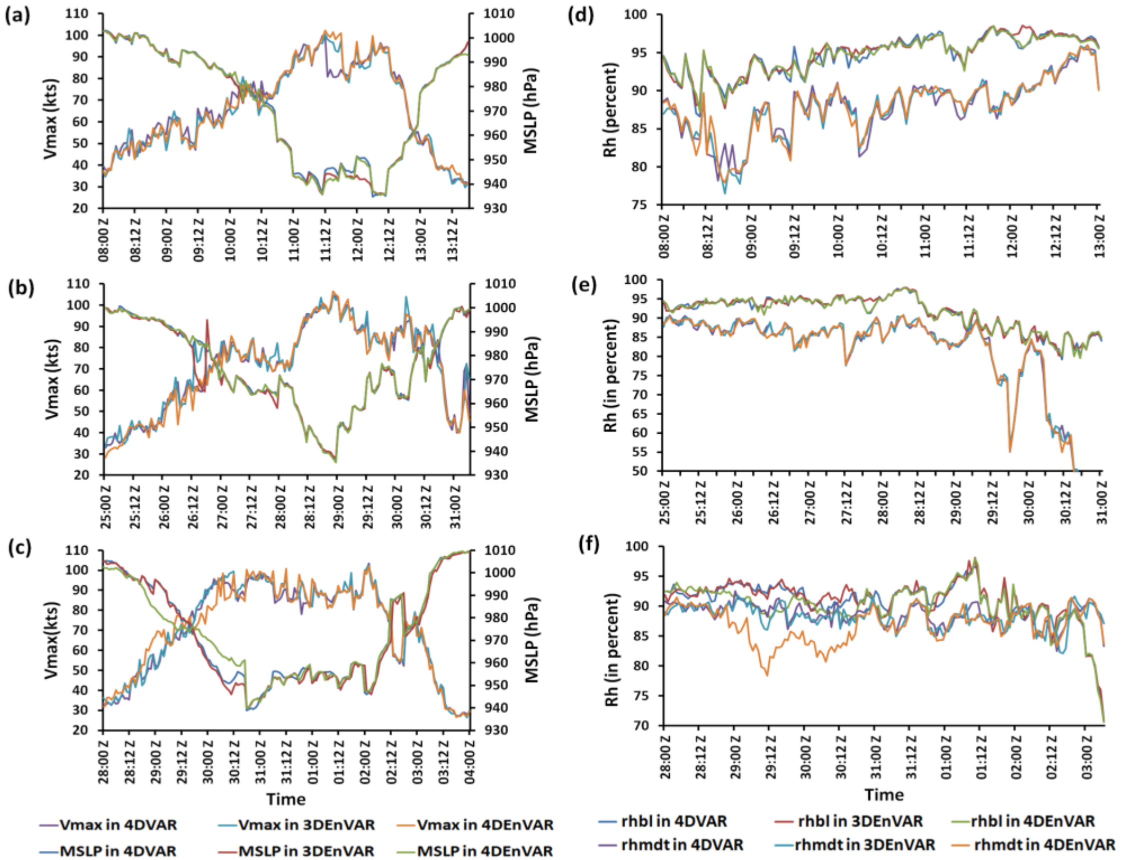

Rapid Intensification captured comparatively well in 4DEnVAR with a time leg /lead

Vertical cross-sectional structure of the TCs

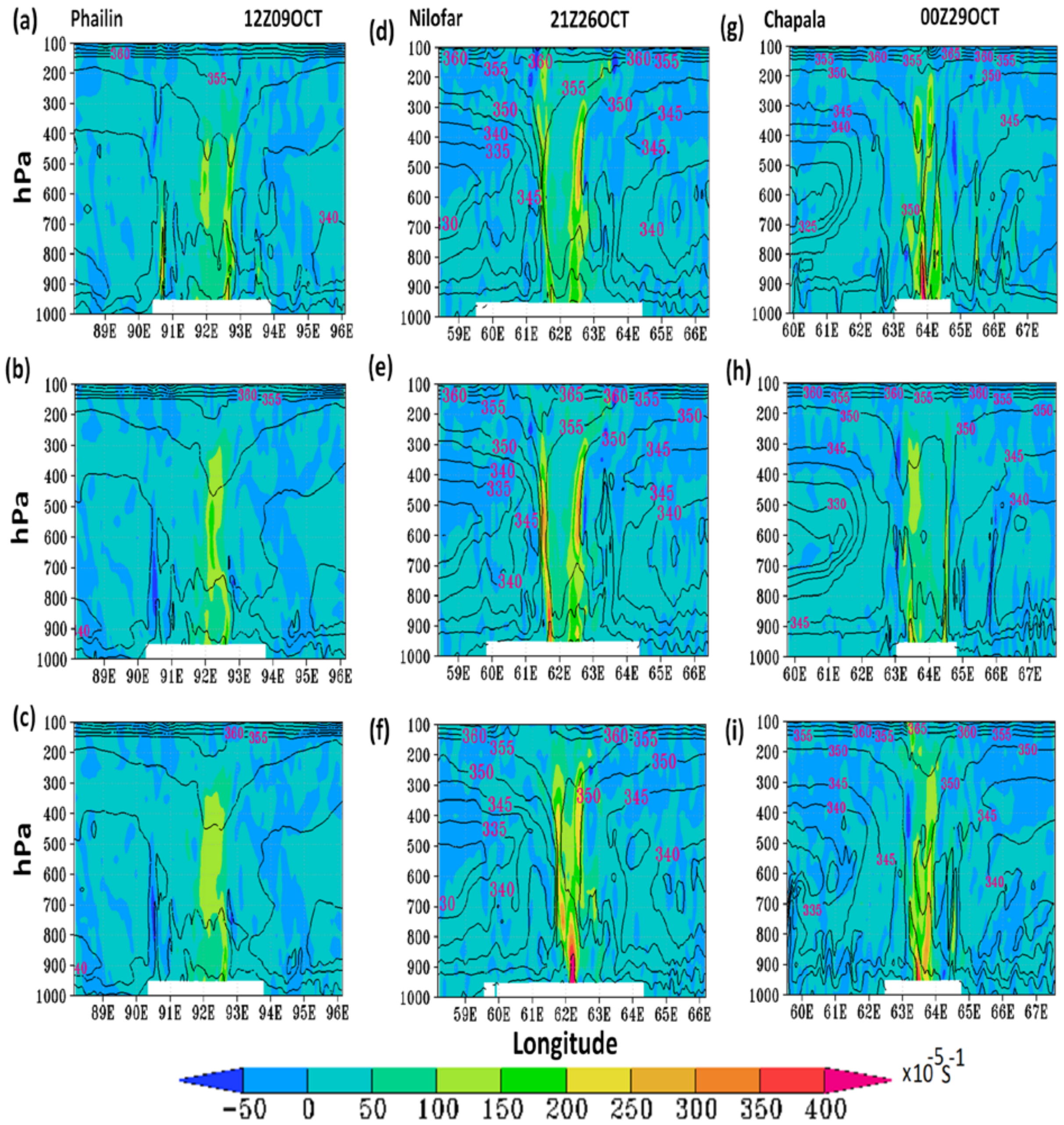

Equivalent potential temperature surfaces (contour) superimposed on relative vorticity (shaded) for cyclonic storm stages of TCs Phailin and Chapala and severe cyclonic storm stage of TC Nilofar.

4DEnVAR captured comparatively more intense and organized vertical structure of the TCs

Summary- Which data assimilation technique?

- Hybrid data assimilation techniques perform better compared to the 4DVAR technique
- 4DEnVAR techniques provide better estimates of Track, intensity, and minimum sea level pressure with comparatively fewer errors.
- The simulations using hybrid DA techniques captured the observed rapid intensity changes in TCs; however, they were not able to predict the exact timing of the RI of the TCs. The temporal error in RI prediction is less than ±6 hours
- 4DEnVAR simulations estimated the most intense and organized vertical structure of TCs.
- Overall, Hybrid DA techniques show improvement over non-hybrid DA, and hybrid 4DEnVAR shows improvement over hybrid 3DEnVAR DA in structure and rapid intensity changes simulation of the TCs
- 4DEnVAR DA is most suitable for the generation of useful reanalysis for the understanding of the physical process involved in structure evolutions and rapid intensity changes of the TCs over NIO.

Scatterometer (Scatsat-1) Data Assimilation

Objective: Real-time/delayed mode assimilation of SCATSAT-1 winds in NARL short-range weather forecast system and impact analysis

Jyoti Bhate, Arpita Munsi, **Amit P Kesarkar,** Govindan Kutty, and Sanjib Kumar Deb, (2021). Impact of assimilation of satellite retrieved ocean surface winds on the tropical cyclone simulations over the north Indian Ocean. Earth and Space Science, 8, e2020EA001517. https://doi.org/10.1029/2020EA001517

Arpita Munsi, **Amit Kesarkar***, Jyoti Bhate, Abhishek Panchal, Kasturi Singh, Govindan Kutty, Ramkumar Giri, (2021), Rapidly intensified, long duration North Indian Ocean tropical cyclones: Mesoscale downscaling and validation, Atmospheric Research, 259, 2021, 105678, ISSN 0169-8095, https://doi.org/10.1016/j.atmosres.2021.105678

Arpita Munsi, **Amit P Kesarkar*,** Jyoti Bhate, et al. (2022) Simulated dynamics and thermodynamics processes leading to the rapid intensification of rare tropical cyclones over the North Indian Oceans. J Earth Syst Sci 131, 211. https://doi.org/10.1007/s12040-022-01951-9.

Arpita Munsi, **Amit P Kesarkar*,** Jyoti N Bhate, Kasthuri Singh, Abhishek Panchal, Govindan Kutty, M. M. Ali, Ashish Routray and R. K. Giri, (2023), Atmosphere-upper-ocean interactions during three rare cases of rapidly intensified tropical cyclones over North Indian Oceans. Journal of Oceanography, 79, 77–89. https://doi.org/10.1007/s10872-022-00664-3.

Arpita Munsi, **Amit P Kesarkar*,** J.N. Bhate, V.P.M Rajasree, G. Kutty, (2023), Helicity evolution during the life cycle of tropical cyclones formed over the north Indian Ocean, Advances in Space Research, 71, 3, 1473-1485, ISSN 0273-1177, https://doi.org/10.1016/j.asr.2022.10.004

Arpita Munsi, **Amit P Kesarkar*,** Jyoti N. Bhate, & Tallapragada Vijay S, (2024), Helicity: A possible indicator of negative feedback initiation of tropical cyclone–ocean interaction. Earth and Space Science, 11, e2023EA003211. https://doi.org/10.1029/2023EA003211

Collaboration with AOSG, SAC, Ahmedabad, and IIST, Thiruvananthapuram

Scatterometer Data Assimilation

- ETKF 3DVAR data assimilation
- Assimilated satellite/wind data:
  - GDAS radiance data,
  - prepbufr data,
  - scatterometer/radiometer data.

Assimilated Ocean surface wind

Instrument name	Oscat-2	ASCAT	Windsat
Satellite name	Scatsat-1	Coriolis	MetOp
Measured wind speed Range	3-20 m/s	3-30 m/s	3-25 m/s
Resolution	50Km x 50Km, 25Kmx 25Km	25Km x 35Km	25 Km x 25Km
Source type	Active	Active	Passive
Frequency(in GHz)	13.5(Ku band)	5.2(C band)	6.8,10.7,18.7,23.8,37
Error	2 m/s, 18°	3.7 m/s, 24°	5 m/s, 20°

Data assimilation in cyclic mode

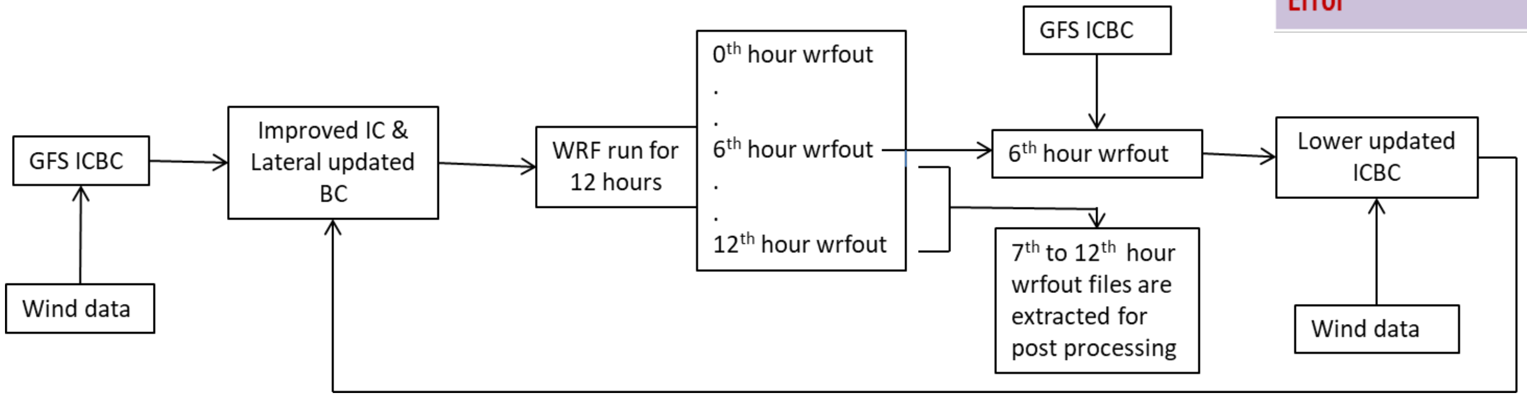

Tropical cyclone Ockhi: Cyclonic storm stage on 12 UTC 01 Dec 2017

Scatsat-I gridded winds

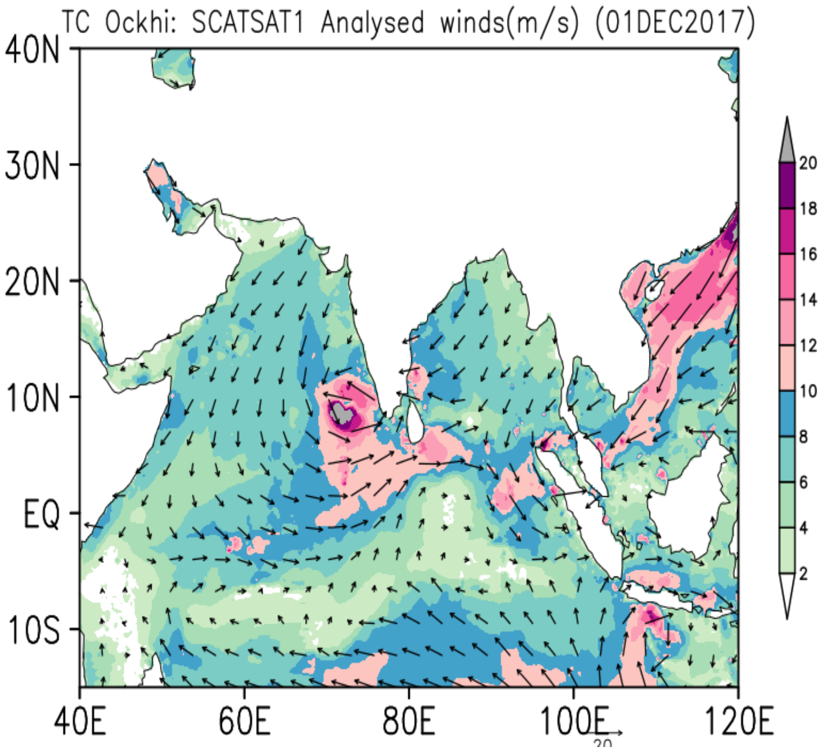

Surface winds with assimilation

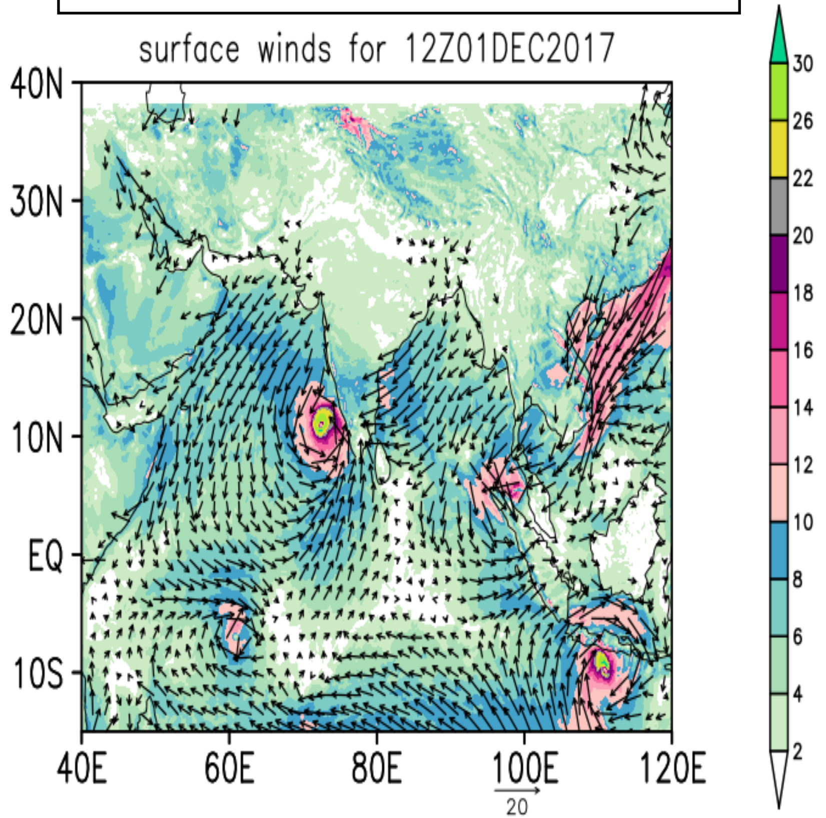

- ✓ SCATSAT-1 ocean winds are assimilated using the hybrid-3DVAR technique for improvement of tropical cyclone prediction and evolution.
- ✓ ANFIS system is being developed to improve the retrievals of ocean winds.
- ✓ The impact of improved retrieval technique will be evaluated in the simulations of tropical cyclones.

Simulation of eyewall wind speed

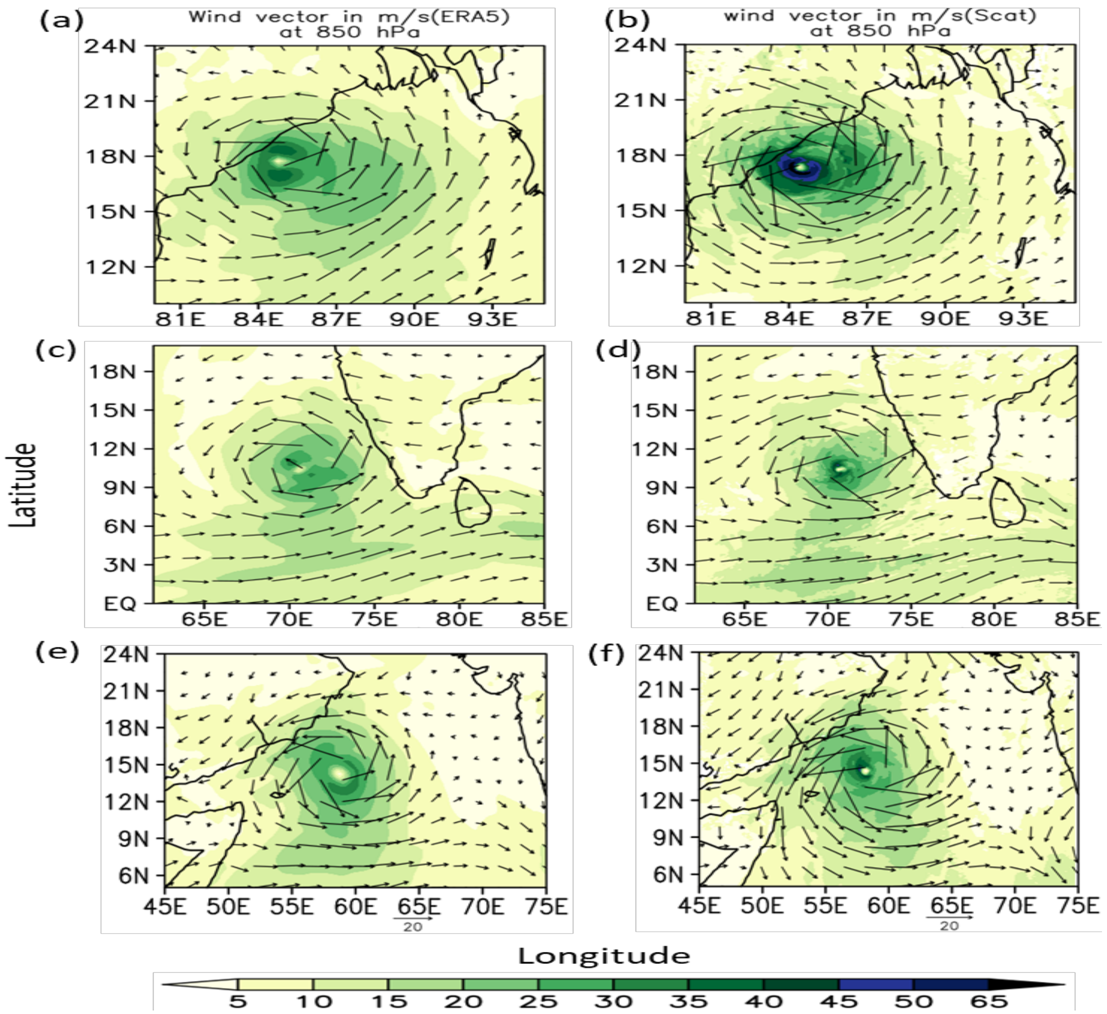

Validation of wind speed at 850hPa

- The location of maximum wind speed is in accordance with each other.
- For TC Fani, ERA5 reanalysis shows maximum wind speed up to 45 m/s and Scat simulation up to 65 m/s.
- For TC Ockhi, ERA5 shows maximum wind speed 40 m/s and that of Scat experiment 45 m/s.
- For TC Luban, ERA5 shows maximum wind speed up to 35 m/s and our simulation 45 m/s.
- Simulation shows higher wind speed in the eyewall region compared to ERA5 reanalysis.

Simulations captured higher wind speeds of the eye wall at the maximum intensified (MI) stage.

Simulation of Rapid Intensification

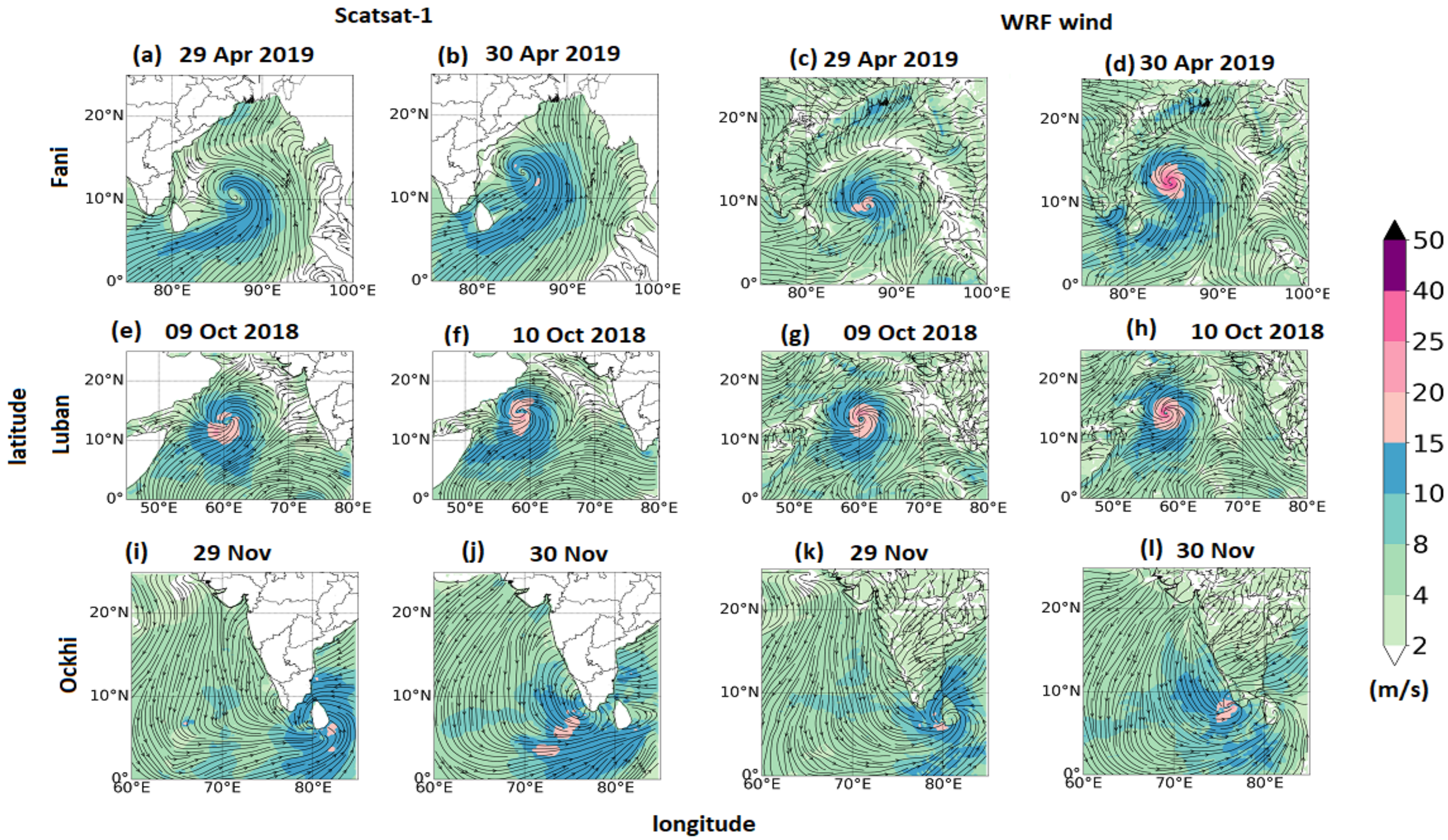

Fani RI: 10-15 to 15-20 m/s by Scatsat-1(S1).
15-20 to 25-40 m/s by WRF simulation.

Luban RI: 15-25 m/s by S1.
15-25 to 25-40 m/s by simulation.

The high-resolution reanalysis successfully captures the RI of TC Fani and Luban, which has not been captured by Scatsat-1.

Simulated rainfall during the lifetime of cyclones

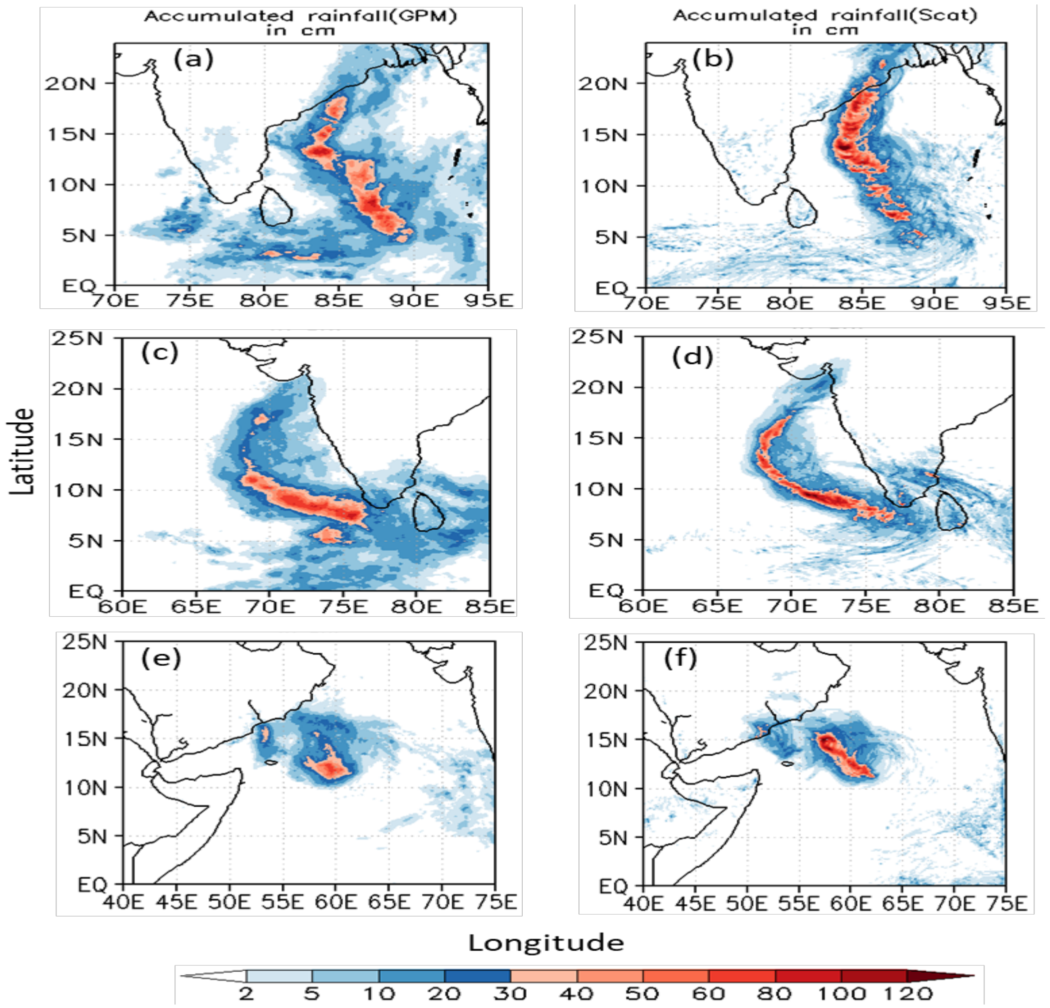

Validation of rainfall

- Scat experiment simulated less intense rainfall in the genesis period and more intense rainfall at the mature stage while compared to the GPM rainfall for heavy rainfall(> 30 cm).
- The areal extent of rainfall distribution for rainfall less than 20 cm is precise compared to GPM rainfall.
- The location of the heavy rainfall band shows accordance.
- The simulation of accumulated rainfall is successful to capture heavy rainfall by position and by magnitude to a good extent.

Simulation of accumulated rainfall is successful in capturing spatial distribution and magnitude of heavy rainfall to a good extent.

Simulation of Diurnal Variation of Convection and Rainfall

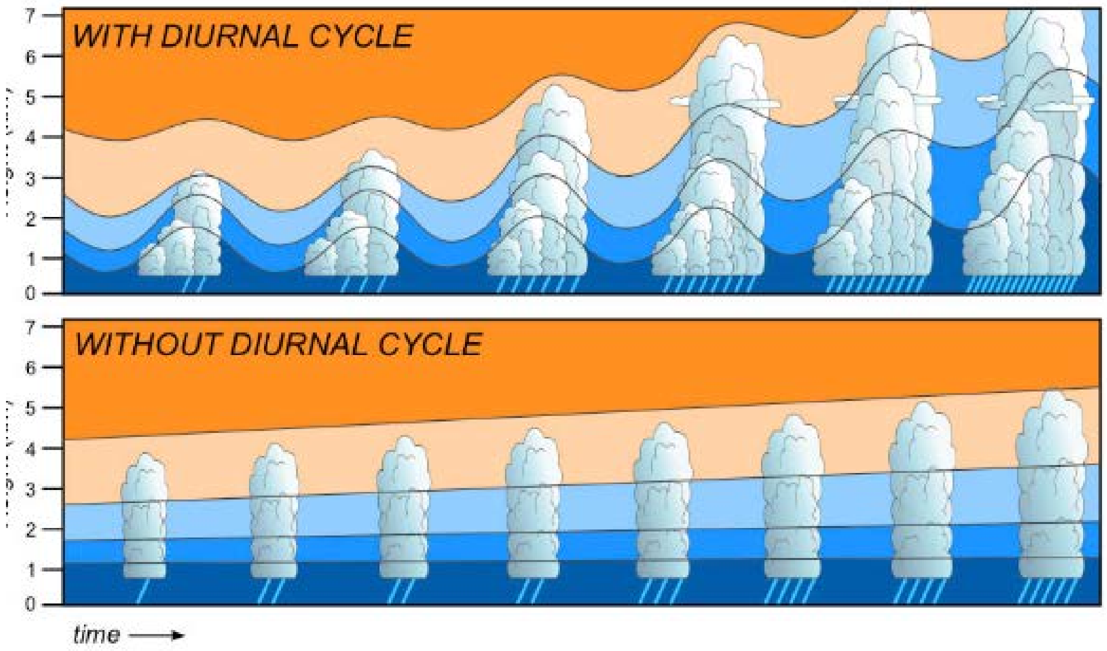

Idealized simulation with and without diurnal cycle

- Jyoti Bhate, Amit P. Kesarkar, Anandakumar Karipot, D. Bala Subrahamanyam, M. Rajasekhar, V. Sathiyamoorthy, C.M. Kishtawal, A sea breeze induced thunderstorm over an inland station over Indian South Peninsula – A case study, Journal of Atmospheric and Solar-Terrestrial Physics, 148, 2016, 96-111, ISSN 1364-6826, https://doi.org/10.1016/j.jastp.2016.09.002.
- Jyoti Bhate, **Amit P Kesarkar,** and Rajasree, V.P.M., (2019), Simulation of the diurnal cycle of rainfall during Indian summer monsoon season using mesoscale model. Theor Appl Climatol 138, 185–200. https://doi.org/10.1007/s00704-019-02777-0
- Jyoti Bhate, and **Amit Kesarkar,** (2019) Sensitivity of diurnal cycle of simulated rainfall to cumulus parameterization during Indian summer monsoon seasons. *Clim Dyn* 53, 3431–3444 (2019). https://doi.org/10.1007/s00382-019-04716-1

Convection Genesis over South Indian Region

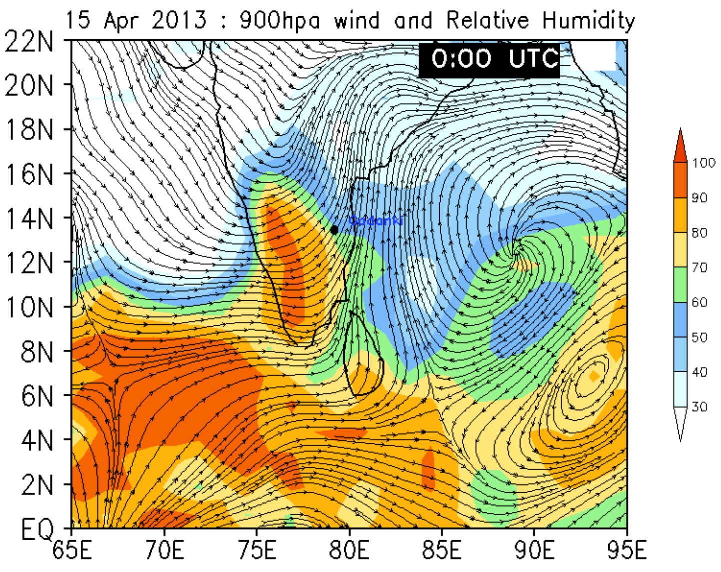

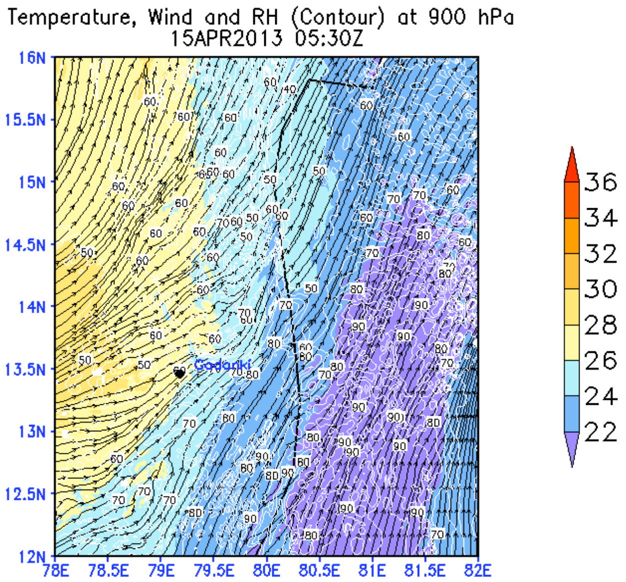

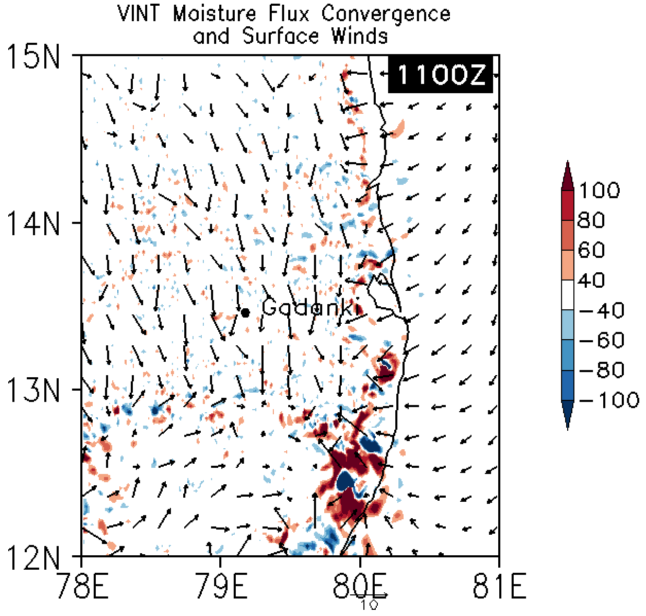

The 900 hPa shows westerly flow over the South Peninsula. Wind discontinuity or troughline shifts towards the East Coast as the day progresses. The analysis fails to show any contribution of the mesoscale phenomenon in convection genesis

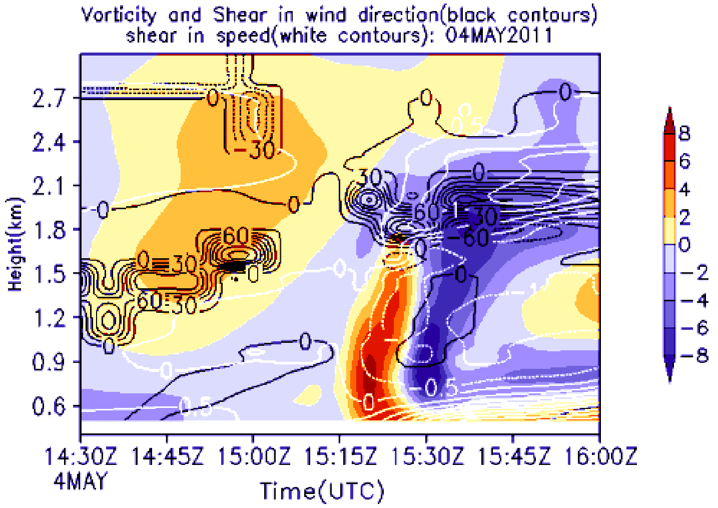

The wind discontinuity observed, extended from surface level to 850 hPa. The low level convergence and divergence pattern present near the discontinuity line produce upward air motion. This upward motion is responsible for initiation of storms over coastal areas.

Prediction of Thunderstorms over Gadanki (2017)

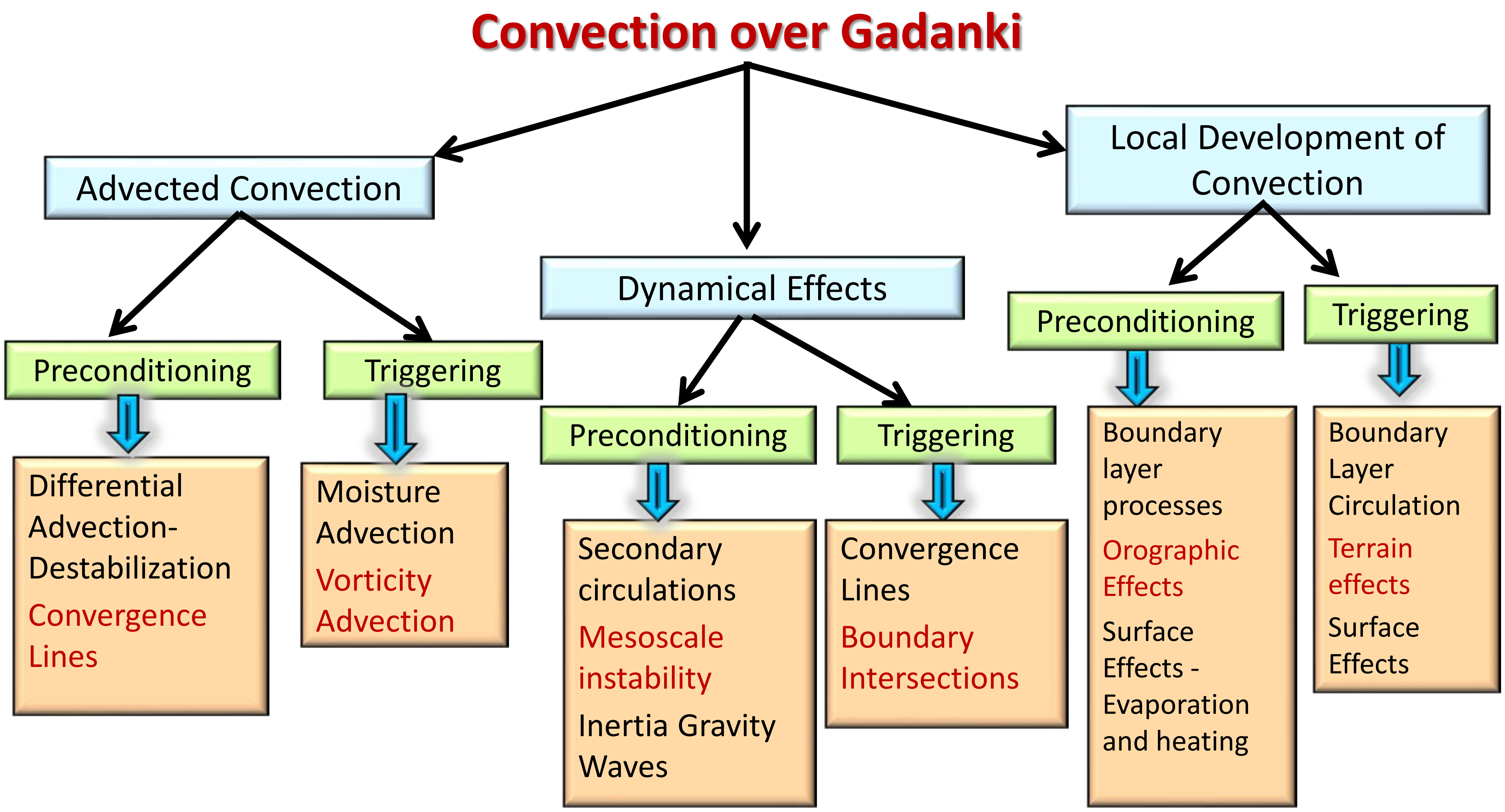

Jyoti Bhate (2018) Physical mechanisms controlling the diurnal cycle of convection over a tropical station

Convective scale data assimilation and assimilation of X-band RADAR Observations

RADAR reflectivity (dBZ) 04 UTC 2019

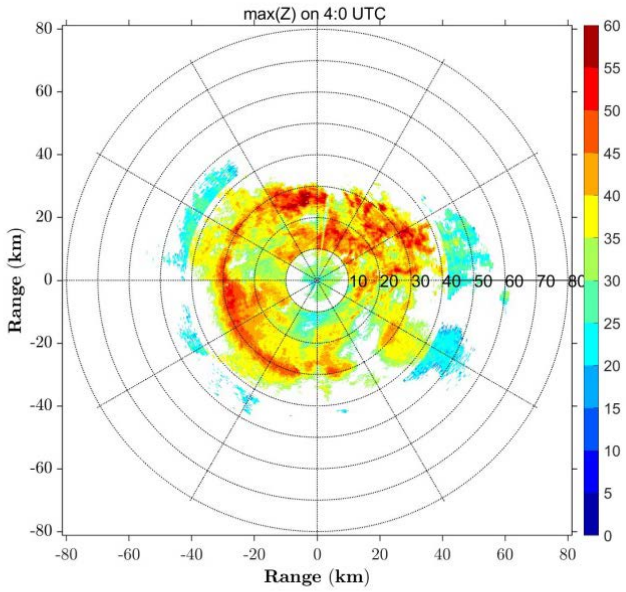

Initial Conditions: 18UTC 16 Aug 2019

- Assimilation of X-band Radar observations (00-04 UTC 16Aug2019 using En4DVAR
- Improved representation of vertical velocity.
- Improved spatial correlation of rainfall in the neighborhood of Gadanki compared to the control run. However, precipitation simulated south of Gadanki
- Improved wind shear, KI, TT, MCAPE, and MCIN.

NARL X-Band Radar data (Radial velocity and reflectivity) is assimilated at convective scale (2km) at hourly interval

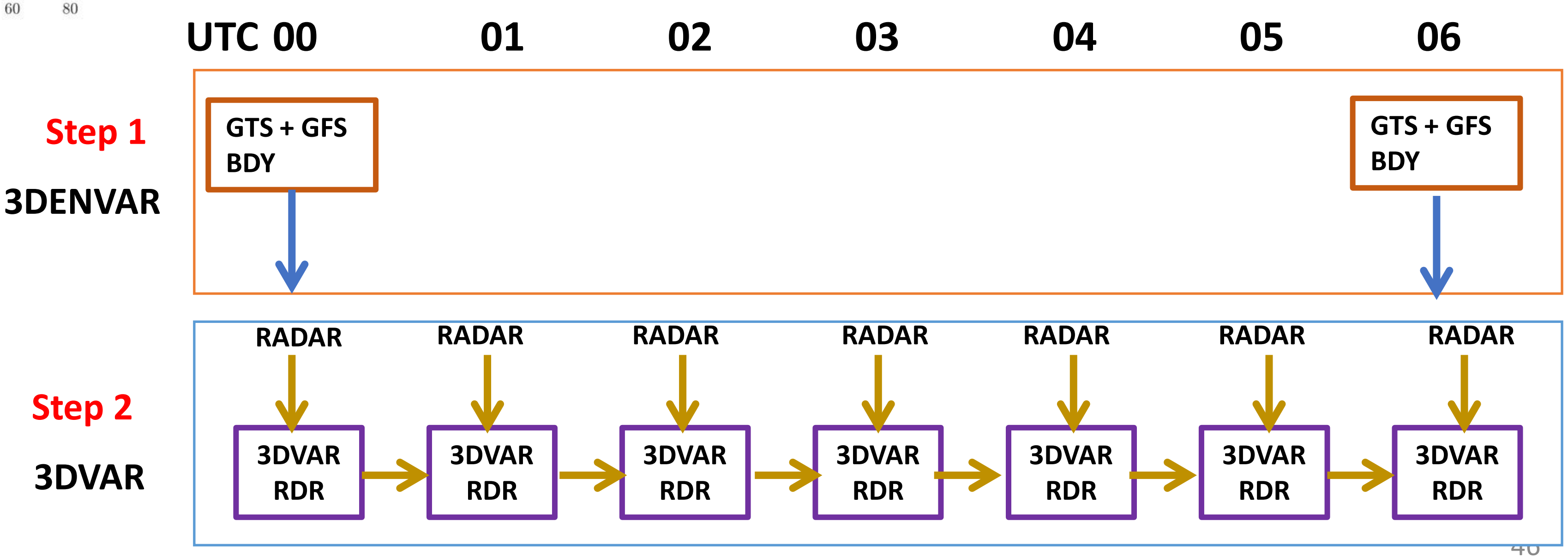

X-band RADAR Observations data assimilation

- Direct data assimilation scheme is implemented (Xiao and Sun (2007)
- **The observation operator for radial velocity is**
- $V_r = u\,\frac{x-x_i}{r_i} + v\,\frac{y-y_i}{r_i} + (w - v_T)\,\frac{z-z_i}{r_i}$,
- Where where (u, v, w) are the wind components, (x, y, z) are the radar location, (x_i, y_i, z_i) are the location of the radar observation, r_i is the distance between the radar and the observation, and v_T is the terminal velocity.
- **The observation operator for the Doppler radar reflectivity is**
- **$Z = 43.1 + 17.5 \log_{10}(pq_r)$**
- where Z is the reflectivity in the unit of dBZ and q_r is the rainwater mixing ratio. (Sun and Crook, 1997)
- Wang and Liu (2019) further developed this operator and added the contribution of snow, and graupel to reflectivity in addition to rainwater mixing ratio.
- The error for the radial velocity is 0.5m/s and error for reflectivity is 1.2dB.for NARL radar

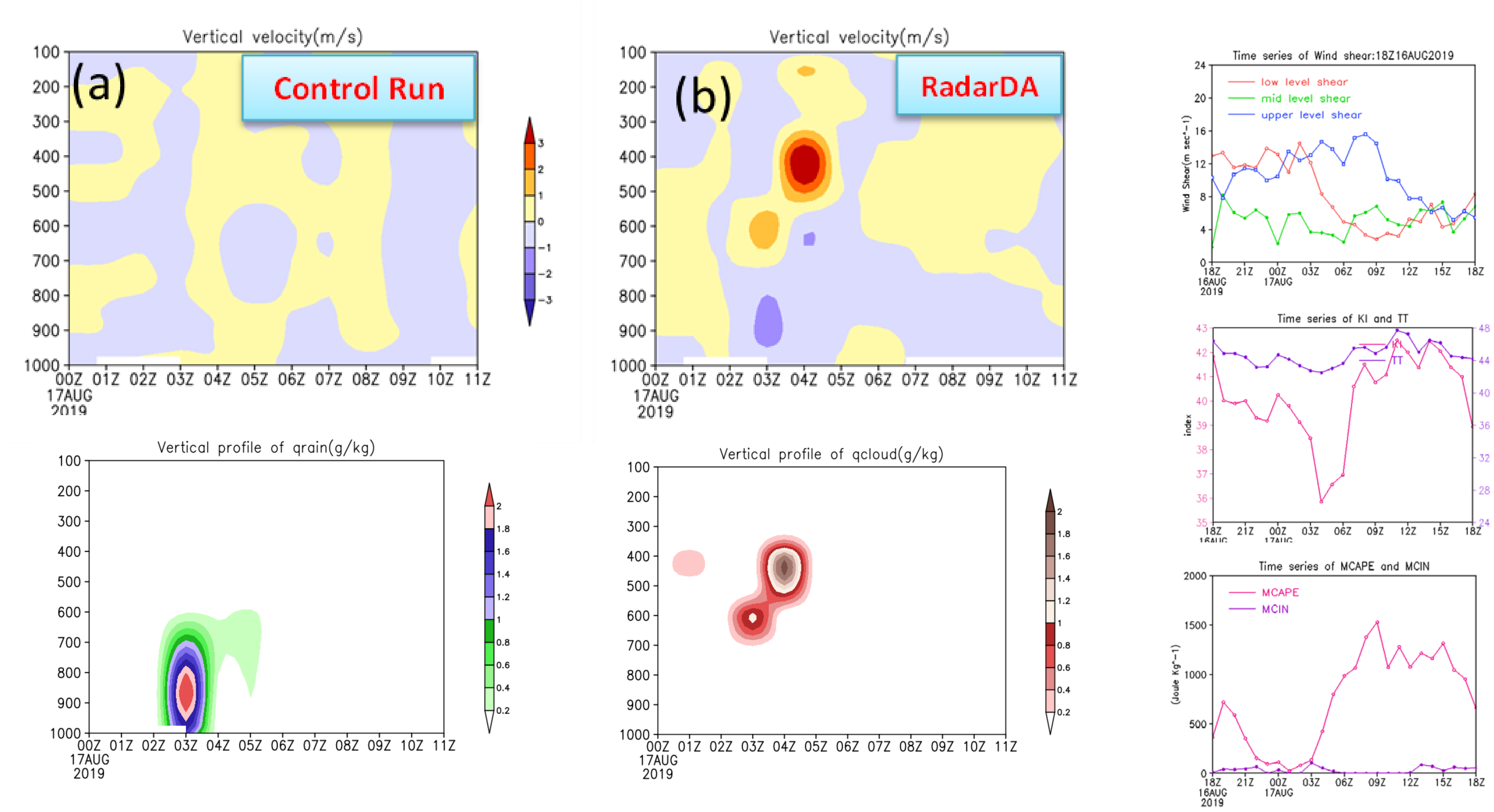
Vertical velocity(m/s)
(a)
Control Run
Vertical velocity(m/s)
(b)
RadarDA
00Z 01Z 02Z 03Z 04Z 05Z 06Z 07Z 08Z 09Z 10Z 11Z
17AUG
2019
Vertical profile of qrain(g/kg)
Vertical profile of qcloud(g/kg)
Time series of Wind shear:18Z16AUG2019
low level shear
mid level shear
upper level shear
Wind Shear(m sec^-1)
Time series of KI and TT
KI
TT
index
Time series of MCAPE and MCIN
MCAPE
MCIN
(Joule Kg^-1)
18Z 21Z 00Z 03Z 06Z 09Z 12Z 15Z 18Z
16AUG
2019
17AUG

X-Band Radar Assimilation on 17 Aug 2022

RADAR reflectivity (dBZ)

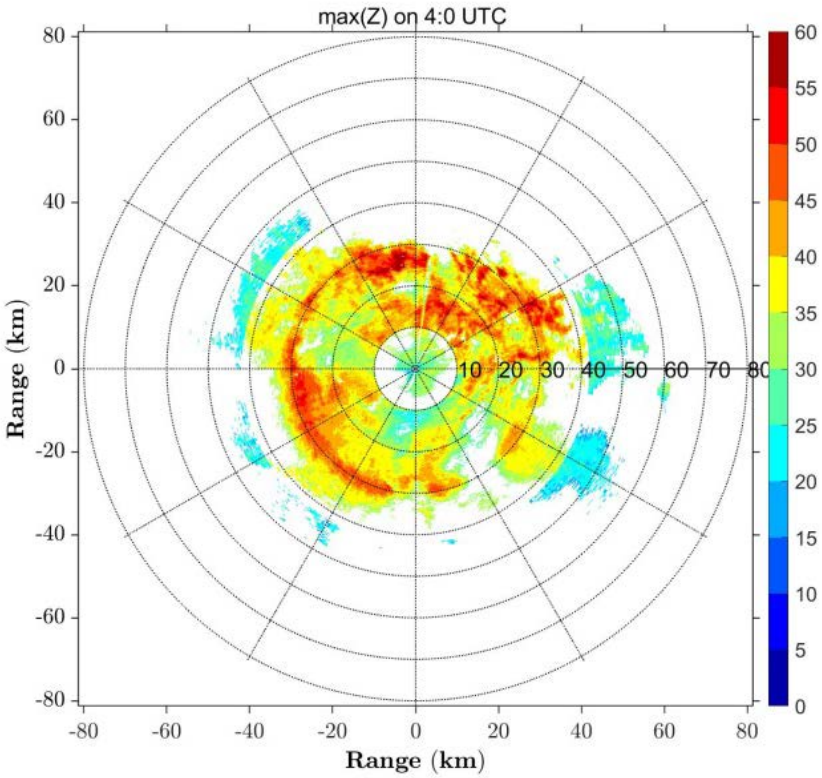

WRF simulation (assimilation of reflectivity)

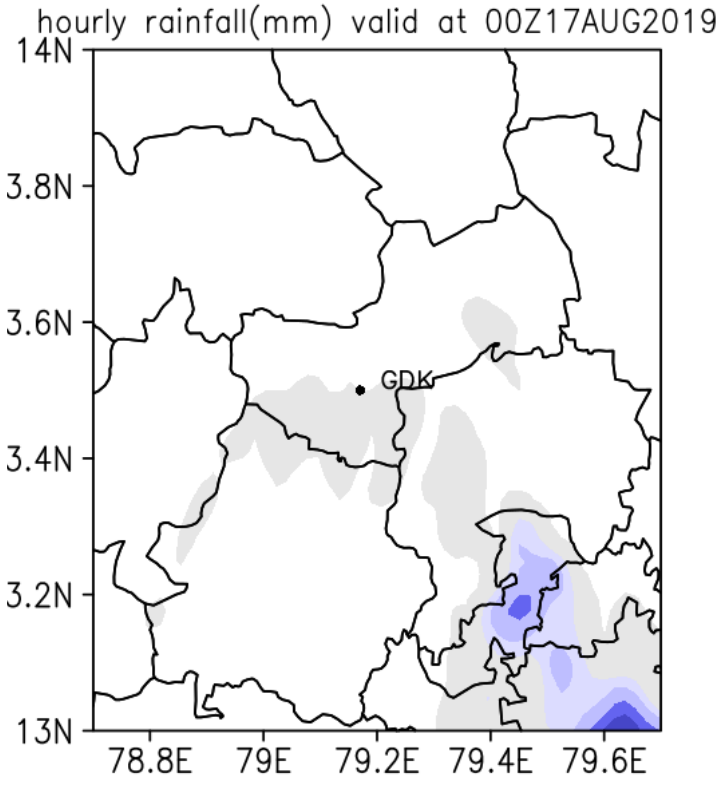

IC: 18Z16Aug2019

GPM-IMERG estimated rainfall (mm)

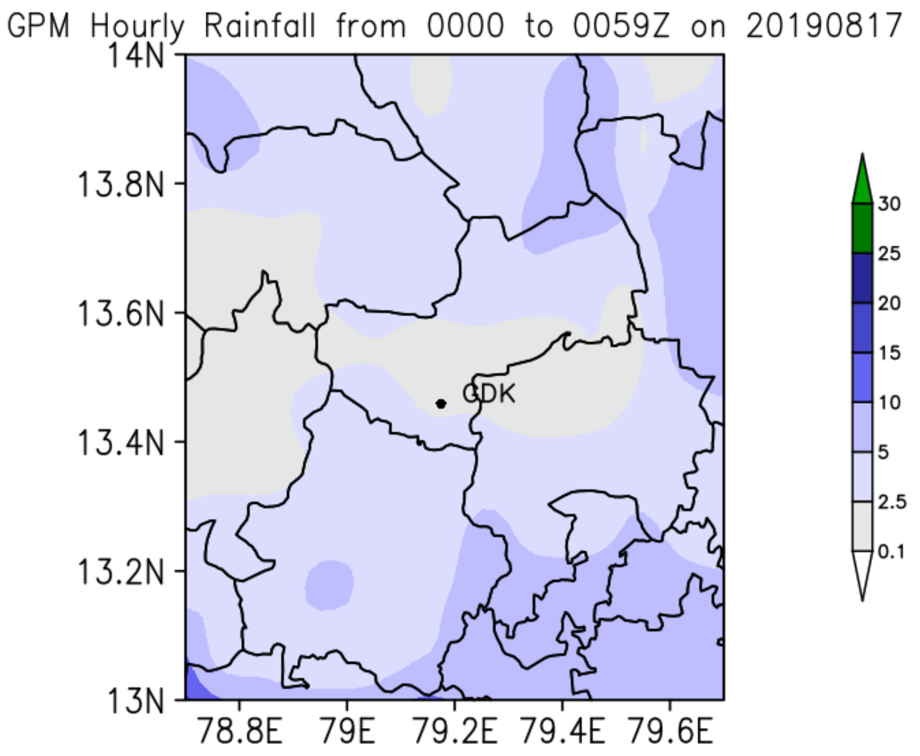

Role of LULC change

Thunderstorm on 30-31 August 2017

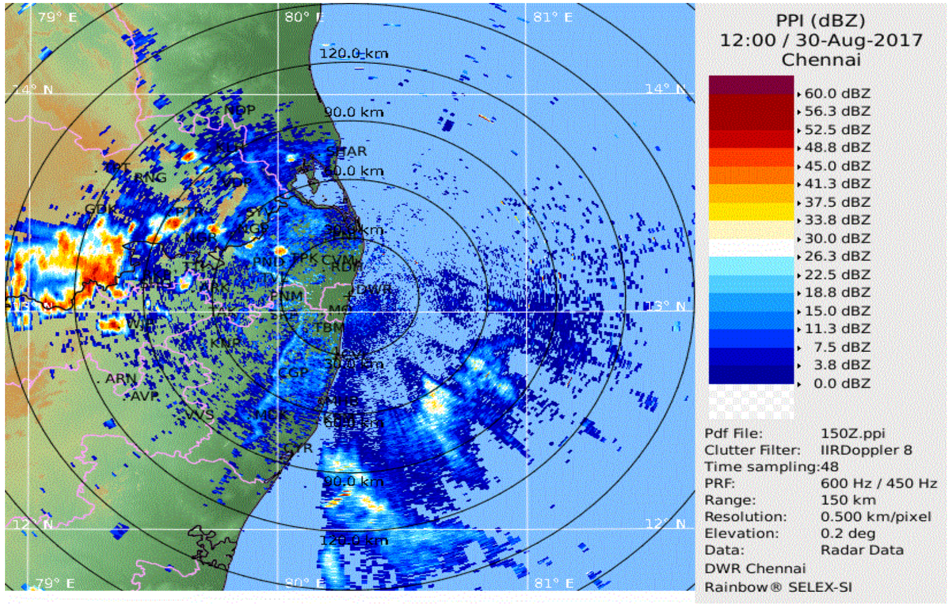

Future research: High-resolution simulations for resolving the influence of lakes, mountains, and land cover on the advected thunderstorms and movement of the troughs over the south Indian region.

Western Disturbances

- Objective: To understand the physical mechanisms of extreme rainfall over the Western Himalayas

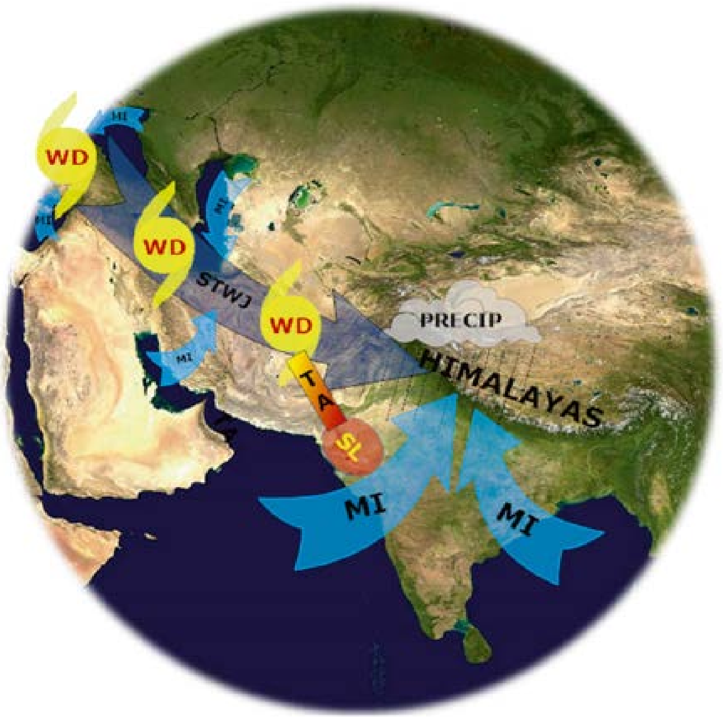

Fig: Conceptual model of WD

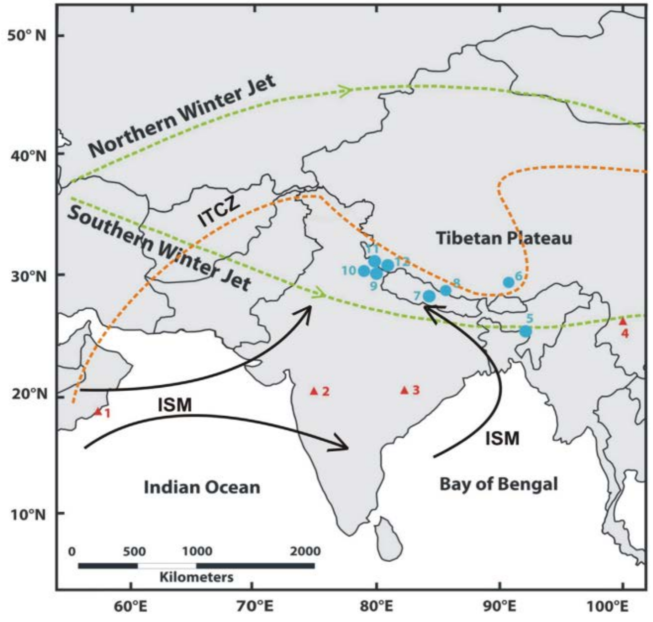

Fig: Position of winter STWJ

Para, J.A., Kesarkar, A., Bhate, J. *et al*. Large-scale dynamics of western disturbances caused extreme precipitation on 24–27 January 2017 over Jammu and Kashmir, India. *Model. Earth Syst. Environ.* **6**, 99–107 (2020). https://doi.org/10.1007/s40808-019-00661-4

Collaboration with Kashmir University, IMD Srinagar

Modelling of Extreme Rainfall Evidences: Kashmir valley (24-27 Jan 2017)

- Extremely heavy rainfall over Kashmir valley
- Maximum daily snowfall at Pahalgam region on 26th January 2017: 11.52 cm highest since 1877
- The **cold air intrusion** from the northern latitudes into the core of western disturbances.
- **Non-conservation of EPV** due to friction and latent heat release causes alteration of static stability and absolute vorticity leading to the development of the intense convective system (low-pressure area) below the level of maximum heating.
- **Baroclinic instability** provided energy of the disturbance (latent heating) by strengthening the influence of baroclinicity on the vertical component of relative vorticity, causing intense precipitation over the J&K region.

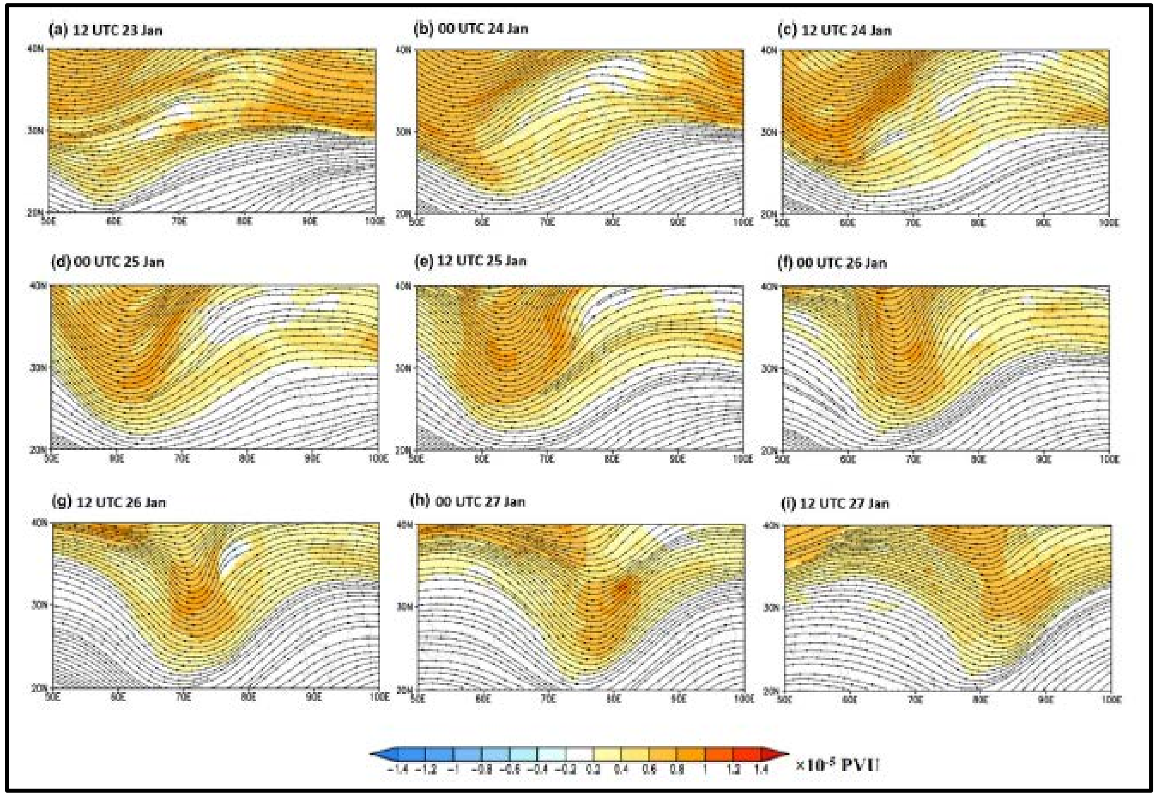

Figure: Ertel potential vorticity ($\times 10^{-5}$ PVU) and 200 hPa wind streamline from 24 to 27 January 2017.

Role of cold dry air intrusion in Western Disturbances on precipitation

- Increase in the kinetic energy on the southwest edge of the trough facilitates two processes.
  - dry and cold air intrusion into the western disturbance system and
  - fetch moist and warm air from the Arabian sea
- Mixing of the air masses over the western Himalayas.
- Decrease in the meridional component of kinetic energy and increase in the zonal component of kinetic energy cause stagnation of cloud mass over western Himalayas.

Passage of WD over the western Himalayas (5 km)

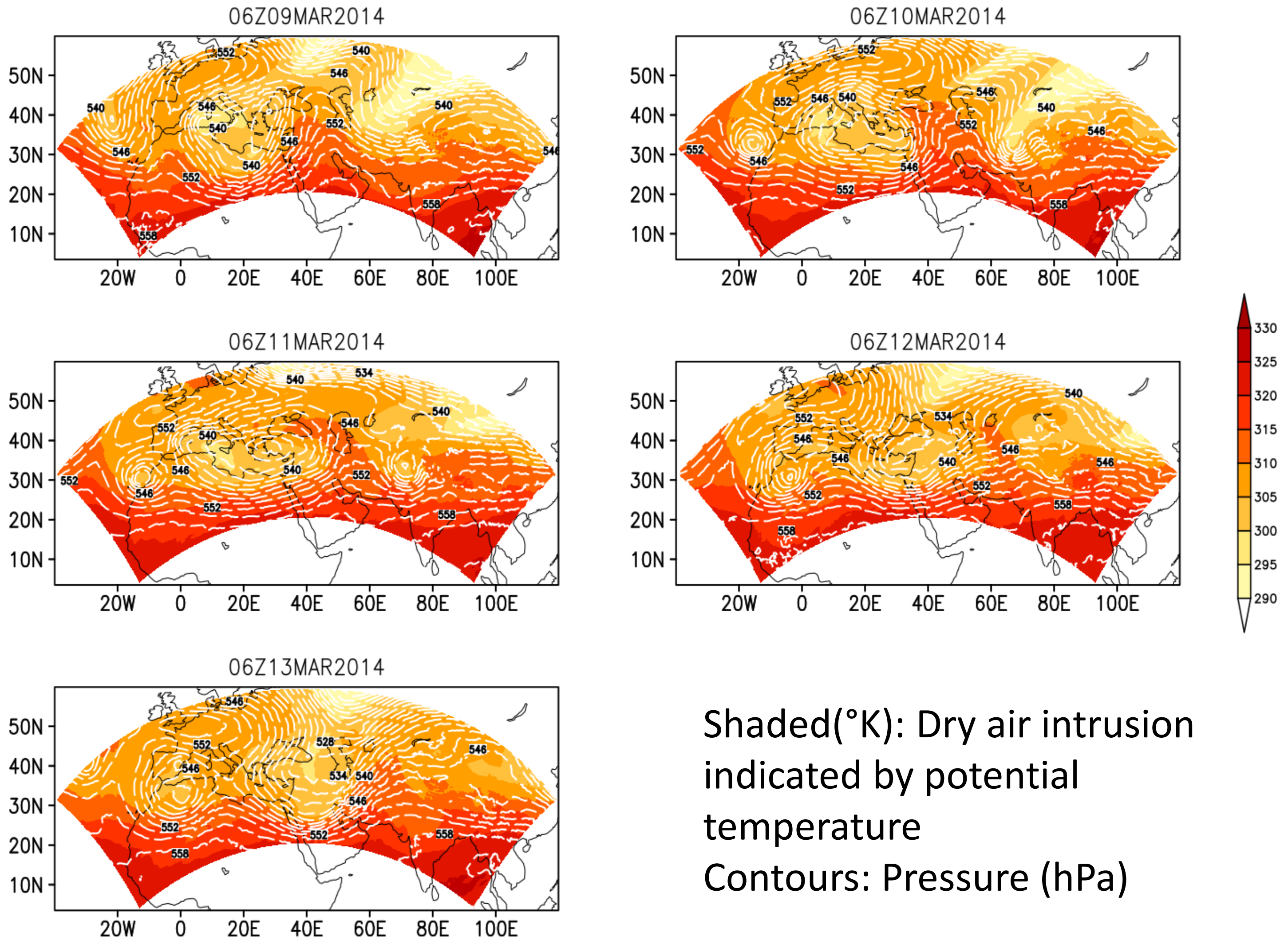

Shaded(°K): Dry air intrusion indicated by potential temperature
Contours: Pressure (hPa)

Impact of Meteorology Assimilation on Simulation of Atmospheric Chemistry – NCAP COALESCE

- Objective: To understand the impact of meteorology assimilation on the simulation of atmospheric chemistry

Sandeep Devaliya, Jyoti N. Bhate, Ramya Sunder Raman, Kaushik Muduchuru, Arushi Sharma, Vikas Singh, Amit P. Kesarkar, Chandra Venkataraman, (2023), Assessment of the impact of atmospheric aerosols and meteorological data assimilation on simulation of the weather over India during summer 2015, Atmospheric Environment, 297, 119586, ISSN 1352-2310, https://doi.org/10.1016/j.atmosenv.2023.119586.

Collaboration with IISER-Bhopal and IIT Bombay

NCAP-COALESCE: Meteorological Assimilation in WRFChem

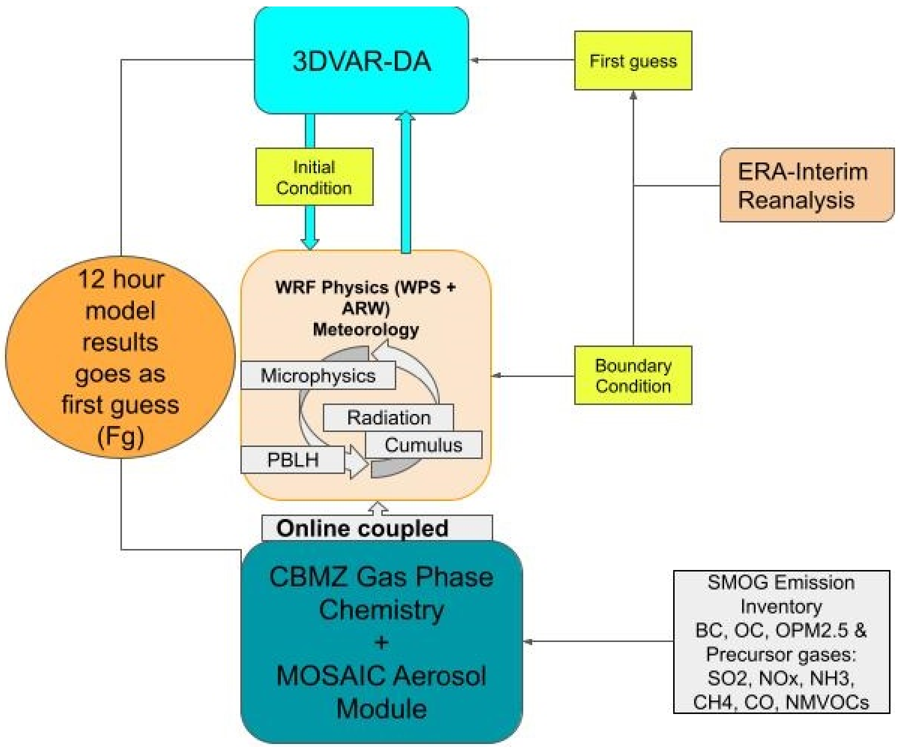

- A reduction in solar radiation (~10 to 60 W/m^2) over India due to the presence of aerosols was observed in WRFChem simulations which is due to the surface dimming effect of aerosols (Fig.).
- Surface dimming effect is also evident in the simulated T2 from the model as the reduction in T2 1-2.5 C is evident..
- Inclusion of 3DVAR further improves the prediction as compared to the results from WRFChemCntrl simulations because the meteorology is being constrained in the model.

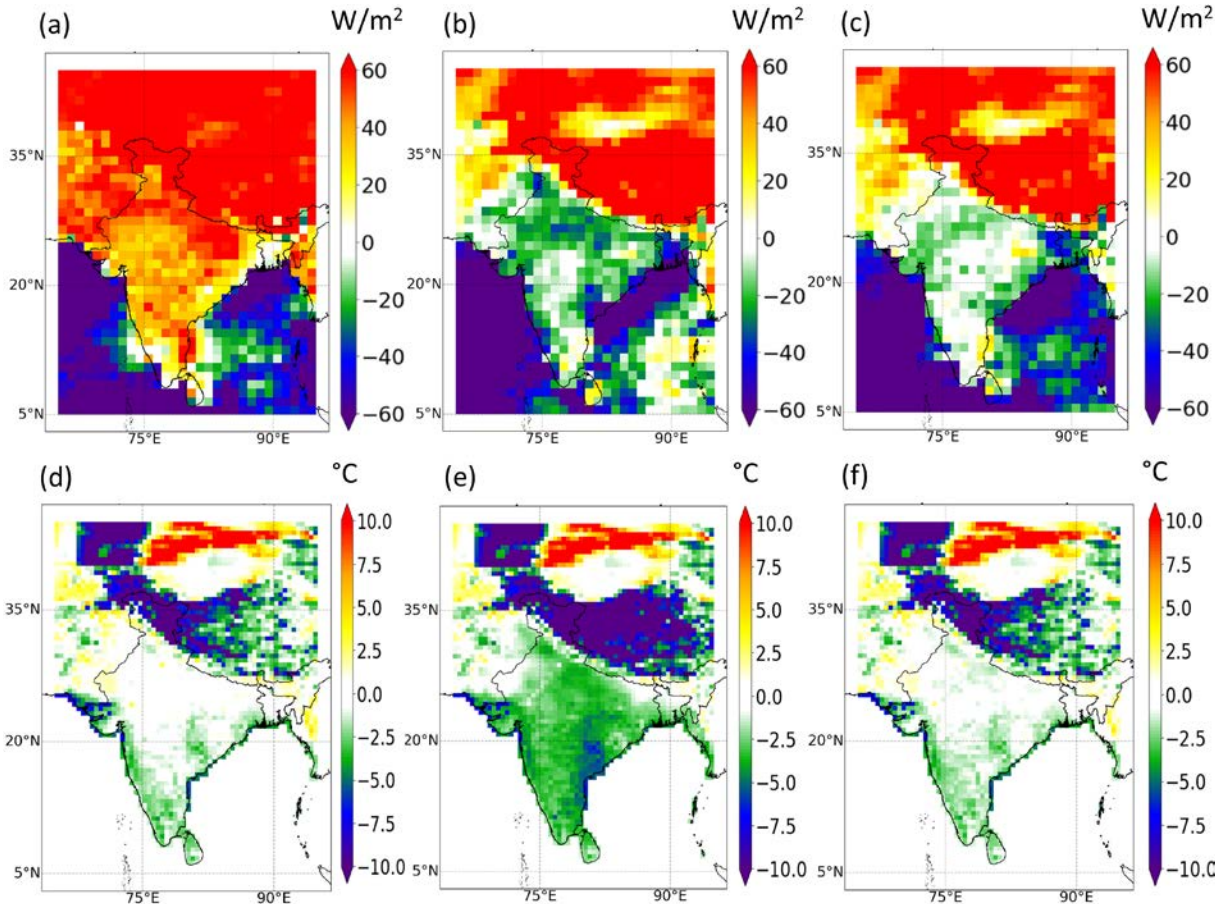

Fig. Incoming downwelling shortwave radiation at the surface: the difference between modeled and CERES products (WRFDA - CERES (a), WRFChemCntrl- CERES (b), WRFChemDA- CERES (c)).

Similarly, 2-meter temperature: the difference between modelled and CRU products (WRFDA-CRU (d), WRFChemCntrl-CRU (e), WRFChemDA-CRU (f))

Three Kinds of Butterfly Effect (BE)

- **BE-first kind:** Sensitivity dependence of solution to initial conditions – data assimilation
- **BE-second kind:** the ability of a tiny perturbation to create an organized circulation at large distances
- **BE-third kind:** hypothetical role of small-scale processes in contributing to finite predictability

Multi-stability vs Mono-stability

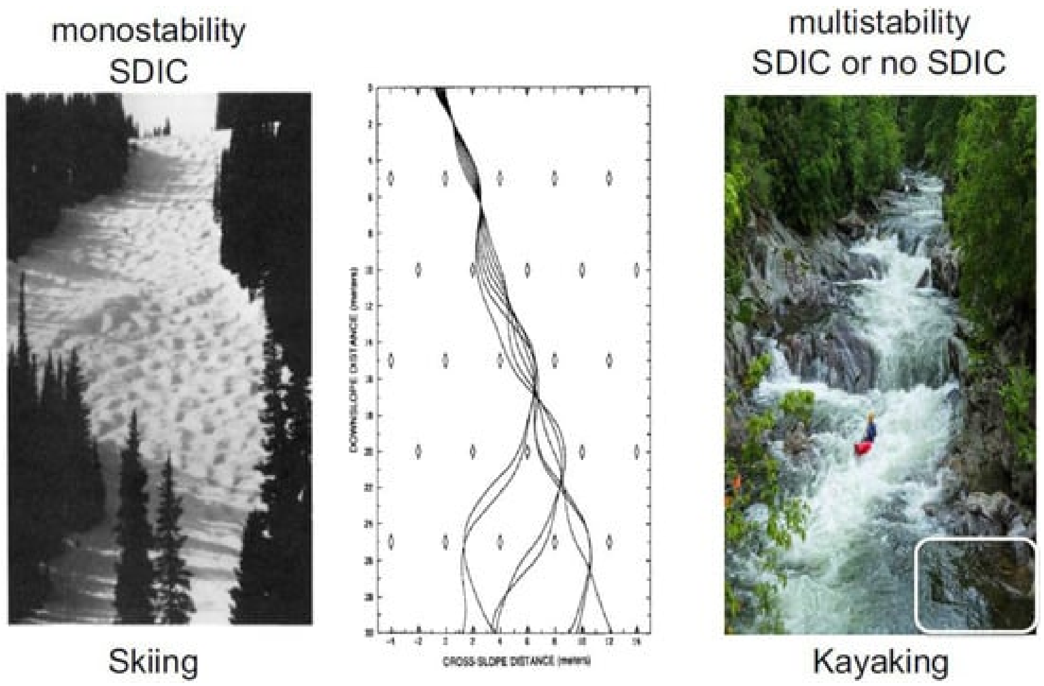

Shen et al., 2022

- Shen, Bo-Wen, Roger Pielke, Sr., Xubin Zeng, Jialin Cui, Sara Faghih-Naini, Wei Paxson, Amit Kesarkar, Xiping Zeng, and Robert Atlas. 2022. "The Dual Nature of Chaos and Order in the Atmosphere" *Atmosphere* 13, no. 11: 1892. https://doi.org/10.3390/atmos13111892
- Shen, Bo-Wen, Roger A. Pielke, Sr., Xubin Zeng, Jialin Cui, Sara Faghih-Naini, Wei Paxson, and Robert Atlas. 2022. "Three Kinds of Butterfly Effects within Lorenz Models" *Encyclopedia* 2, no. 3: 1250-1259. https://doi.org/10.3390/encyclopedia2030084

Unified Modelling Framework for Weather and Climate Modelling

Multiscale Adaptive Mesh Refinement on Ellipsoid

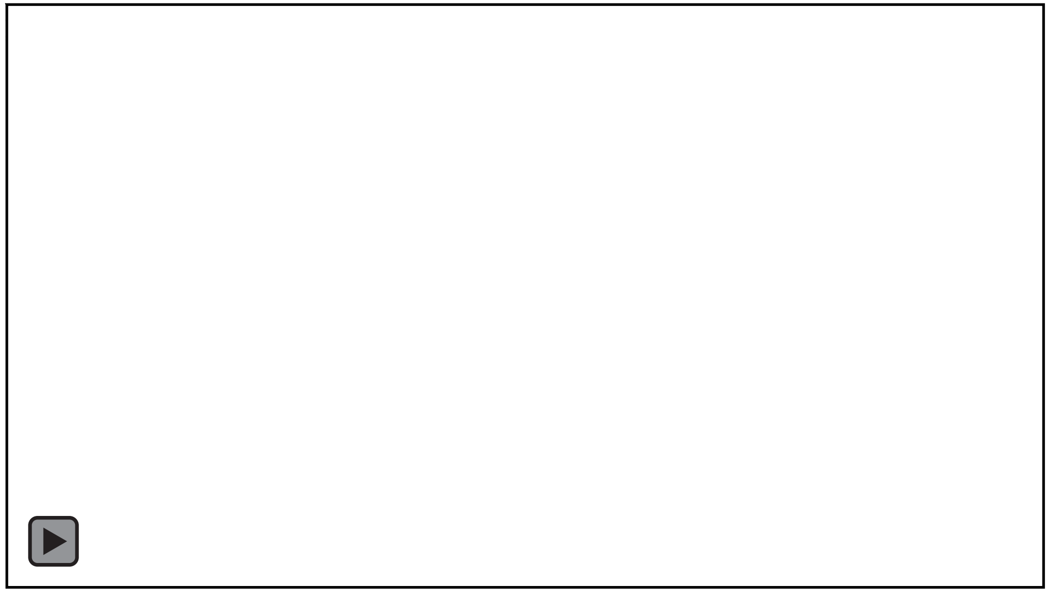

- Ellipsoid: WGS 1984
- Multiscale compressible nonhydrostatic equations of motions over ellipsoid
- Multiresolution spectral collocation framework for solving governing equations of dynamical core
- Earth Gravity Model 2008
- High resolution topography and LULC
- Coordinate Axis: Latitude, Longitude and Lagrangian coordinate
- 32 bit geo-hashing for collocated nodes along equator and meridian for static data and data assimilation

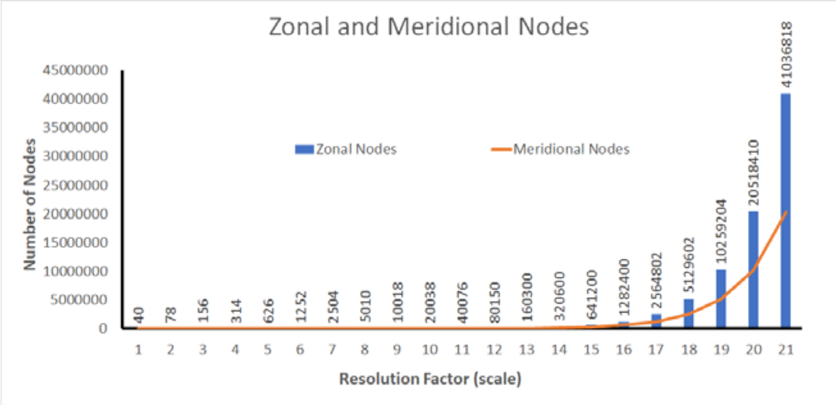

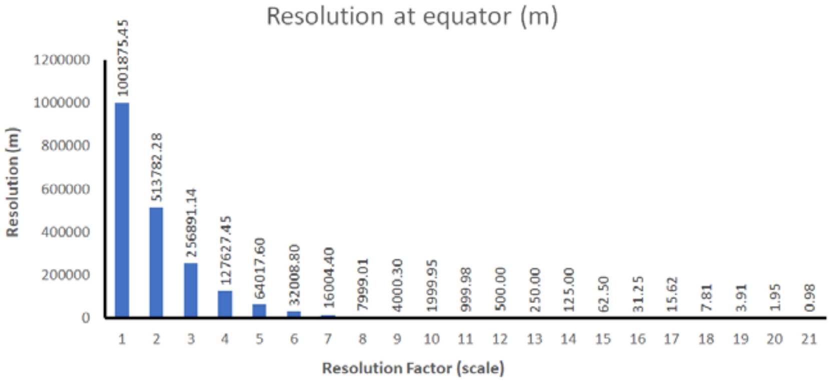

Adaptive Mesh Refinement Criterion
- Coastlines +/- 20km
- Topography / Orography slope
- Land use Land Cover
- Atmospheric processes

Concurrency and Computations, (2020)

i. Kavita Patnaik, Amit P. Kesarkar, Subhrajit Rath, Jyoti N. Bhate, Anantharaman Chandrasekar (2024) A 1-D model to retrieve the vertical profiles of minor atmospheric constituents for cloud microphysical modeling: III. Disturbed weather situations, Science of The Total Environment, 907, 167959, ISSN 0048-9697, https://doi.org/10.1016/j.scitotenv.2023.167959.

ii. Kavita Patnaik, Amit P. Kesarkar, Subhrajit Rath, Jyoti N. Bhate, Anantharaman Chandrasekar, (2023), A 1-D model to retrieve the vertical profiles of minor atmospheric constituents for cloud microphysical modeling: II. Simulation of diurnal cycle, Science of The Total Environment, 905, 167377, ISSN 0048-9697, https://doi.org/10.1016/j.scitotenv.2023.167377.

iii. Kavita Patnaik, Amit P. Kesarkar, Subhrajit Rath, Jyoti N. Bhate, Abhishek Panchal, Anantharaman Chandrasekar, Ramakumar Giri, (2023), A 1-D model to retrieve the vertical profiles of minor atmospheric constituents for cloud microphysical modeling: I. Formulation and validation, Science of The Total Environment, 881, 163360, ISSN 0048-9697, https://doi.org/10.1016/j.scitotenv.2023.163360.

iv. Debojit Sarkar, Amit P Kesarkar, Jyoti Bhate, Pavani Goriparthi, and Anantharaman Chandrasekar, Cloud burst over the complex terrain of Sauni Binsar, Uttarakhand: I. Appraisal of collision efficiencies. Revision Submitted to JESS.

v. Debojit Sarkar, Amit P Kesarkar, Jyoti Bhate, Pavani Goriparthi, and Anantharaman Chandrasekar, Cloud burst over Sauni Binsar, Uttarakhand: II. Appraisal of coalescence efficiencies. Revision Submitted to JESS.

vi. Subhrajit Rath, Amit P Kesarkar, Kavita Patnaika, Jyoti Bhate, and Govindan Kutty, Infrared heating/cooling-induced perturbation in vertical velocity inside convective clouds. Submitted to JESS

vii. Subhrajit Rath, Amit P Kesarkar, Kavita Patnaika, Jyoti Bhate, and Govindan Kutty, Infrared heating/cooling-induced perturbation in vertical velocity inside stratiform clouds, Submitted to JESS

viii. Debojit Sarkar, Amit Kesarkar, Jyoti Bhate, Pavani Goriparthi, and Anantharaman Chandrasekar, In-cloud Turbulence and Flow regimes separation during the Cloud Burst event of Sauni Binsar, Uttarakhand, India, submitted to Atmospheric Research

ix. Debojit Sarkar, Amit Kesarkar, Jyoti Bhate, Pavani Goriparthi and Anantharaman Chandrasekar, Classification of droplet breakup processes and its impact over a cloud burst event over Sauni Binsar, Uttarakhand, Modeling of Earth System and Environment

High-resolution microphysics parameterization – NARL scheme

Objective: To develop high resolution microphysics parameterization for prediction of extreme weather events

The kinetic equations for PSD of the p^th^ hydrometeor type of $f_p(m)$ used in the bin category for i^th^ bin,

$$\frac{\partial \rho f_{i,p}}{\partial t} + \frac{\partial \rho u f_{i,p}}{\partial x} + \frac{\partial \rho v f_{i,p}}{\partial y} + \frac{\partial \rho w f_{i,p}}{\partial z} = \left(\frac{\delta f_{i,p}}{\delta t}\right)_{nucl} + \left(\frac{\delta f_{i,p}}{\delta t}\right)_{c/e} + \left(\frac{\delta f_{i,p}}{\delta t}\right)_{d/s} + \left(\frac{\delta f_{i,p}}{\delta t}\right)_{f/m} + \left(\frac{\delta f_{i,p}}{\delta t}\right)_{col} + \cdots \ldots \ldots \ldots \ldots + \frac{\partial}{\partial x_j}\left(K \frac{\partial}{\partial x_j} \rho f_{i,p}\right)$$

- Three-moment bin scheme
- Representation of 57 microphysical processes in terms of exchange of mass and number concentration.
- 15 solid hydrometeors-ice types
- Multiscale, multiphysics representation
- Representation of impact of aerosol / dry mass intrusion on cloud development
- Representation of impact of infrared heating on cloud development

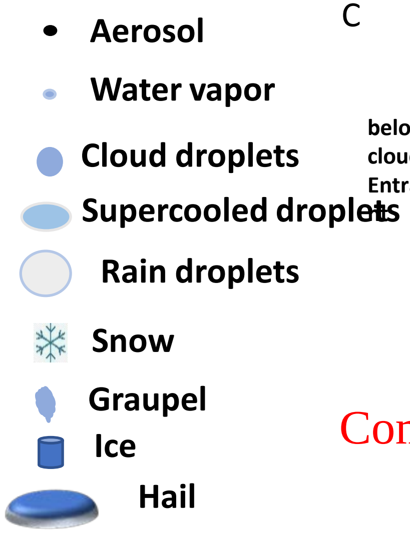

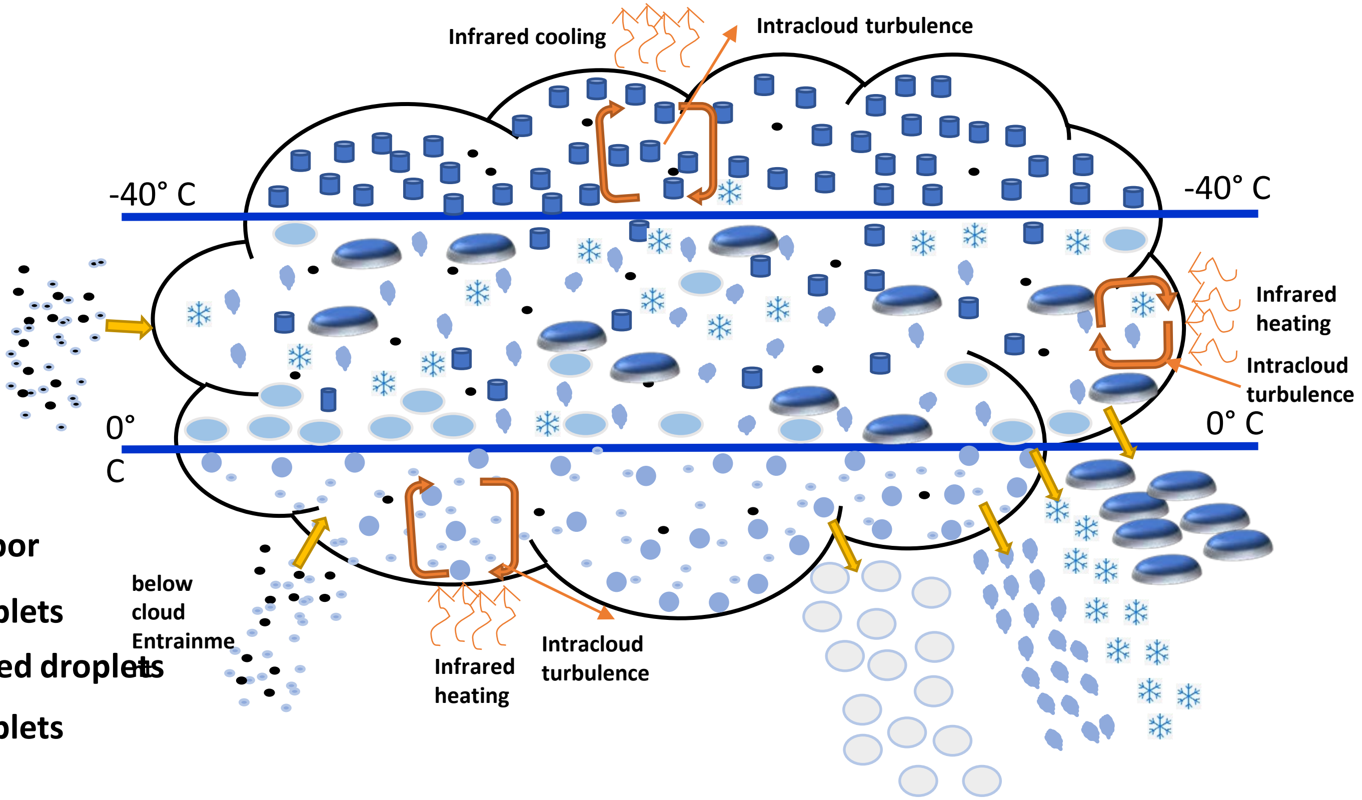

Complex microphysical processes interact inside the cloud and with an environment

NARL Scheme: Multiscale and Multiphysics representation

Multiscale

Bulk representation of Bins: 10015

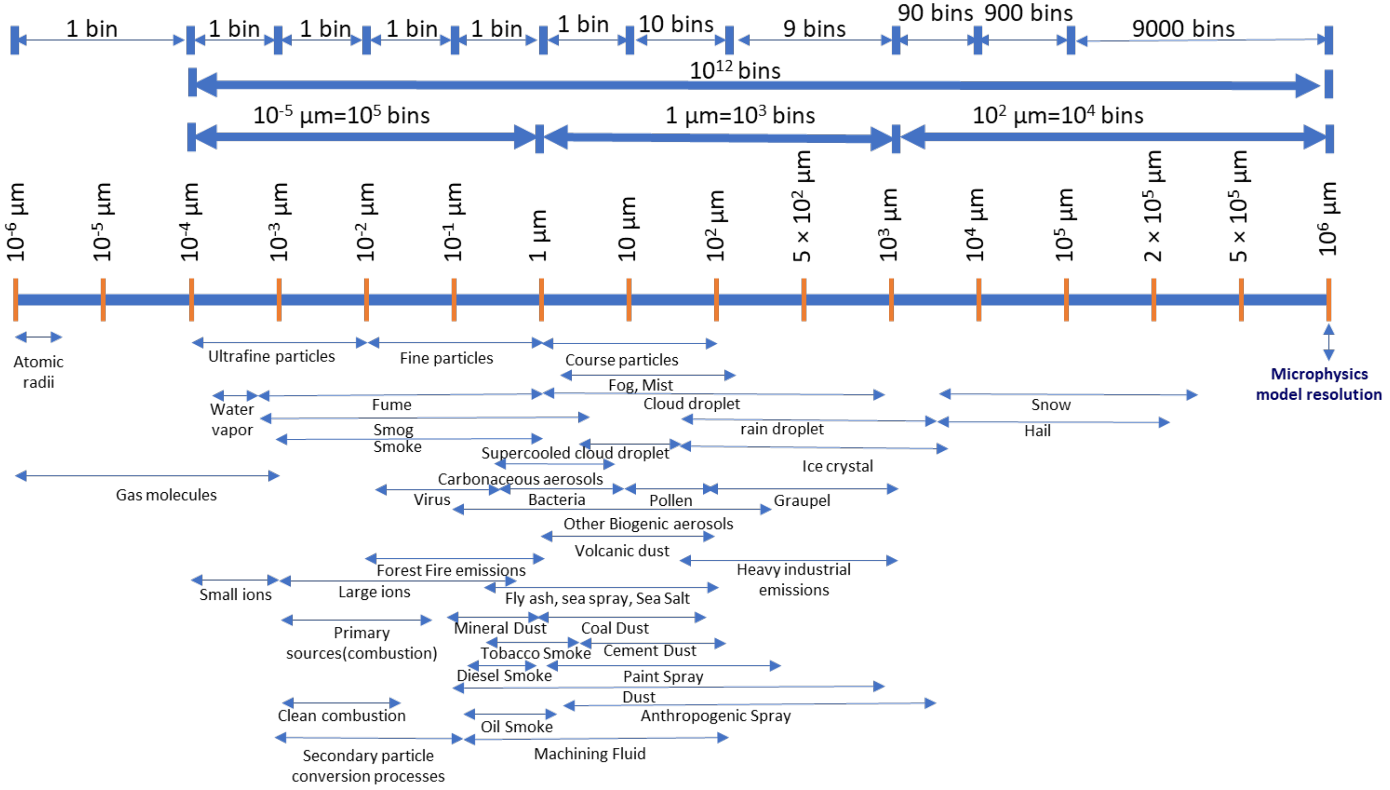

Multiphysics

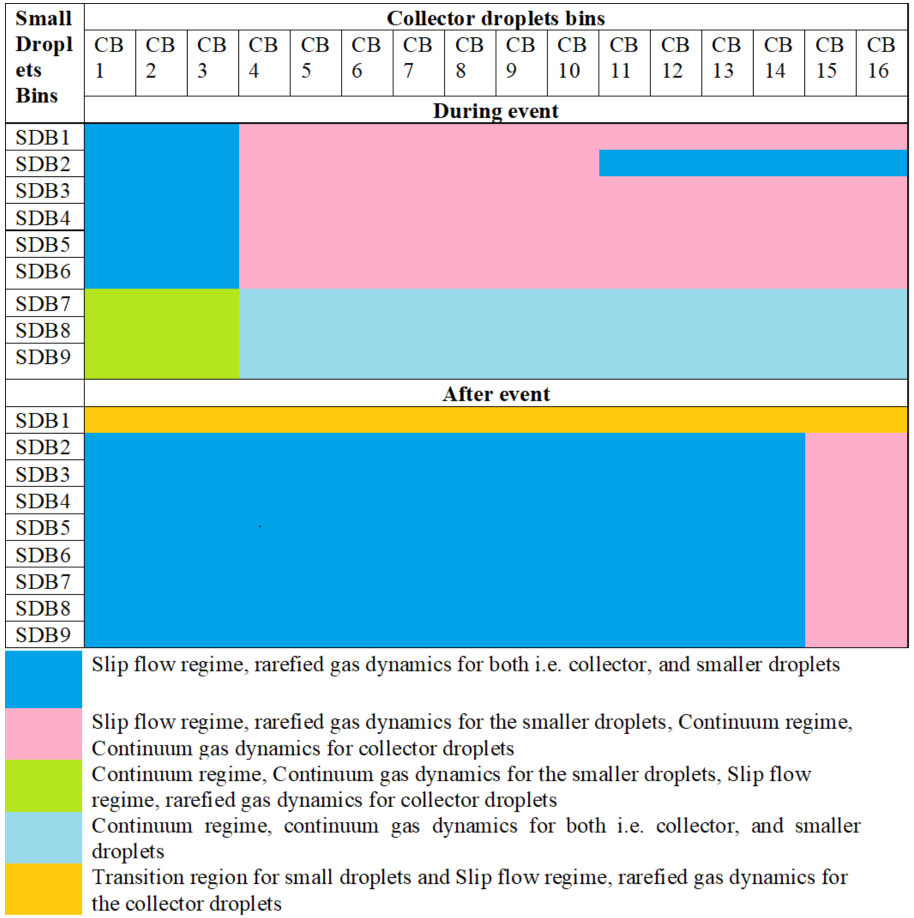

Atmospheric Research- in review

Simulation of cloud burst event over Suni Binsar, Uttarakhand (10 June 2021) using high resolution NARL microphysics

June 10, around 11:45 a.m. IST, Sauni Binsar/ Bindar, Kosi river, Block: Ranikhet, Almora

cloud burst >10 cm hr^{-1}

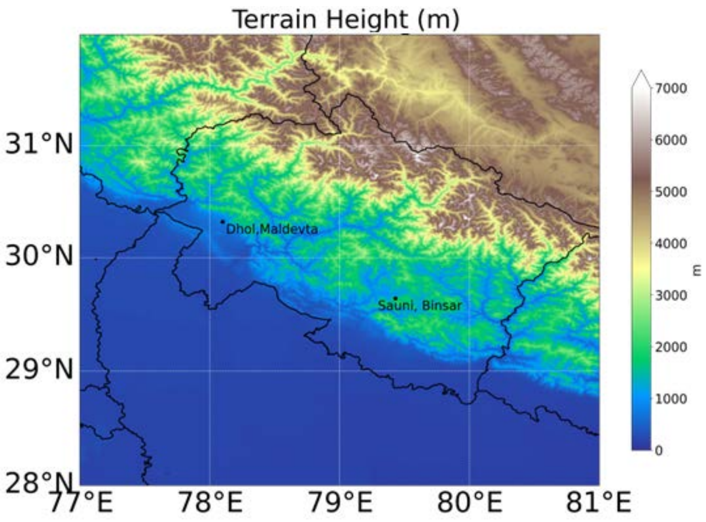

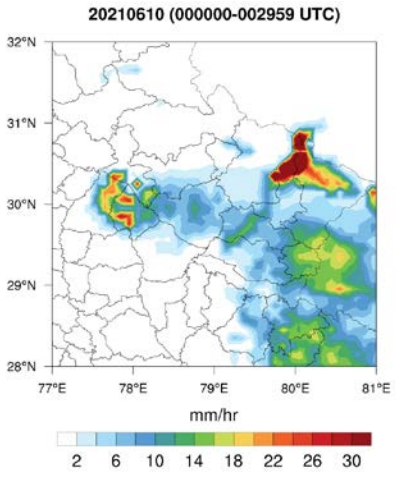

850 hPa

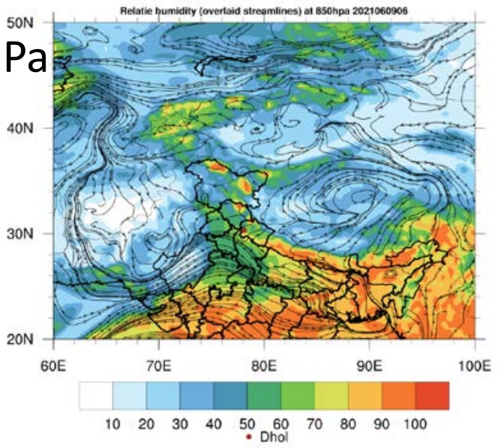

500 hPa

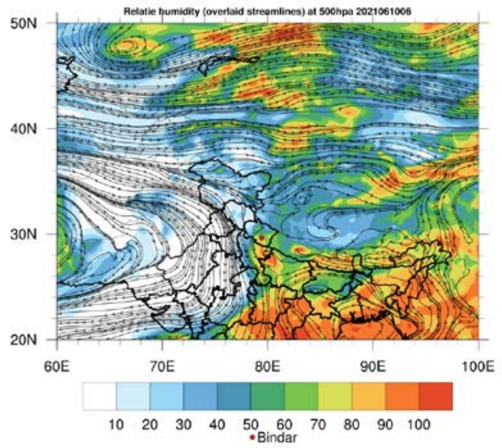

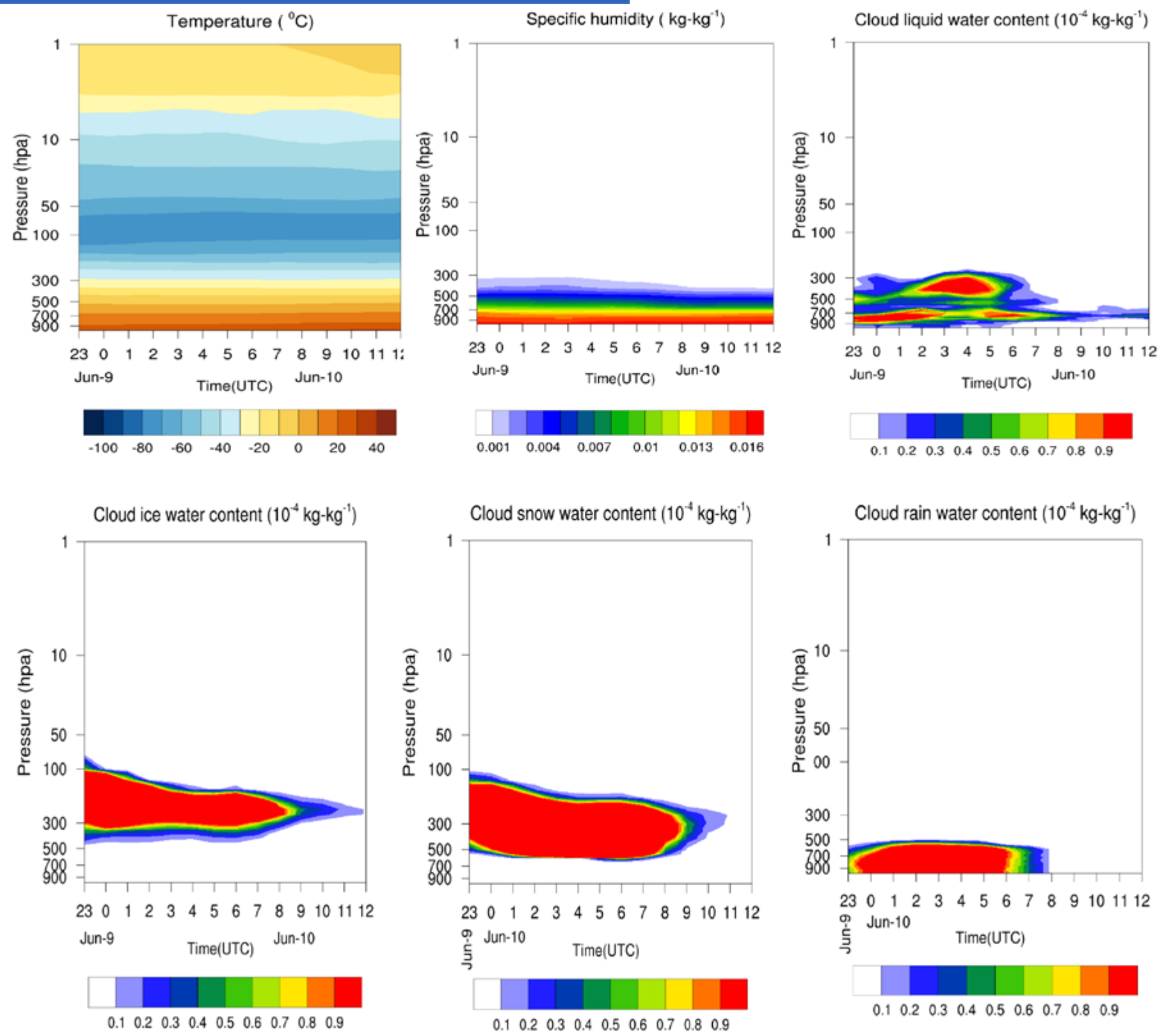

Atmospheric Research - in review

Collision-Coalescence and breakup mechanism

Collision efficiencies
Collector droplet radius: 5000-6000 μm

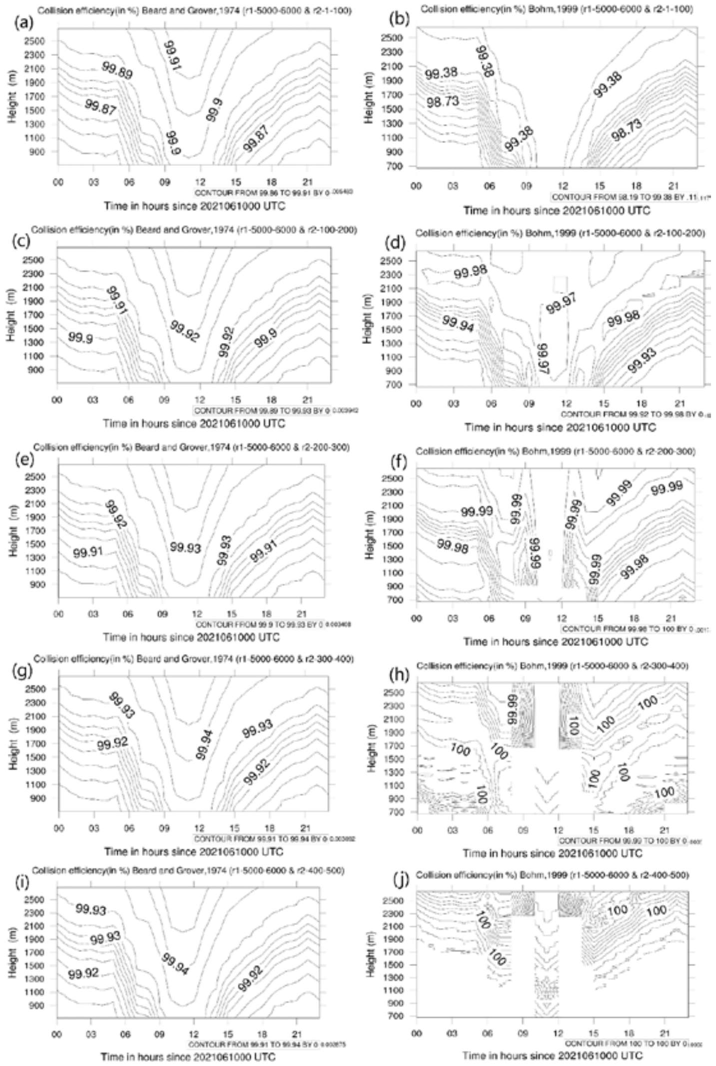

JASTP1 - in review

Coalescence efficiencies
Collector droplet radius: 5000-6000 μm

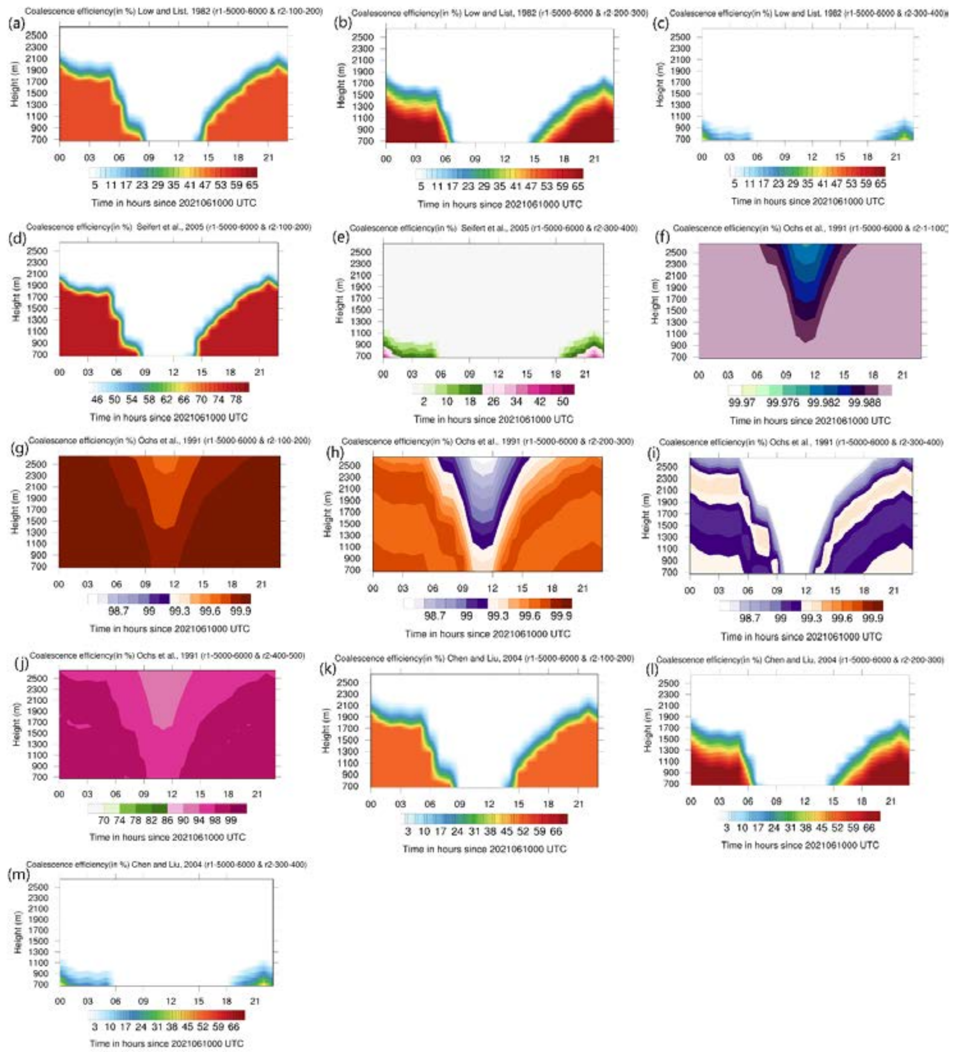

JASTP2 - in review

- Collision, Coalescence, and breakup mechanisms determine the non-inductive charging mechanism inside the cloud.
- High values of Collision and Coalescence efficiencies indicate the large amount of charge separation

NARL microphysics scheme - cloud chemistry: Hybrid Monte Carlo-Gear Solution Solver

Objective: To develop hybrid Monte Carlo – Gear Solution Solver for estimating CCNs for microphysics models

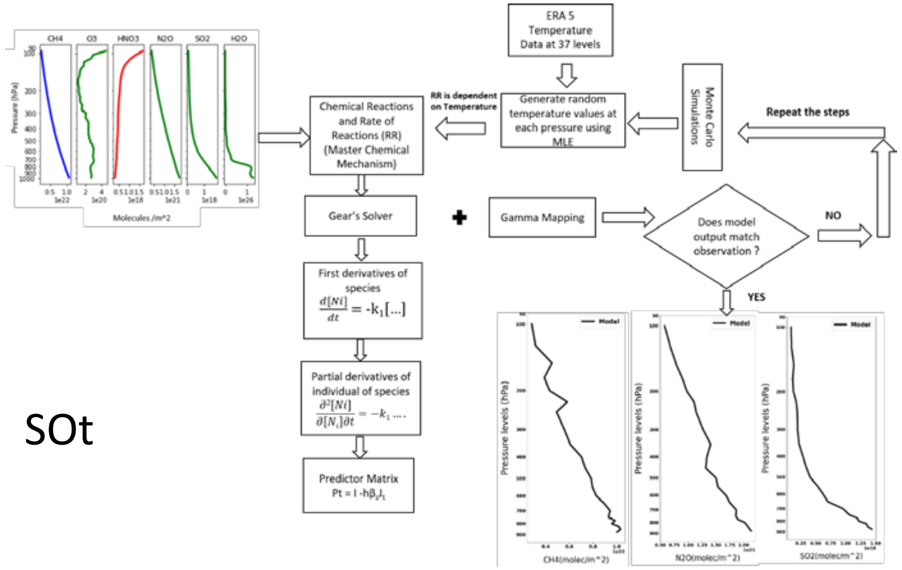

SOt

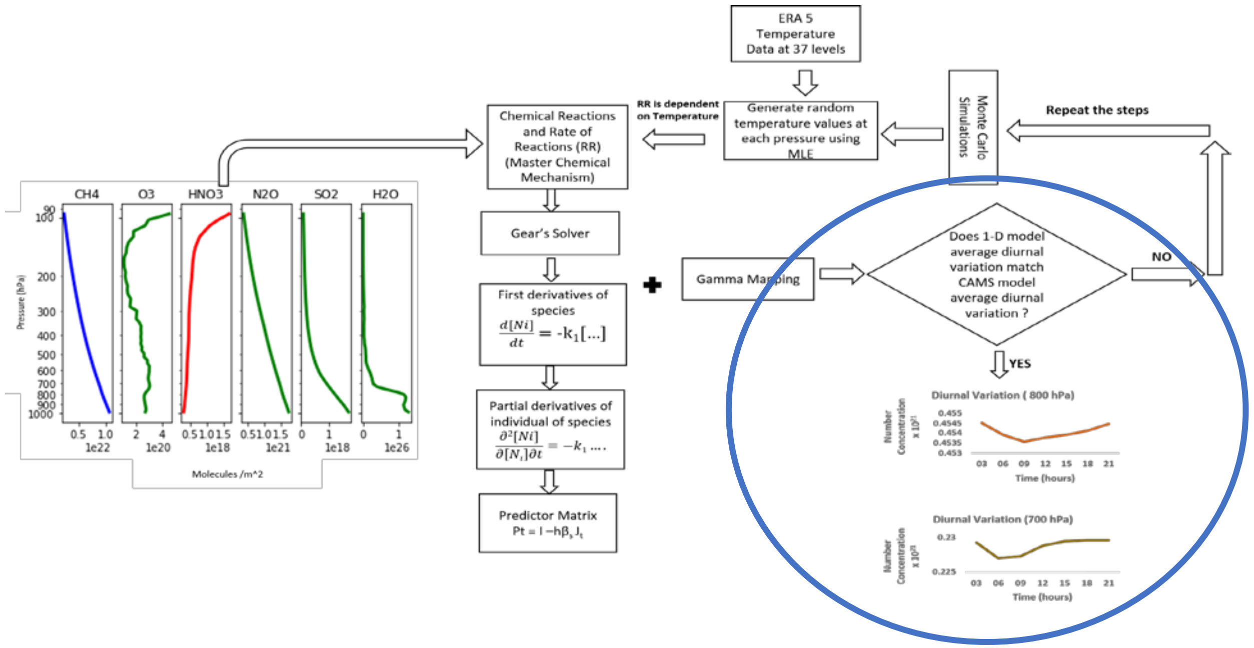

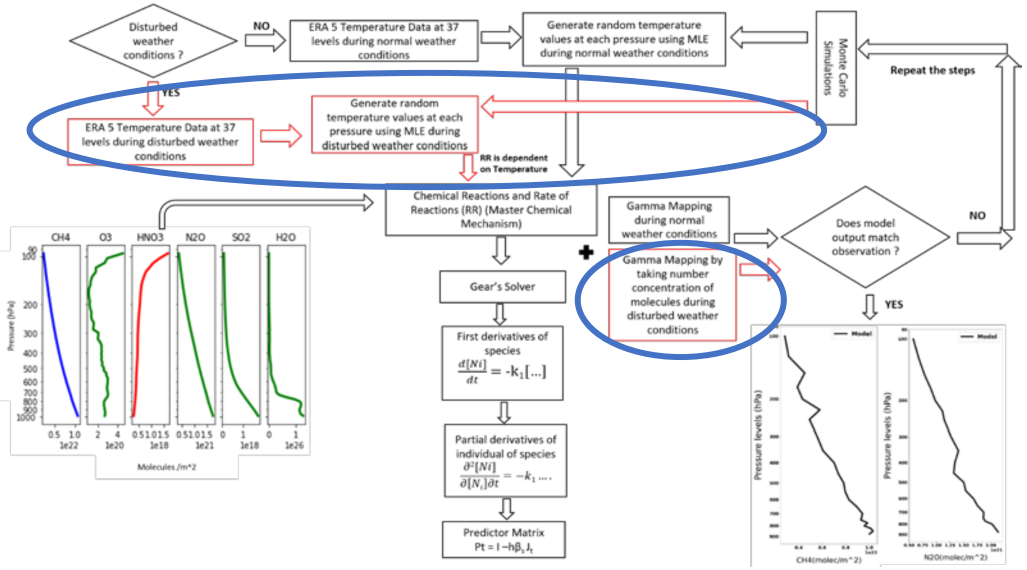

- Retrieved profiles and CLIMCAPS products are in very good agreement.
- The accuracy of retrieved profiles is impacted due to the passage of synoptic scale disturbance.
- Developed solver is useful for estimating the profiles of CCN number concentration.

NARL microphysics scheme: Representation of the impact of infrared heating

Stratiform rainfall case over Gadanki, Rainfall: 48.5 mm Date: 30 July 2017 06:00 IST

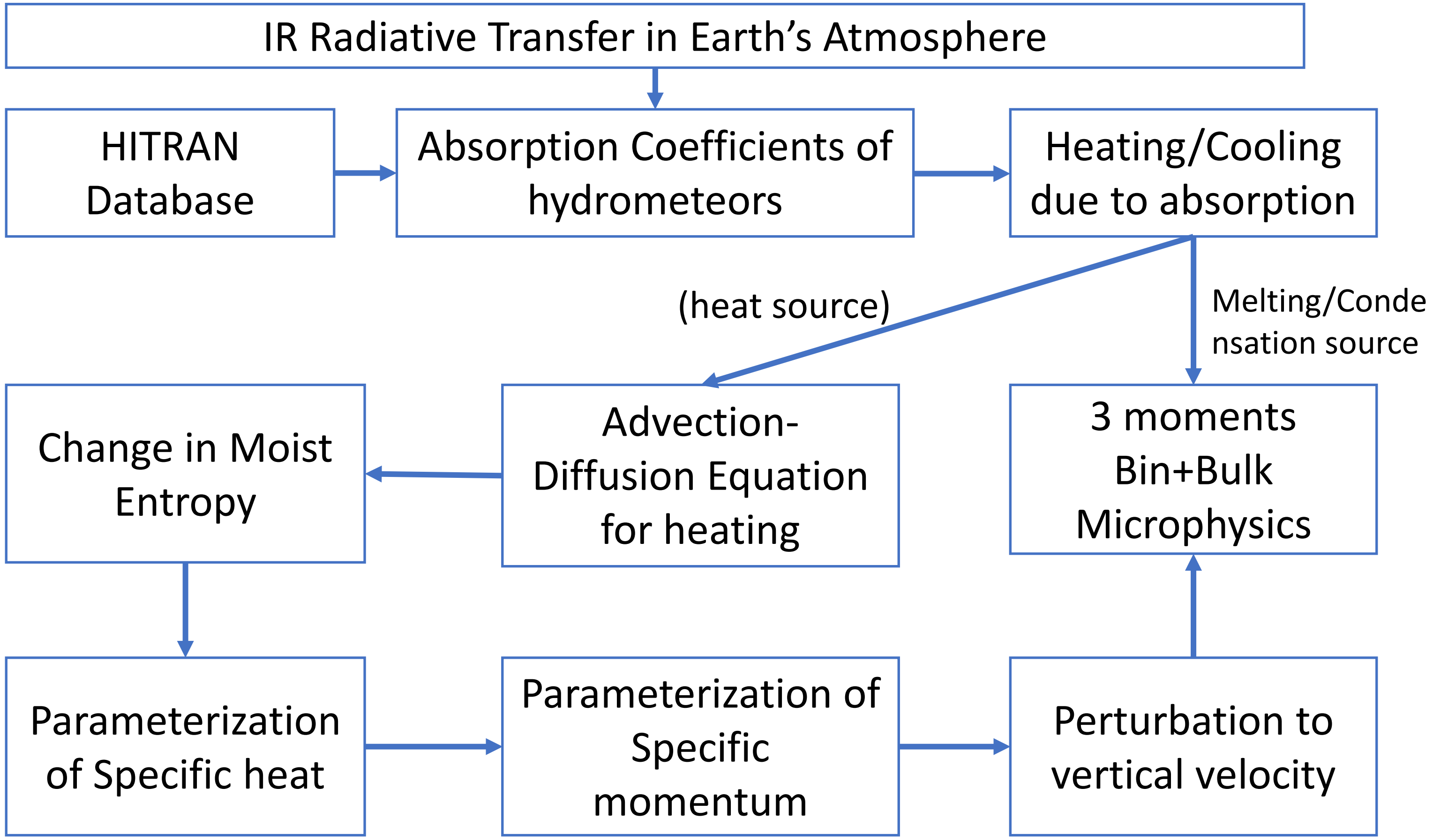

JESS in review

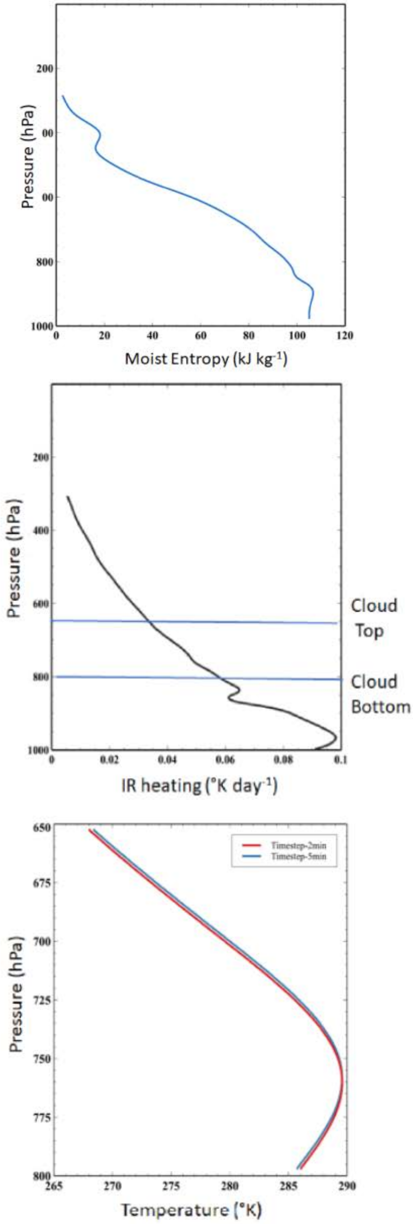

- Heat generation is higher in the lower part of the cloud than in the upper part. It creates the vertical gradient of the temperature inside the cloud and alters condensation and melting profiles.
- Perturbation to vertical velocities are of the order of 1-12 cm s^{-1} per unit mass

NRSC-Lightning Detection Sensor Network and NARL Collaboration

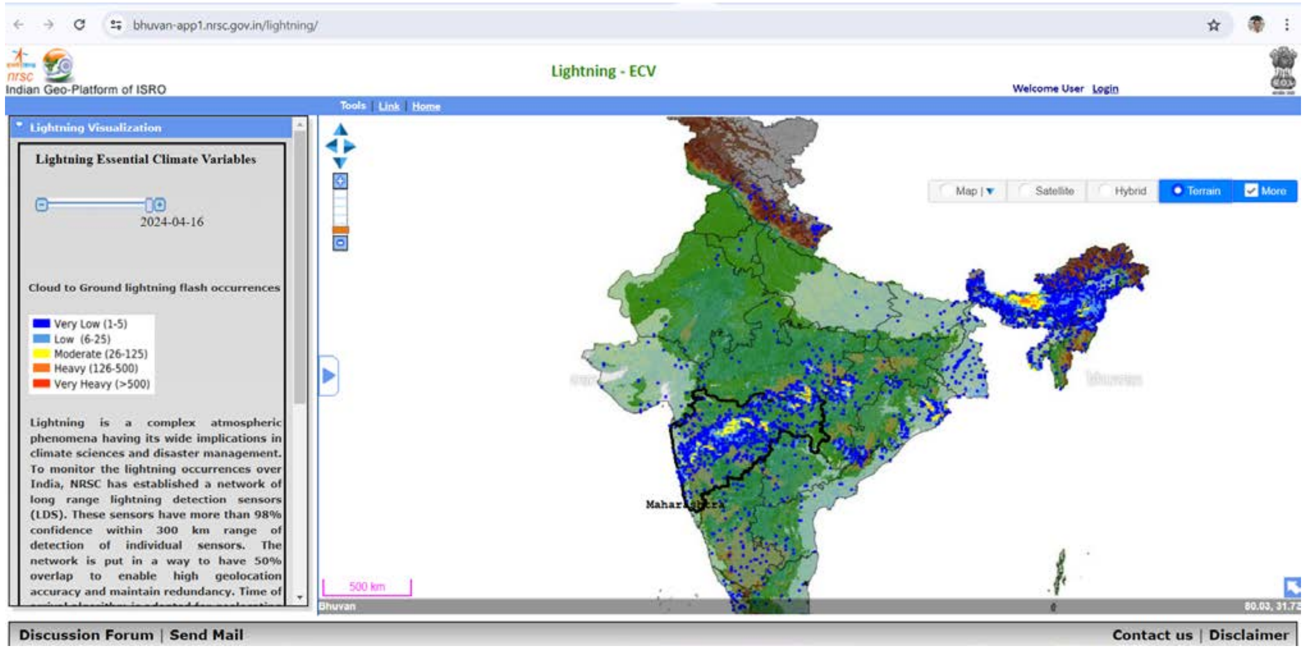

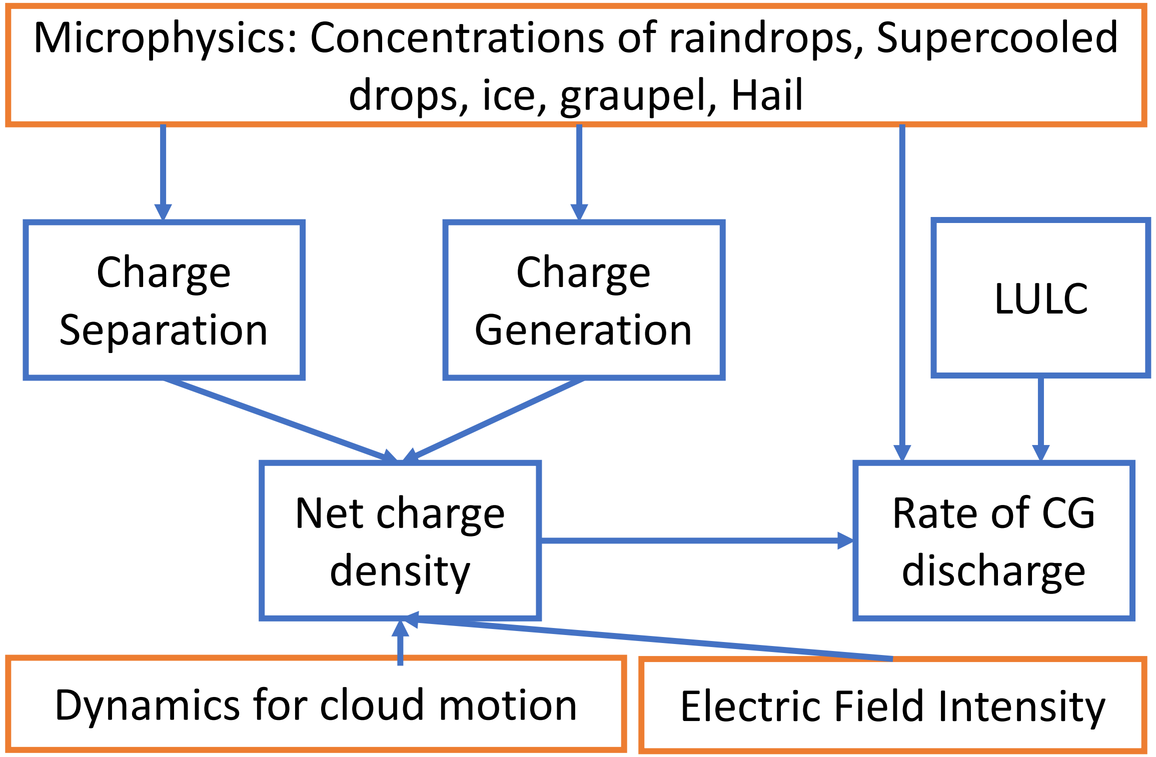

Source: https://bhuvan-app1.nrsc.gov.in/lightning/

Objectives:

- To develop cloud charge distribution parameterization
- To validate mesoscale lightning flash count forecast.
- To parameterize lightning flash count
- To develop algorithms for nowcasting and short-range prediction of lightning flash count

Overview and Summary

- Rapid improvement in the development of DA techniques and their operationalization in the last 2 decades
- However with new challenges of three kinds of butterfly effect
- Future generation models will be more complex leading to complex DA algorithums
- New avenue/challenges for researchers: convective scale data assimilation, assimilation in multi-resolution, multiscale, Multiphysics, and multistable models (Chaotic and non-chaotic models) to improve predictability

Thank you very much for your kind attention **e-mail: amit@narl.gov.in**